

The self-tuning of the cosmological constant and the holographic relaxion

Yuta Hamada[‡], Elias Kiritsis^{‡b}, Francesco Nitti[‡], Lukas T. Witkowski[†]

[‡] *APC, AstroParticule et Cosmologie, Université de Paris, CNRS/IN2P3, CEA/IRFU, Observatoire de Paris, 10, rue Alice Domon et Léonie Duquet, 75205 Paris Cedex 13, France*

^b *Crete Center for Theoretical Physics, Institute for Theoretical and Computational Physics, Department of Physics, Voutes University Campus, GR-70013, Vasilika Vouton, Heraklion, GREECE*

[†] *Institut d'Astrophysique de Paris, GReCO, UMR 7095 du CNRS et de Sorbonne Université, 98bis boulevard Arago, 75014 Paris, France*

ABSTRACT: We propose a brane-world setup based on gauge/gravity duality that permits the simultaneous realisation of self-tuning of the cosmological constant and a stabilisation of the electroweak hierarchy. The Standard Model dynamics including the Higgs sector is confined to a flat 4-dimensional brane, embedded in a 5-dimensional bulk whose dynamics is governed by Einstein-dilaton-axion gravity. The inclusion of a dynamical bulk axion is new compared to previous implementations of the self-tuning mechanism. Because of the presence of the axion, the model generically exhibits a multitude of static solutions, with different values for the equilibrium position for the brane. Under mild assumptions regarding the dependence of brane parameters on bulk fields, a number of these solutions exhibit electroweak symmetry breaking with a small Higgs mass as compared to the cutoff-scale of the brane theory. The realisation of self-tuning of the cosmological constant is generic and as efficient as in previous constructions without a bulk axion. Vacua with a small Higgs mass can sometimes be found, regardless of whether the brane theory depends explicitly on the bulk axion. Because it is expected on general principles that the brane action will depend on the axion, the generation of solutions with a hierarchy is a robust feature.

Contents

1. Introduction and results	2
1.1 Setup and summary of results	5
1.2 Open questions and future work	11
2. The bulk theory and its dual QFT	13
2.1 Constraints on the effective gravitational action	15
2.2 The first order formalism	18
3. The brane theory and its couplings to the bulk fields	22
4. Brane-bulk interactions: the Israel matching conditions	23
5. Solutions in the small axion backreaction approximation	28
6. General numerical solutions	30
6.1 Brane potential choice 1: No explicit axion dependence	32
6.2 Brane potential choice 2: linear axion dependence of Higgs mass parameter	39
6.3 Brane potential choice 3: axion cosine potential	45
6.4 Brane potential choice 4: $\Lambda_{QCD} + \Lambda_a$	45
6.5 Summary of the section	47
7. The gauge hierarchy problem and outlook	48
Acknowledgements	50
Appendices	51
A. Calculation of on-shell action, free energy and topological susceptibility	51
A.1 Small axion backreaction approximation	53
B. Small axion backreaction approximation	54
C. Brane equilibrium position in the near-UV or near-IR regions: analytic results	58
C.1 Brane equilibrium position in the near-UV region	58
C.2 Brane equilibrium position in the near-IR region	59
D. Overshooting constraint	60

E. Positivity constraints	63
E.1 Linear Perturbations	64
E.2 KK expansion	65
E.2.1 Ghosts	66
E.2.2 Tachyons	67
E.3 Simple models estimates	68
E.3.1 Discrete models	68
E.3.2 Continuous models (abridged)	72
E.4 General remarks	73

1. Introduction and results

The idea of naturalness in effective field theory emerged in the second half of the twentieth century, as one of the main guidelines for model building in the context of theories of fundamental physics. One of the main drives was the realization that the most complete theory of fundamental interactions, i.e. the Standard Model of particle physics plus semiclassical gravity, suffers from (at least) two *naturalness problems*, i.e. the fact that some dimensionful parameters of the theory, which are sensitive to UV physics, are nevertheless much smaller than one would expect compared to other mass scales in the theory.

The first is the *Electroweak hierarchy problem*, which does not involve (directly) gravitational physics and concerns the Higgs mass (equivalently, its vacuum expectation value). In a natural EFT, the latter should be of the order of the high-energy cut-off, i.e. the energy scale where the theory breaks down (for example because new heavy degrees of freedom which had been integrated out at low energy have to be included). The appearance of novel UV scales in the SM is guaranteed by the fact that the electromagnetic coupling is IR-free and the theory is not UV complete. There are other good reasons to believe that a few such scales exist well above the Higgs mass scale of around 1 TeV. On the one hand, we have many hints for the existence of physics beyond the Standard Model at a high energy scale (dark matter, inflation, neutrino masses if they are generated via a see-saw mechanism). On the other hand, ultimately the need for a quantum description of gravity at the Planck scale M_p most likely needs new physics at or below this scale.¹

The second problem concerns the *cosmological constant* (CC), a parameter whose only effect can be felt when the theory is coupled to gravity. In a natural theory,

¹The holographic realization of gravity via the AdS/CFT correspondence and its generalizations indicate that novel physics always appears *well-below* the Planck scale. The relevant scale is (most of the time) the string scale.

the CC is expected to receive contributions from the vacuum energy of all quantum fields in the model, each contribution scaling like the respective mass-scale to the fourth power. However, the observed cosmological constant today (which in Einstein gravity is related to the four-dimensional curvature of the universe on very large scales) is measured to be many orders of magnitude below all known mass scale of particle physics. Unlike the electroweak hierarchy problem, we have *direct* evidence for the existence of physics above the CC scale (namely, all of particle physics apart from Maxwell electromagnetism and neutrinos).

Although many attempts have been made to address one or the other of the two problems by introducing new physics, rarely both issues have been attacked at the same time, or using the same underlying mechanism.² The aim of the present paper is to present a coherent framework that potentially addresses both hierarchy problems.

Recently, a class of models was put forward [7] to address the cosmological constant problem in the context of holographic brane-worlds. In this framework, the Standard Model fields are confined on a 4-dimensional brane immersed in a 5-dimensional warped, non-compact bulk, similar to the original Randall-Sundrum (RS) brane-world model [8].³ However, the model proposed in [7] departs from the RS model in several crucial ways:

1. The SM brane is not an “end-of-space” brane, but it is rather a defect in a geodesically complete bulk, which has an asymptotically Anti-de Sitter (AdS) region. In the holographic language, the UV of the geometry is kept. This setup has a dual holographic interpretation in terms of a UV-complete holographic QFT dual to the bulk theory and a coupling to the SM realized on the brane, [10]. IT is also crucial for the success of the self-tuning mechanism.
2. The bulk theory contains one or more scalar fields which have a non-trivial profile in the vacuum (ground-state) solution. Their backreaction causes the bulk geometry to depart from AdS in the interior.
3. The localized brane action contains all terms allowed by the symmetries, up to second order in derivatives. In particular, it contains a localized Einstein-Hilbert term.

As a consequence of these features, the model displays a mechanism of *self-tuning* of the cosmological constant: the curvature observed on the brane is decoupled from the vacuum energy of the brane-localized fields. In particular, for arbitrary values of the vacuum energy there generically exist solutions with a flat and stabilized brane.

²There are a few notable exceptions, [1]-[6].

³See [9] for recent work on theoretical obstacles to exactly localizing fields on 3-branes in 5-dimensional brane-worlds.

Moreover, thanks to the last property in the list above,⁴ a DGP-like mechanism of gravity quasi-localisation [12] allows the four-dimensional observers on the brane to experience ordinary four-dimensional gravity in a range of scales.⁵ In [18] it was shown that the self-tuning mechanism is robust, in the sense that stabilized solutions with curved branes require a modification of the boundary conditions at the AdS boundary, and therefore belong to a different superselection sector than flat solutions. A dynamical study of this model in the cosmological setting was initiated in [19].

The self-tuning mechanism of [7] relies on the interplay between bulk and brane dilaton potentials. In that work, only gravity and the bulk dilaton were kept as dynamical fields, and the Standard Model fields were considered non-dynamical (they were “integrated out”). In this work, we improve on that model by adding two new ingredients: the Higgs field on the brane, and the axion field in the bulk. Both are necessary to have a complete realistic model.

The brane Higgs sector. In the full theory, the brane-localized Higgs field is expected to also play an important role in the self-tuning dynamics: even at the classical level, the Higgs has a non-trivial brane-localized potential, and its vacuum expectation value enters the determination of the brane vacuum energy.⁶ In particular, the latter depends on whether the electroweak gauge group is in the broken or unbroken phase. Therefore, in order to find the correct self-tuning vacuum, it is necessary to minimize the potential for the dilaton and the Higgs field at the same time.⁷

The bulk axion. An extra bulk field other than the dilaton is universally present in holographic duals to large- N gauge theories: it is the bulk axion field, dual to the gauge theory instanton operator $Tr[F \wedge F]$. This field enjoys a shift symmetry in the bulk, which however may be broken on the brane due to the coupling with the

⁴Even in the presence of a brane-localized Einstein-Hilbert term it generally remains challenging to reproduce realistic gravitational interactions for a four-dimensional observer localized on a brane, as discussed in e.g. [11].

⁵Several works in the past displayed some, but not all, of the features listed above. Dilatonic brane-worlds were extensively studied, including in the context of self-tuning models [15, 16], but in these works the absence of a gravity-localisation mechanism and/or the presence of bulk singularities made these models untreatable. On the other hand, models like DGP or RS-DGP [17] without a bulk scalar are unsuitable for self-tuning.

⁶In orientifold realizations of the SM in string theory there are always two Higgs fields necessary in order to realize the symmetry breaking patterns of the Standard Model, even in the absence of supersymmetry, [20, 21, 22]. These Higgses and the breaking are intertwined with anomalous $U(1)$'s that are always present, [23]. We do not consider these subtleties in this paper.

⁷In contrast, the other SM fields can still be neglected for this purpose, as they do not take on a vacuum expectation value. There is an exception to this and this involves chiral symmetry breaking, but the correction for the self-tuning dynamics is negligible for our purposes.

Standard Model.⁸ The general bulk dynamics of Einstein-axion-dilaton theories (including axion backreaction) was recently discussed extensively in [24]. A peculiarity of the axion field is that the gauge theory coupling to which it is dual (namely the θ -angle) is periodic. This implies the existence of several inequivalent bulk solutions corresponding to different branches of $\theta + 2\pi k$, which correspond to the same physical θ -angle but different boundary conditions for the bulk axion. This phenomenon is already known from gauge theory dynamics, [25], and has been seen in several related holographic contexts, [26, 27]. Moreover it matches the analysis of the QCD chiral Lagrangian, [25, 27].

In this work, we study the self-tuning and brane-stabilisation problem in the framework of [7], enriched by the dynamical bulk axion and the SM Higgs field. We ask the question whether the electroweak hierarchy problem can be resolved at the same time as the CC problem: do vacua with a small CC *and* a small Higgs vacuum expectation value (with respect to the high energy cut-off) exist, for generic model parameters? As we shall see, a positive answer relies on the existence of multiple, densely packed axion vacua, which gives rise to multiple flat extrema of the bulk-brane system, some of which lie in the region where the Higgs vev is small.

The idea of exploiting multiple axionic-like vacua (in four dimensions or in conjunction with extra dimensions) has been explored in the past, to solve either the cosmological constant problem, [2], or the electroweak hierarchy problem like in the relaxion scenario [28]. The latter had the feature, in addition to realizing the existence of vacua with small Higgs vev, of providing a dynamical mechanism (cosmological relaxation) for vacuum selection. Here we do not address this problem, which is of dynamical nature and we leave it for future work. Rather, we provide a proof of principle that a vacuum with a small Higgs mass and a self-tuned vacuum energy may generically exist in this class of models, given suitable (but non finely tuned) potentials. For other related work where the two hierarchy problems are correlated, see [1]-[6].

In the rest of this introductory section we summarize our setup and our main results.

1.1 Setup and summary of results

We consider an Einstein-axion-dilaton theory in the bulk, dual to a non-trivial holographic QFT. Although we employ a single scalar and a single pseudoscalar (dual to an instanton density) our results generalize to the multiscalar case.

We add a codimension-1 brane on whose world-volume the SM fields are localized. One of these fields is the Higgs scalar which will play a central role in our discussion.

⁸The shift symmetry is also broken in the bulk by string theory instantons. Such a breaking is negligible at large N as it is exponentially small, $\mathcal{O}(e^{-N})$.

The bulk dynamics is described by the general two-derivative action which after field redefinitions reads,

$$S_{bulk} = M_p^3 \int d^5x \sqrt{-g} \left[R - \frac{1}{2} g^{ab} \partial_a \varphi \partial_b \varphi - \frac{1}{2} Y(\varphi) g^{ab} \partial_a a \partial_b a - V(\varphi) \right] + S_{GHY}, \quad (1.1)$$

where g_{ab} is the metric of the 5-dimensional bulk space-time, φ is the bulk dilaton field and a is the bulk axion which only enters the bulk action via derivative terms. We shall consider the following ansatz for the bulk fields

$$ds^2 = du^2 + e^{2A(u)} \eta_{\mu\nu} dx^\mu dx^\nu, \quad \varphi = \varphi(u), \quad a = a(u), \quad (1.2)$$

which is also employed in the description of holographic axionic RG flows [24]. The explicit Poincaré symmetry of the ansatz indicates that we are looking for ground state solutions.

Implementing the self-tuning mechanism of [7], we shall seek solutions with a *flat* 4-dimensional brane embedded into a bulk described by (1.1). One way of achieving this is to embed the brane in such a way that it coincides with a constant- u -slice of the bulk geometry:

$$\text{brane locus: } u = u_0, \quad \text{with } \varphi_0 \equiv \varphi(u_0), \quad a_0 \equiv a(u_0). \quad (1.3)$$

The brane has localized curvature terms on its world-volume. However, for a brane with a flat world-volume, only the cosmological constant term, denoted by W_B , will be non-vanishing in this sector, as all terms involving the brane curvature vanish. In addition, the brane supports the SM fields. In this work, we wish to study the interplay between the self-tuning mechanism and the stabilisation of the electroweak hierarchy, and hence we leave the Higgs sector explicit. The rest of the SM fields are present but do not play a role in our arguments. Therefore, for our study, the relevant terms of the brane action are given by

$$S_{brane} = M_p^3 \int d^4x \sqrt{-\gamma} \left[-W_B(\varphi, a) - Z_H(\varphi, a) |\partial_\mu H|^2 - X_H(\varphi, a) |H|^2 - S_H(\varphi, a) |H|^4 \right], \quad (1.4)$$

where $\gamma_{\mu\nu}$ is the induced metric on the brane, W_B is the cosmological constant term (mentioned above) and H is the Higgs doublet of the SM (in units of M_p). The quantities X_H and S_H correspond to the Higgs mass-squared and the Higgs quartic coupling, respectively and everything is a function of the two bulk scalars φ, a . All the bulk scalars are dimensionless but the Higgs has dimensions of mass. Therefore W_B, X_H^{-1} have dimensions of mass, while Z_H, S_H have dimensions of $(\text{mass})^{-3}$.

The precise functional form of the dependence on φ, a is in principle calculable from a UV completion of the model. This has been discussed in [10], and this UV

completion via bifundamental messenger fields determines the couplings between bulk fields to brane operators. SM model quantum corrections then generate a localized action for the bulk fields, which in this case corresponds to W_B as well as quantum corrections to the functions Z_H , X_H and S_H .

Calculating these is beyond the scope of the analysis in this work. Instead, here we shall make educated guesses for these functions based on results from string compactifications.⁹ Independent of the UV completion, we can make a few observations regarding the brane potentials. In particular, if the theory on the brane has a UV cutoff given by the energy scale Λ , then we shall expect quantum corrections due to fields on the brane to make the brane potentials UV sensitive to the UV cutoff as follows:¹⁰

$$W_B \sim \frac{\Lambda^4}{M_p^3}, \quad X_H \sim \frac{\Lambda^2}{M_p^3}, \quad Z_H, S_H \sim \frac{\log \Lambda^2}{M_p^3} \quad (1.5)$$

The goal of this construction is to realise the self-tuning of the cosmological constant, while at the same time stabilising the electroweak hierarchy. In the context of this class of models, this implies the following:

1. **Self-tuning:** Self-tuning is realised successfully as long as our bulk-brane system exhibits a solution with a flat brane. Therefore by construction, the brane is flat, despite the presence of a non-vanishing cosmological constant W_B and contributions from the Higgs sector, which can be of the order of the cutoff-scale. This is the essence of the self-tuning mechanism.
2. **Stable electroweak hierarchy:** Given a solution of the brane-bulk system, we can calculate the corresponding Higgs mass on the brane, which (in both vacua with intact and broken electroweak symmetry) is given by

$$m_h^2 \sim M_p^3 |X_H(\varphi_0, a_0)|. \quad (1.6)$$

Here we define the Higgs mass to be low if it is small compared to the cutoff scale on the brane i.e.

$$\frac{m_h^2}{\Lambda^2} \ll 1. \quad (1.7)$$

⁹An explicit dependence of at least one of the brane potentials W_B , X_H , S_H on a would correspond to a breaking of the axionic shift symmetry $a \rightarrow a + \text{const}$. While we exclude such a breaking in the bulk sector, here we permit this breaking as long as it only occurs in the brane sector of the theory. The reason is that as with the QCD axion, brane non-perturbative effects (that are not suppressed exponentially in N will generically generate a potential for the axion on the brane.

¹⁰In the UV completion of this model along the lines of [10] the scale Λ is identified with the ‘messenger scale’.

However, note that from (1.5) and (1.6) it follows that for a generic self-tuning vacuum, the condition (1.7) is not automatically satisfied. A large electroweak hierarchy is only generated if in the self-tuning vacuum we also have that

$$M_p^3 |X_H(\varphi_0, a_0)| \ll \Lambda^2. \quad (1.8)$$

Not every solution will exhibit this property, and hence, in contrast to self-tuning of the cosmological constant, a large electroweak hierarchy is not a priori guaranteed. However, as we explain in more detail below, the setup described here typically exhibits a large number of vacua satisfying (1.8) and hence a small Higgs mass (in addition to a large number of vacua with no significant hierarchy). The key to this is the presence of the bulk axion, and a holographic interpretation of the bulk solutions, as we now explain.

An important property of the type of brane-world model considered here is that the bulk geometry permits an interpretation in terms of holographic RG flow solutions, i.e. the 5-dimensional bulk solutions are dual to the RG flow of a particular 4-dimensional gauge theory. The relevance of this for successful self-tuning has been thoroughly explored in [7] and hence we refer readers to this work for details.

Here we focus on what is new compared to the setups considered in [7] which is the existence of a non-trivial flow for a bulk axion and the Higgs dynamics. According to the standard holographic dictionary, the bulk axion a is dual to the instanton density operator of the dual gauge theory. The coupling to this operator is known as the θ -angle, whose RG running is then encoded in the bulk solution of the axion a . Part of the definition of the dual gauge theory (and thus our brane-world model) is the value of the θ -angle at the UV fixed point of the RG flow, denoted by θ_{UV} . This is a parameter we are free to choose and which is part of the definition of the model. In the dual geometry, a choice of θ_{UV} is equivalent to a choice of the value a_\star of the bulk axion on the UV boundary of the geometry (here reached for $u \rightarrow -\infty$, i.e.

$$a(u) \underset{u \rightarrow -\infty}{=} a_\star + \mathcal{O}(e^{4u/\ell}), \quad (1.9)$$

where the ellipsis denotes subleading terms. The precise map between a_\star and θ_{UV} , however, is many-to-one and given by [26]:

$$a_\star = c \frac{\theta_{UV} + 2\pi k}{N_c}. \quad (1.10)$$

Here, N_c specifies the number of colors of the dual gauge theory and c is a dimensionless constant whose value is determined by the precise implementation of the gauge-gravity correspondence. Most importantly, k is an integer parametrizing different branches which exhibit the same value of θ_{UV} , but different values of a_\star .

Thus, a model with a definite value of θ_{UV} will in fact correspond to a family of brane-worlds with different values of a_\star related to θ_{UV} via (1.10). For every value of

a_\star we shall obtain a different solution $a(u)$ for the axion flow, which will backreact differently on the geometry. Solutions for different values of a_\star will generically exhibit different values for the equilibrium position u_0 of the brane, and hence different φ_0, a_0 . A model with a unique value θ_{UV} hence gives rise to a set of vacua (labelled by k), all with different values of φ_0, a_0 . As the Higgs mass depends on φ_0, a_0 through X_H as in (1.6), the various vacua will typically exhibit different values of the Higgs mass.

We should stress that as we work in a bottom-up setup, it is important to accommodate the constraints on axion actions as arising from string theory and further encapsulated in the form of swampland conjectures on theories with axions, [29, 30, 31, 32, 33]. They boil down to a constraint on the axion decay constant being sub-Planckian as well as having excursions in axion field space that are also sub-Planckian. However, in our setup the axion decay constant is field dependent and care is needed to assess the proper constraints. We will discuss them in detail in section 2.1, following [24].

To determine whether a particular model permits vacua with a large electroweak hierarchy one can proceed as follows. One can treat a_\star as a free parameter and map the space of solutions for the equilibrium position of the brane u_0 as a function of a_\star . For every such equilibrium position one then records the values of φ_0, a_0 , which then allows to calculate X_H . In this way one can extract X_H as a function of a_\star .

A key point in the space of solutions is the value of a_\star (we denote it henceforth by $a_{\star,0}$) that leads to a vanishing effective Higgs mass, $X_H(a_{\star,0}) = 0$. If this happens, then we expect that around this value and in the regime in which $X_H < 0$, we will have electroweak symmetry breaking with a small Higgs mass. Then, for any value of θ_{UV} , as long as there exist branches that satisfy¹¹

$$c \frac{\theta_{UV} + 2\pi k}{N_c} \approx a_{\star,0} \tag{1.11}$$

these correspond to vacua with a low Higgs mass. Moreover, the steps with which the Higgs mass changes for these vacua is set by $1/N_c$. For large N_c (as is assumed here) there will typically be many such solutions. It follows that a zero in $X_H(a_\star)$ is a sufficient condition for the existence of vacua with a low Higgs mass in our setup, i.e. such vacua are guaranteed to exist if X_H as a function of a_\star exhibits at least one zero.

The goal of this work is then to check for the existence of such self-tuning vacua with large electroweak hierarchy, in models with several broadly generic choices for the brane potentials W_B, X_H and S_H . In practice this is done by scanning the space of solutions as a function of a_\star and identifying zeros of X_H at the brane locus for specific values of a_\star as explained above. If the backreaction of the axion flow on the

¹¹ c is an $\mathcal{O}(1)$ number that depends on the particular duality pair. It can be computed only in string theory dual pairs. For N=4 sYM, $c = \frac{1}{2\pi}$.

geometry is sufficiently weak, this can be analysed partly analytically (sec. 5), but otherwise we turn to numerical methods (sec. 6).

In situations where the axion backreaction on the bulk geometry is sufficiently “small”, we can employ a probe approximation to assess how the presence of the axion affects a given self-tuning solution obtained without axion running. In this framework the modifications due to the axion can be calculated analytically and we display the analysis and the resulting formulae in sec. 5. The effect of the axion in this case is to slightly shift the brane equilibrium position leading to ‘small’ changes in the quantities governing the physics of the brane.

For finite values of the axion data, we consider the following four distinct classes of models:

- **Case 1:** The brane potential W_B , X_H and S_H are functions of φ only, and do not depend explicitly on a . See sec. 6.1.
- **Case 2:** All brane potentials depend on φ but in addition the brane potential X_H (the Higgs-mass-squared) is taken to also depend linearly on a . See sec. 6.2.
- **Case 3:** All brane potentials depend on φ but in addition the brane cosmological constant W_B has a periodic dependence on a . See sec. 6.3.
- **Case 4:** All brane potentials depend on φ , X_H also depends linearly on a and W_B also has a periodic dependence on a , i.e. a combination of cases 2 and 3. See sec. 6.4.

Our results can be summarised as follows:

- In all four cases examined, we find that the existence of a bulk axion does not destabilize or inhibit the holographic self-tuning mechanism for the cosmological constant. That is, for generic brane potentials, there typically exists at least one equilibrium position for the brane, as in the case without the axion field.
- In cases 2 and 4, i.e. models where the Higgs-mass-squared parameter X_H depends on the bulk axion field a explicitly, we find that (for generic model parameters) X_H as a function of a_* generically crosses zero and hence solutions with a small Higgs mass generically exist in these models.
- In contrast, in cases 1 and 3, i.e. models where the Higgs-mass-squared parameter X_H does not depend on the bulk axion field a , this is not generically the case. Then, a zero of X_H as a function of a_* only occurs when the model parameters are chosen carefully and hence these models require a certain level of tuning to exhibit a significant electroweak hierarchy. Such a choice of parameters for case 1 is presented in sec. 6.1.

In conclusion we find that for several classes of brane data, the mechanism for the stabilisation of the electroweak hierarchy is viable and can appear in tandem with the self-tuning of the brane cosmological constant. This positive conclusion is however a first step towards obtaining a feasible and detailed model of the mechanism as we expand upon in the next subsection.

1.2 Open questions and future work

There are several open issues and future directions of our work:

- The analysis in this work constitutes a proof of principle that the self-tuning of the cosmological constant and a stable electroweak hierarchy can be achieved together in brane-world models based on axionic holographic RG flows. What we have not attempted is to propose a model that is quantitatively consistent with all current observations, e.g. a model that reproduces the correct numerical value for the electroweak scale, which is therefore left for future work. One of the important constraints on such a model is that the function W_B , as well as the corrections to the other brane functions, should come from known SM corrections, in which the effective SM parameters are functions of the bulk fields along the lines described in [35, 36].
- For our construction to be applicable to the existing universe, the interactions mediated by these fluctuations should reproduce four-dimensional Einstein gravity on the brane, at least over observable scales. It was observed that there exist two sets of propagating modes, with one corresponding to a spin-two mode associated to the 5d graviton realising a DGP-like scenario [12]. Interestingly, both at short and long distances the graviton propagation is four-dimensional with the graviton exhibiting a mass. A five-dimensional phase may exist at intermediate distances if parameters are chosen accordingly. One of the main goals for future work is to construct an explicit model in which self-tuning is effective and at the same time four-dimensional gravitational physics is reproduced at the observed scales.
- An important question concerns the stability of the brane equilibrium position, and under what circumstances fluctuations about an equilibrium position are neither tachyonic nor ghost-like. A key quantity controlling the gravitational coupling and the graviton mass is the induced Einstein term on the brane. For the holographic brane-world model of [7] including a bulk dilaton, but without a bulk axion or brane Higgs field, such an analysis of fluctuations has been performed in that work. Overall, it was observed that parametric regimes exist where all fluctuation modes are non-tachyonic and not ghost-like. More specifically, in [7] it was shown that if certain inequalities are obeyed by the various potentials evaluated at the brane, then stability is guaranteed.

It is plausible that the key aspects of the analysis of [7] may carry over to setup including a bulk axion, whose presence will alter the aforementioned inequalities but not the general picture, as long as the bulk theory satisfies some positive energy conditions, e.g. the NEC (which we always assume to be the case).

The picture changes qualitatively, however, when we include the brane-localized Higgs field. Even if we ensure that the latter has a positive kinetic term and a positive mass (in the EW-breaking vacuum) on the brane, bulk-brane mixing may result in the presence of an additional ghost or tachyon. In particular, a healthy brane Higgs can become ghost-like or tachyonic by linear mixing with the infinite tower of bulk KK modes in the scalar sector. This question is addressed in Appendix E of this work. There, we study the Higgs-bulk mixing in a general model, and we formulate the conditions under which the effective four-dimensional Higgs field stays healthy after diagonalizing the kinetic and mass matrices. Again these constraints take the form of inequalities, which this time involve sums or integrals over the tower of KK modes. In order to have a definite answer, one should evaluate these constraints on a specific model, which is beyond the scope of the present work. Nevertheless, we estimate the correction to the Higgs mass and kinetic term in simplified settings (two toy-models with a discrete and a continuous KK spectrum, respectively) and we find that, in each case, the effect is generically suppressed by powers of the four-dimensional Planck scale and/or the DGP-like transition length r_c . This suggests that generically, in reasonable models, the mixing of the Higgs with the KK tower does not lead to new instabilities (although a definite answer can only be provided by an explicit computation in a specific model).

- As discussed above, the phenomenology of our construction is highly sensitive to the dependence of the brane potentials W_B , X_H , S_H on the bulk scalars φ and a . For example, the existence of vacua with a small Higgs mass is favoured if X_H depends on a explicitly. Here we considered several simple functional forms for the brane potentials, but ideally this should be computed from a UV completion of our construction. More detailed knowledge regarding the functional form of W_B , X_H , S_H would also help determine whether a large electroweak hierarchy is generic in our construction or whether it only occurs in certain corners of parameter space (i.e. how much tuning is needed).
- Even if a model exhibits a multitude of vacua with ‘small’ Higgs mass, there typically also exist vacua where the Higgs mass is not small. For our brane-world scenario to reproduce the observed universe, we hence need to specify a dynamical mechanism that preferably populates (at late times) the vacua with small Higgs mass over those with no significant hierarchy.

Therefore, the next important question is how the vacuum realizing the light Higgs mass is selected in our world. If the vacuum with a small Higgs mass minimizes the free energy of the total system, then the system evolves to this state after a sufficiently long time. In the absence of the brane, it is well known that the minimum free energy occurs for minimal values of $k = 0, 1$, [26]. However, the brane contributes to the free energy and the minimization problem becomes complex, especially as it is affected by the scalar-dependent functions on the brane.

- On the other hand, if the vacuum with a small Higgs mass does not minimize the free energy of the total system, this state could be realized as a metastable vacuum. Transitions to and from this state and rates are important in assessing the viability of this option, [26, 37].

- We are therefore led to study the real time evolution of the bulk solutions as well as the brane along the lines studied in [38, 19]. In our case, we have two effects that can happen in tandem. The first is a semiclassical tunneling that interpolates between different k -bulk solutions. Moreover, we also have the brane motion in a single bulk solution which will also be affected by the axion.

One of the relevant dynamical questions concerns the bulk motion of the brane that will generate the associated cosmology. This was studied in the absence of the axion in [38, 19], in the probe approximation where this is solvable. What was found is that the setup corresponds to a brane moving in the radial bulk potential whose minimum (or minima) are at the places where the brane is flat and the brane cosmological constant cosmologically invisible. If the brane starts in a different bulk position it will move generating a non-trivial brane cosmology. This motion is affected, beyond the initial velocity and potential, by the presence of matter densities on the brane and brane-bulk energy exchange, [39, 40].

In the presence of a bulk axion we expect a similar behavior, but now the brane motions will also be affected by the axion. It is important to find how the system may evolve to the metastable vacuum by studying the associated cosmology. At the same time, the lifetime of this vacuum should be long enough. An alternative possibility is to rely on anthropic arguments for the Higgs mass [41, 42, 43, 44, 45].

- Our setup described in this paper has several similarities to the standard relaxion scenario [28]. These are discussed in our concluding section 7.

2. The bulk theory and its dual QFT

As a bulk theory, we consider an Einstein-axion-dilaton theory in a 5-dimensional

bulk space-time, parameterized by coordinates $x^a \equiv (u, x^\mu)$ where u is the holographic coordinate. In the Einstein frame, the most general two-derivative action compatible with the axion shift symmetry is

$$S_{bulk} = M_p^3 \int d^5x \sqrt{-g} \left[R - \frac{1}{2} g^{ab} \partial_a \varphi \partial_b \varphi - \frac{1}{2} Y(\varphi) g^{ab} \partial_a a \partial_b a - V(\varphi) \right] + S_{GHY}, \quad (2.1)$$

where M_p is the bulk Planck scale, g_{ab} is the bulk metric, R is its associated Ricci scalar, φ is the bulk scalar field, and a is the bulk axion field. $V(\varphi)$ is a bulk scalar potential, and $Y(\varphi)$ is a function controlling the axionic kinetic term. S_{GHY} is the Gibbons-Hawking-York term at the space-time boundary (e.g. the UV boundary if the bulk is asymptotically AdS).

The bulk field equations are given by:

$$R_{ab} - \frac{1}{2} g_{ab} R = \frac{1}{2} \partial_a \varphi \partial_b \varphi + \frac{Y}{2} \partial_a a \partial_b a - \frac{1}{2} g_{ab} \left(\frac{1}{2} (\partial \varphi)^2 + \frac{Y}{2} (\partial a)^2 + V \right), \quad (2.2)$$

$$\partial_a (\sqrt{-g} g^{ab} \partial_b \varphi) - \frac{\partial V}{\partial \varphi} - \frac{Y}{2} (\partial a)^2 = 0 \quad , \quad \partial_a (\sqrt{-g} Y g^{ab} \partial_b a) = 0. \quad (2.3)$$

We shall consider holographic RG flow geometries, which display 4-dimensional Poincaré invariance and correspond therefore to vacuum states of the dual QFT. In the domain-wall (or Fefferman-Graham) gauge, the metric and scalar field are:

$$ds^2 = du^2 + e^{2A(u)} \eta_{\mu\nu} dx^\mu dx^\nu, \quad \varphi = \varphi(u), \quad a = a(u). \quad (2.4)$$

We take the coordinate u to increase towards the IR region. In this paper, we consider solutions which have an asymptotic AdS-like boundary for $u = -\infty \equiv u_{UV}$. The bulk theory is dual to a field theory with a UV conformal fixed point, deformed by a relevant operator dual to the dilaton and, generically, a θ -angle which is dual to the axion. One important aspect of our analysis concerns the boundary conditions one should impose in the interior of the bulk geometry. There the metric scale factor generically vanishes at some coordinate value u_{IR} (corresponding to the deep IR on the field theory side), which may be finite or infinite.

With (2.4), the bulk equations of motion (2.2, 2.3) become

$$6\ddot{A} + \dot{\varphi}^2 + Y\dot{a}^2 = 0, \quad (2.5)$$

$$12\dot{A}^2 - \frac{\dot{\varphi}^2}{2} - \frac{Y\dot{a}^2}{2} + V = 0, \quad (2.6)$$

$$\ddot{\varphi} + 4\dot{A}\dot{\varphi} - V' - \frac{Y'}{2}\dot{a}^2 = 0, \quad (2.7)$$

$$\partial_u (Y e^{4A} \dot{a}) = 0, \quad (2.8)$$

where a dot stands for a u -derivative while a prime stands for a φ -derivative. Equation (2.8) can be solved as

$$\dot{a} = \frac{Q}{Y e^{4A}} \quad (2.9)$$

with Q an integration constant. By substituting (2.9) into (2.5, 2.6, 2.7), the remaining bulk equations become

$$6\ddot{A} + \dot{\varphi}^2 + \frac{Q^2}{Y e^{8A}} = 0, \quad (2.10)$$

$$12\dot{A}^2 - \frac{\dot{\varphi}^2}{2} - \frac{Q^2}{2Y e^{8A}} + V(\varphi) = 0, \quad (2.11)$$

$$\ddot{\varphi} + 4\dot{A}\dot{\varphi} - V' - \frac{Y'Q^2}{Y^2 e^{8A}} = 0. \quad (2.12)$$

2.1 Constraints on the effective gravitational action

The effective actions we use involve arbitrary functions of the scalar field φ . However, string theory puts constraints on such functions. Especially for solutions in which scalars run towards the end of the moduli space, it is well known that they produce bulk metrics that are (mildly singular). This is an effect that has been observed in the dimensional reduction of many well known solutions in string theory, (deformations of the AdS/CFT correspondence), [13]. It was observed that such singularities were artifacts of the dimensional reduction, and once the solutions were lifted to the higher dimensions, the solutions were regular.

Gubser introduced constraints on the lower-dimensional gravitational theory that imply that the higher-dimensional theories are regular, [50]. Such constraints are conjectures in the general case, but they have been tested in many holographic examples, and it is known that all holographic observables are finite despite the mild bulk singularities.¹² For example, for a scalar potential that at large values of the scalar behaves as

$$V \sim e^{b\varphi} \quad (2.13)$$

the Gubser criterion becomes

$$b \leq \sqrt{\frac{2d}{d-1}}, \quad (2.14)$$

where d is the dimension of the AdS boundary. Eq. (2.14) does not allow arbitrarily steep potentials in the regime of large φ .

The Gubser constraints were refined in [49, 51, 61], where the notion of a repulsive singularity was introduced. As in general the mild singularity is resolved by the inclusion of the (missing) KK states, we have two possibilities.

1. The correlator in the lower dimension depends on the details of the singularity resolution.

¹²Our use of the word ‘‘mild singularity’’ translates into one that satisfies the Gubser criteria.

2. The correlator in the lower dimension *does not* depend on the details of the singularity resolution.

In theories that we are in case 2 above, we call the singularity *repulsive*. Low energy observables in such cases can be computed reliably without resolving the singularity. The precise criteria to have a repulsive singularity were derived in [49, 51, 61] and for the example of a single scalar sharpen the Gubser bound in (2.14) to

$$b \leq \sqrt{\frac{2(d+2)}{3(d-1)}}. \quad (2.15)$$

Therefore, theories that satisfy (2.15) have a well-defined holographic description and well-defined and finite correlation functions. Moreover, the precise holographic dictionary, boundary conditions and holographic renormalization have been rigorously specified in [57] for generic scalars and in [58] for the case of the Einstein-dilaton axion system we use in this paper. The scaling symmetries that appear when the dilaton runs to infinity were also interpreted in terms of the scaling symmetries of the higher-dimensional theories, [62].

The addition of the axion pseudoscalar raises additional issues. It does not have a potential, but is constrained by the axion swampland conjectures, [29, 30, 31, 32, 33]. They state that in cases where the axion kinetic term is constant, its scale f_a^2 must be at most as large as the Planck scale, $f \leq M_P$. Also the field excursion of the axion must be (in Planck units as we use in this paper) smaller than one. However, upon dimensional reductions these conditions are modified. First, the axion kinetic term becomes field dependent, as is the case we consider here. Moreover, for large φ the kinetic term coefficient, $Y(\varphi)$ behaves as

$$Y(\phi) \sim e^{\gamma\varphi} \quad , \quad \gamma \geq \gamma_{min} \equiv \frac{2d}{(d-1)b} - b \geq 0, \quad (2.16)$$

with γ positive and this behavior seems to violate our constraints.

To convert our conditions on constraints on field dependent couplings we can dimensionally reduce the RR forms and metric on a N -dimensional sphere to $d+1$ dimensions. In that case the scale factor of the sphere acquires a potential as in (2.13) with

$$b = \sqrt{\frac{2(d+N-1)}{N(d-1)}}, \quad (2.17)$$

which is confining, [62]. When $N=1$ one obtains a potential at the Gubser bound, (2.14), while the limit $N \rightarrow \infty$ gives a potential at the border of losing confinement, [62, 49]. The repulsive constraint in (2.15) translates to $N \geq 3$.

The lower-dimensional axion acquires a kinetic function $Y(\varphi)$ as in (2.16) with

$$\gamma = \sqrt{\frac{2N(d-1)}{d+N-1}} = \frac{2}{b}, \quad (2.18)$$

which automatically satisfies the inequality (2.16) if $d > 1$. The runaway $\varphi \rightarrow \infty$ solutions corresponds in $d + N$ dimensions to the volume of the N-sphere shrinking to zero, but without a curvature singularity.

Therefore, the constraint $f_a \leq M_p$ in the higher dimension translates to b satisfying the Gubser bound in the lower dimension and¹³

$$\gamma \leq \frac{2}{b}. \quad (2.19)$$

We impose this inequality in all our models later on in section 6 and in particular in equation (6.3).

We now proceed to the second constraint on the axion, namely that its field range in Planck units should be sub-Planckian. This implies that the variation of the axion, as it is normalized here should be smaller than one. As shown in [24] the axion starts as $a = a_{UV}$ in the AdS boundary and then varies monotonically down to zero, as it evolves towards the IR end of the geometry. This implies that the constraint translates to

$$a_{UV} \lesssim 1. \quad (2.20)$$

It has been shown in [24] that the possible values of a_{UV} that lead to a regular bulk solutions is restricted to the interval

$$|a_{UV}| \leq a_{UV}^{max}, \quad (2.21)$$

with the upper bound a_{UV}^{max} being constrained by the detailed effective action and in particular, by the bulk dilaton potential $V(\varphi)$ and the axion kinetic term $Y(\varphi)$. The bound derived analytically in [24] is

$$a_{UV}^{max} \leq \int_{\phi_{UV}}^{\infty} \frac{d\varphi}{\sqrt{Y(\varphi)}}, \quad (2.22)$$

where ϕ_{UV} is the value of the dilaton at the AdS boundary. For potentials that in the IR behave as in (2.16) the bound is determined essentially by the value of γ . Moreover, in many examples analyzed numerically, we found that a_{UV}^{max} is below the bound implied by (2.22), a fact that suggests that the bound in (2.22) can be improved. In the cases we numerically analyse later on in this paper $a_{UV}^{max} < 1$ and therefore in agreement with the axion swampland bounds.

Finally, the presence of a_{UV}^{max} , implies that the number n of distinct saddle points, labelled by integers, is finite and of order $\mathcal{O}(N_c)$

$$n = \left\lfloor \frac{N_c a_{UV}^{max}}{2\pi} \right\rfloor, \quad (2.23)$$

where where $\lfloor z \rfloor$ is the maximum integer smaller than or equal to the real number z .

¹³This is in fact a sufficient condition. In the higher dimension, the RR kinetic terms are further suppressed compared to the NS-NS kinetic terms with an extra factor of g_s^2 . Via the holographic duality, this extra factor is matching the fact that the θ^2 correction to the vacuum energy in the gauge theory is suppressed by a factor of N_c^2 compared to the leading term, [26, 63].

2.2 The first order formalism

Following [24], we introduce three scalar functions of the bulk field φ , which we denote by $W(\varphi)$, $S(\varphi)$ and $T(\varphi)$. In terms of these scalar functions, the bulk equations of motion (2.10)–(2.12) reduce to the system of first order differential equations, as we shall show explicitly below.

The functions $W(\varphi)$, $S(\varphi)$ and $T(\varphi)$ are defined as

$$\dot{A} \equiv -\frac{W(\varphi)}{6}, \quad (2.24)$$

$$\dot{\varphi} \equiv S(\varphi), \quad (2.25)$$

$$T(\varphi) \equiv \frac{Q^2}{e^{8A}}. \quad (2.26)$$

We immediately observe that $T \geq 0$ as $e^{4A} \geq 0$ by definition.

Using these definitions, it can be shown that the bulk equations of motion (2.10)–(2.12) can be written as the following set of first order differential equations in the φ variable:

$$S^2 - W'S + \frac{T}{Y} = 0, \quad (2.27)$$

$$\frac{T'}{T} = \frac{4}{3} \frac{W}{S}, \quad (2.28)$$

$$\frac{W^2}{3} - \frac{S^2}{2} - \frac{T}{2Y} + V = 0. \quad (2.29)$$

The u -derivative of the axion field is given by

$$\dot{a} = \text{sign}(Q) \frac{\sqrt{T}}{Y}, \quad (2.30)$$

from (2.9). Note that, as $Y \geq 0$ and $T \geq 0$, the sign of Q determines the monotonicity properties of the axion evolution, which do not change along the flow.

The two equations in (2.27), (2.28) are first order differential equations while the equation in (2.29) is algebraic. Therefore, the solutions for W , S and T will depend on two integration constants. One of them can be taken to be Q , which then enters in the axion flow equation (2.9). The second one will be denoted by C_{UV} , and can be shown to be related to the vev of the operator dual to φ . Then, solving for a , A and φ by integrating (2.30), (2.24) and (2.25) will introduce three further integration constants. However, the integration constant associated with A , just redefines the constant Q , and is hence not a physical parameter. Equivalently, it can be chosen so that the boundary metric has unit normalization, thus fixing the unit of measuring scales and other parameters such as Q .

We can compute asymptotic expressions for W , S , T and hence a , A , φ analytically both in the UV (near-boundary) and the IR region. Here we summarize the most important results. The reader can find the full analysis in [24].

Consider a maximum of the scalar potential $V(\varphi)$, which we can always locate at $\varphi(u_{UV}) = 0$ by a shift in φ . As expected, a maximum of V will be associated with a UV fixed point of a holographic RG flow. In the vicinity of that maximum, the bulk functions $V(\varphi)$, $Y(\varphi)$ can be expanded in a regular power series in φ ,¹⁴

$$V = -\frac{12}{\ell^2} - \frac{1}{2} \frac{m^2}{\ell^2} \varphi^2 + \mathcal{O}(\varphi^3), \quad Y = Y_0 + Y_1 \varphi + \mathcal{O}(\varphi^2), \quad (2.31)$$

and we define

$$\Delta_{\pm} \equiv 2 \pm \sqrt{4 - m^2 \ell^2}. \quad (2.32)$$

For a maximum, $m^2 > 0$, $2 < \Delta_+ < 4$ and $0 < \Delta_- < 2$. The length scale ℓ is defined via (2.31) as

$$\ell^2 = -\frac{12}{V(0)}. \quad (2.33)$$

It can be shown to correspond to the radius of the AdS space-time which the bulk space-time asymptotes to when approaching the boundary. The functions $W(\varphi)$, $S(\varphi)$ and $T(\varphi)$ can also be expanded in a series for small φ , but this type of series turns out to be a trans-series that contains also non-analytic powers.

The expansions for W, S, T for small φ can be found using similar techniques as in [46], [47]. The leading terms in this expansion are universal. As in the standard case of purely dilatonic flows, there are two branches for the solutions for W, S, T depending on the coefficient of the leading φ^2 term in W , given either by $\frac{\Delta_+}{2}$ (plus-branch) or $\frac{\Delta_-}{2}$ (minus-branch) [46]. In the following, we focus on the minus branch solution, which will be relevant for our later applications.

The UV expansions for W, S and T on the minus-branch will contain two integration constants denoted by C_{UV} and q_{UV} . The first is related to the vev of the QFT operator dual to the dilaton φ . The constant q_{UV} determines the vev of the QFT operator dual to the axion and is related to Q introduced in (2.9). The precise relation will be given later, in (2.52). Collecting the universal terms and the leading terms containing C_{UV} and q_{UV} the near-UV expansions of W, S and T on the minus branch are given by:

$$W_-(\varphi) = \frac{6}{\ell} + \frac{\Delta_-}{2\ell} \varphi^2 + \dots + C_{UV} |\varphi|^{\frac{4}{\Delta_-}} + \dots + \frac{q_{UV}}{8Y_0} |\varphi|^{\frac{8}{\Delta_-}} + \dots, \quad (2.34)$$

$$S_-(\varphi) = \frac{\Delta_-}{\ell} \varphi + \dots + \frac{4C_{UV}}{\Delta_-} |\varphi|^{\frac{\Delta_+}{\Delta_-}} + \dots + \frac{q_{UV} Y_1}{2Y_0^2 (4 + \Delta_-)} |\varphi|^{\frac{8}{\Delta_-}} + \dots \quad (2.35)$$

$$T_-(\varphi) = q_{UV} |\varphi|^{\frac{8}{\Delta_-}} \left[1 + \dots - \frac{32C_{UV}}{(\Delta_+ - \Delta_-)\Delta_-^2} |\varphi|^{\frac{\Delta_+ - \Delta_-}{\Delta_-}} + \dots \right]. \quad (2.36)$$

Further details regarding the UV expansion can be found in section 4.1 and appendix A of [24].

¹⁴This is the case in all known supergravity examples that are low energy limits of string theories.

Next, we discuss the asymptotic behavior of the solutions to (2.27)–(2.29) in the deep IR region. In [24], the regularity of general axionic flows was studied. If the flow ends at a finite end-point, φ_{end} , then regularity requires that $Y(\varphi)$ diverges at φ_{end} . This is not permissible in string theory, though. Therefore, regular axionic flows exist only when φ runs to the boundaries of its space,¹⁵ i.e. as $\varphi \rightarrow \pm\infty$. One may expect that a ‘mild-enough’ singularity in this regime can be resolved by KK or stringy states as advocated by Gubser, [50].

In the following, we choose the IR to be reached for $\varphi \rightarrow +\infty$. Then, motivated by top-down results from string theory, we assume that for large dilaton-values V and Y can be approximated by exponentials in φ , i.e.

$$V \simeq -\frac{V_\infty}{\ell^2} e^{b\varphi} \quad , \quad Y \simeq Y_\infty e^{\gamma\varphi} \quad , \quad (2.37)$$

with V_∞, Y_∞, b and γ constant. The corresponding solutions for W, S, T in this regime are [24]

$$W = W_\infty e^{\frac{b}{2}\varphi} - \frac{D_{IR}}{2} \frac{e^{-(\frac{b}{2} + \gamma - \frac{8}{3b})\varphi}}{\frac{b}{2} + \gamma - \frac{4}{3b}} + \dots \quad , \quad (2.38)$$

$$S = \frac{b}{2} W_\infty e^{\frac{b}{2}\varphi} - \frac{D_{IR}}{2} \frac{\frac{b}{2} + \gamma}{\frac{b}{2} + \gamma - \frac{4}{3b}} e^{-(\frac{b}{2} + \gamma - \frac{8}{3b})\varphi} + \dots \quad , \quad (2.39)$$

$$T = \frac{b}{2} D_{IR} W_\infty Y_\infty e^{\frac{8}{3b}\varphi} + \dots \quad , \quad (2.40)$$

with

$$W_\infty = \sqrt{\frac{8V_\infty}{\frac{8}{3} - b^2}} \quad , \quad (2.41)$$

and D_{IR} an integration constant which is related to q_{UV} as

$$\frac{q_{UV}}{D_{IR}} = \lim_{\varphi(u_{UV}) \rightarrow 0, \varphi(u_{IR}) \rightarrow \infty} \frac{\frac{b}{2} W_\infty Y_\infty e^{\frac{8}{3b}\varphi(u_{IR})}}{|\varphi(u_{UV})|^{8/\Delta_-} \exp\left(\frac{4}{3} \int_{\varphi(u_{UV})}^{\varphi(u_{IR})} d\varphi \frac{W}{S}\right)} \quad . \quad (2.42)$$

If the asymptotic form of V satisfies the Gubser bound, [50, 51], which here corresponds to

$$b \leq \sqrt{\frac{8}{3}} \quad , \quad (2.43)$$

then the solutions, although singular, are expected to have a resolvable singularity. We also require

$$\gamma \geq \frac{8}{3b} - b = \frac{8 - 3b^2}{3b} \quad , \quad (2.44)$$

¹⁵This is the behavior in top-down holographic theories like the Witten realization of QCD once it is dimensionally reduced to 5 dimensions, [48]. It is also the behavior in Improved Holographic QCD (IHQCD), [49], a bottom-up holographic theory constructed to emulate the dynamics of YM in four dimensions. Moreover, it is also the behavior in V-QCD, [27], which emulates the dynamics of QCD in the Veneziano limit.

for the validity of the expansion. Note that the backreaction due to the axion flow on W and S enters only at subleading order in the IR. There exists another solution in which the axion field backreacts at the leading order. However, as discussed in [24], this solution does not have a holographic interpretation, and therefore we discard it. The reader can find all the details of the IR expansion in section 4.2 and appendix B of [24].

Last, we review the holographic interpretation of the various integration constants appearing in the solutions. As was argued below equation (2.30), the physical system in question is characterized by four physical integration constants. As we shall describe below, these correspond to two pairs of the form (source, vev) for the operators dual to the dilaton and axion fields, respectively.

The axion bulk profile is characterized by the two coefficients a_\star and Q , which enter as the integration constants of the second order axion equation of motion and control the leading and subleading terms in the near-boundary expansion,

$$a(u) = a_\star + Q \frac{\ell}{4Y_0} e^{4u/\ell} + \dots \quad u \rightarrow -\infty, \quad (2.45)$$

In the holographic dictionary, a_\star is related to the value of the θ -term in the UV field theory (modulo 2π shifts) and Q is proportional to the vacuum expectation value of the corresponding topological density operator $O_a(x)$. More precisely, the relation between the source a_\star and the UV θ -angle θ_{UV} in the dual QFT is

$$a_\star = c \frac{\theta_{UV} + 2\pi k}{N_c} \quad (2.46)$$

where N_c is the number of the color in the dual QFT, $\theta_{UV} \in [0, 2\pi)$, $k \in \mathbb{Z}$ and c a dimensionless number of $\mathcal{O}(N_c^0)$. In instances where the dual geometry including the compact internal manifold is known, the parameter c can in principle be computed. For example, in the conventional IIB normalization of the RR axion, $c = 1$. The expectation value of the operator O_a , dual to the axion is

$$\langle O_a \rangle = Q \frac{M_p^3}{N_c}. \quad (2.47)$$

Due to the exact axion shift symmetry of the bulk Lagrangian, of the two parameters a_\star and Q , only Q enters non-trivially in the non-linear equations for the metric and dilaton (2.10)–(2.12). Therefore, seemingly, a_\star remains a free parameter. This, however, would go against the expectation from holography where one does not expect any additional freedom in the interior. Instead, a solution should be completely fixed by the choice of boundary sources plus some universal requirement in the IR. In [24] we therefore proposed such an IR condition in the form of the requirement that the axion field should vanish at the IR endpoint,

$$a(u_{IR}) = 0. \quad (2.48)$$

This axion regularity condition (2.48) leads to a relation between the axion source a_\star to the axion vev Q , and hence no free parameter remains. The condition (2.48) is motivated by top-down string theory constructions, where the axion is a form field component along an internal cycle, which shrinks to zero-size in the IR as in [26]. Single-valuedness then demands that the axion field vanishes at such IR end-points. Combining (2.48) with (2.30), the axion source is expressed as

$$a_\star = \text{sign}(Q) \int_{\varphi(u_{IR})}^{\varphi(u_{UV})} d\varphi \frac{\sqrt{T}}{YS}, \quad (2.49)$$

Similarly, the dilaton bulk profile in the minus branch is characterized by two integration constants φ_- and C , which also control the leading and subleading terms in the near-boundary expansion:

$$\varphi = \varphi_- \ell^{\Delta_-} e^{\Delta_- u/\ell} + 4C_{UV} \frac{(|\varphi_-| \ell^{\Delta_-})^{\frac{\Delta_+}{\Delta_-}}}{(\Delta_+ - \Delta_-)\Delta_-} e^{\Delta_+ u/\ell} + \dots \quad u \rightarrow -\infty, \quad (2.50)$$

where φ_- determines the UV coupling constant of the scalar operator $O(x)$ dual to φ , and C_{UV} is related to its vev. The vev of $O(x)$ is given by

$$\langle O \rangle = C_{UV} (M_p \ell)^3 \frac{4}{\Delta_-} |\varphi_-|^{\frac{\Delta_+}{\Delta_-}}. \quad (2.51)$$

Again, one can show that the IR regularity condition (2.48) leads to a relation between C_{UV} and a_\star . For completeness, we also recall that the integration constants Q and q_{UV} are related as

$$Q^2 = q_{UV} \frac{1}{\ell^2} (\ell |\varphi_-|^{1/\Delta_-})^8. \quad (2.52)$$

For details we once more refer readers to [24].

3. The brane theory and its couplings to the bulk fields

Given the bulk system discussed in the previous section, we now introduce a co-dimension-1 brane at a fixed value $u = u_0$ in the bulk. The world-volume of this brane is taken to model our universe and correspondingly we assume that SM fields are localized on this brane. At the two derivative level, the brane action is

$$S_{brane} = S_g + S_{SM}, \quad (3.1)$$

where

$$S_g = M_p^3 \int d^4x \sqrt{-\gamma} \left[-W_B(\varphi, a) - \frac{1}{2} Z_B(\varphi, a) \gamma^{\mu\nu} \partial_\mu \varphi \partial_\nu \varphi - \frac{1}{2} Y_B(\varphi, a) \gamma^{\mu\nu} \partial_\mu a \partial_\nu a + U_B(\varphi, a) R_B \right], \quad (3.2)$$

and

$$S_{SM} = M_p^3 \int d^4x \sqrt{-\gamma} \left[-T_H(\varphi, a) |\partial_\mu H|^2 - X_H(\varphi, a) |H|^2 - S_H(\varphi, a) |H|^4 + U_H(\varphi, a) R_B |H|^2 + \dots \right]. \quad (3.3)$$

The ellipsis represent omissions corresponding to higher-dimensional terms involving the Higgs field, higher curvature terms as well as higher derivative terms for the other SM fields. Here, $\gamma_{\mu\nu}$ is the induced metric on the brane, which from (2.4) is given by

$$\gamma_{\mu\nu} = e^{2A(u)} \eta_{\mu\nu}, \quad (3.4)$$

and R_B is the corresponding scalar curvature. H is Higgs field of the SM (in units of M_p), and $W_B, Z_B, Y_B, U_B, X_H, S_H, T_H$ and U_H are scalar potentials generated by quantum corrections of the brane-localized fields. In particular, $W_B(\varphi, a)$ is the ‘‘cosmological constant’’ on the brane. From the ansatz (2.4), we can set the kinetic term of the Higgs field to be

$$T_H = M_p^{-1}, \quad (3.5)$$

without loss of generality.¹⁶

The brane separates the bulk into two parts, denoted by ‘‘UV’’ ($u < u_0$, which contains the conformal AdS boundary region or more generally, in non-asymptotically AdS solutions, the region where the volume form becomes infinite) and ‘‘IR’’ ($u > u_0$, which may contain the AdS Poincaré horizon, or a good singularity, or a black hole horizon etc.).

4. Brane-bulk interactions: the Israel matching conditions

We denote the bulk solutions and scalar functions in the UV and IR regions by

$$(A(u), \varphi(u), a(u)) \equiv \begin{cases} (A_{UV}(u), \varphi_{UV}(u), a_{UV}(u)) & \text{for } u < u_0 \\ (A_{IR}(u), \varphi_{IR}(u), a_{IR}(u)) & \text{for } u > u_0 \end{cases}, \quad (4.1)$$

and

$$(W(\varphi(u)), S(\varphi(u)), T(\varphi(u))) \equiv \begin{cases} (W_{UV}(\varphi(u)), S_{UV}(\varphi(u)), T_{UV}(\varphi(u))) & \text{for } u < u_0 \\ (W_{IR}(\varphi(u)), S_{IR}(\varphi(u)), T_{IR}(\varphi(u))) & \text{for } u > u_0 \end{cases}. \quad (4.2)$$

¹⁶With our choice of ansatz in (2.4), φ and a do not depend on x^μ . Therefore, the rescaling of the Higgs field does not generate terms including $\partial_\mu T_H$.

Both sets (W_{UV}, S_{UV}, T_{UV}) and (W_{IR}, S_{IR}, T_{IR}) are solutions to the bulk equations (2.27)–(2.29). The integration constant Q will in principle differ in the UV and IR regions as we have

$$\dot{a} \equiv \begin{cases} \frac{Q_{UV}}{Y e^{4A_{UV}}} = \text{sign}(Q_{UV}) \frac{\sqrt{T_{UV}}}{Y} & \text{for } u < u_0 \\ \frac{Q_{IR}}{Y e^{4A_{IR}}} = \text{sign}(Q_{IR}) \frac{\sqrt{T_{IR}}}{Y} & \text{for } u > u_0 \end{cases}. \quad (4.3)$$

In the following it will be convenient to define the jump of a quantity X across the brane by

$$\left[X \right]_{UV}^{IR} \equiv \lim_{\epsilon \rightarrow 0^+} (X(u_0 + \epsilon) - X(u_0 - \epsilon)). \quad (4.4)$$

The solutions in the UV and IR regions are then to be matched at the locus of the brane. The relevant conditions are known as Israel matching conditions and are given by the following:

1. Continuity of the metric and scalar fields:

$$\left[g_{ab} \right]_{UV}^{IR} = 0, \quad \left[\varphi \right]_{UV}^{IR} = 0, \quad \left[a \right]_{UV}^{IR} = 0. \quad (4.5)$$

For later convenience, we can define

$$A_0 \equiv A(u_0) = A_{UV}(u_0) = A_{IR}(u_0), \quad (4.6)$$

$$\varphi_0 \equiv \varphi(u_0) = \varphi_{UV}(u_0) = \varphi_{IR}(u_0), \quad (4.7)$$

$$a_0 \equiv a(u_0) = a_{UV}(u_0) = a_{IR}(u_0). \quad (4.8)$$

$$Y_0 \equiv Y(\varphi_0). \quad (4.9)$$

Only φ_0 and a_0 (not u_0) are gauge-invariant quantities.¹⁷

2. Discontinuity of the extrinsic curvature and normal derivatives of φ and a :

$$\left[K_{\mu\nu} - \gamma_{\mu\nu} K \right]_{UV}^{IR} = \frac{1}{\sqrt{-\gamma}} \frac{\delta S_{brane}}{\delta \gamma^{\mu\nu}}, \quad (4.10)$$

$$\left[n^a \partial_a \varphi \right]_{UV}^{IR} = -\frac{1}{\sqrt{-\gamma}} \frac{\delta S_{brane}}{\delta \varphi}, \quad \left[n^a \partial_a a \right]_{UV}^{IR} = -\frac{1}{\sqrt{-\gamma}} \frac{\delta S_{brane}}{\delta a}, \quad (4.11)$$

where $K_{\mu\nu}$ is the extrinsic curvature of the brane, $K = \gamma^{\mu\nu} K_{\mu\nu}$ is its trace, and n^a is a unit normal vector to the brane, oriented towards the *IR*.

¹⁷By gauge invariant, we mean invariant under bulk diffeomorphisms.

Using the form of the brane action in (3.2) and (3.3), equations (4.10, 4.11) are given explicitly by:

$$\begin{aligned} \left[K_{\mu\nu} - \gamma_{\mu\nu} K \right]_{UV}^{IR} &= \frac{1}{2} \hat{W}_B(\varphi, a, H) \gamma_{\mu\nu} + \hat{U}_B(\varphi, a, H) G_{\mu\nu}^B - (\nabla_\mu \nabla_\nu - \gamma_{\mu\nu} \square) \hat{U}(\varphi, a, H) \\ &\quad - Z_B \left(\partial_\mu \varphi \partial_\nu \varphi - \frac{1}{2} \gamma_{\mu\nu} (\partial\varphi)^2 \right) - Y_B \left(\partial_\mu a \partial_\nu a - \frac{1}{2} \gamma_{\mu\nu} (\partial a)^2 \right) \\ &\quad - \left((\partial_\mu H \partial_\nu H^* + c.c.) - \gamma_{\mu\nu} |\partial H|^2 \right) \Big|_{u=u_0}, \end{aligned} \quad (4.12)$$

$$\left[n^a \partial_a \varphi \right]_{UV}^{IR} = \frac{\partial \hat{W}_B}{\partial \varphi} - \frac{\partial \hat{U}_B}{\partial \varphi} R_B + \frac{1}{2} \frac{\partial Y_B}{\partial \varphi} (\partial a)^2 - \frac{1}{\sqrt{-\gamma}} \partial_\mu (Z_B \sqrt{-\gamma} \gamma^{\mu\nu} \partial_\nu \varphi) \Big|_{u=u_0}, \quad (4.13)$$

$$\left[n^a \partial_a a \right]_{UV}^{IR} = \frac{\partial \hat{W}_B}{\partial a} - \frac{\partial \hat{U}_B}{\partial a} R_B + \frac{1}{2} \frac{\partial Z_B}{\partial a} (\partial \varphi)^2 - \frac{1}{\sqrt{-\gamma}} \partial_\mu (Y_B \sqrt{-\gamma} \gamma^{\mu\nu} \partial_\nu a) \Big|_{u=u_0} \quad (4.14)$$

where $G_{\mu\nu}^B$ is the Einstein tensor constructed from $\gamma_{\mu\nu}$, and

$$\hat{W}_B(\varphi, a, H) = W_B(\varphi, a) + X_H(\varphi, a) |H|^2 + S_H(\varphi, a) |H|^4, \quad (4.15)$$

$$\hat{U}_B(\varphi, a, H) = U_B(\varphi, a) + U_H(\varphi, a) |H|^2. \quad (4.16)$$

In the following we rewrite the conditions (4.12, 4.13, 4.14) for the physical system at hand. For one, in this work we shall be exclusively interested in situations with a constant Higgs field on the brane world-volume,

$$H = \text{const.} \quad . \quad (4.17)$$

Further, for the ansatz of the bulk geometry and the chosen brane embedding, the extrinsic curvature and normal derivatives of φ and a can be written as:

$$K_{\mu\nu} = \dot{A} e^{2A} \eta_{\mu\nu}, \quad K_{\mu\nu} - \gamma_{\mu\nu} K = -3\dot{A} e^{2A} \eta_{\mu\nu}, \quad n^a \partial_a \varphi = \dot{\varphi}, \quad n^a \partial_a a = \dot{a}. \quad (4.18)$$

Then, the matching conditions can be cast in a gauge-invariant form using the scalar functions (W, S, T) on each side of the brane: making use of the expressions (2.24, 2.25, 2.30) for \dot{A} , $\dot{\varphi}$ and \dot{a} , as well as (4.18), equations (4.12, 4.13, 4.14) become conditions specifying the discontinuities in the scalar functions across the brane in terms of brane-localized terms:

$$\left[W \right]_{UV}^{IR} = \hat{W}_B(\varphi_0, a_0, H) \quad (4.19)$$

$$\left[S \right]_{UV}^{IR} = \frac{\partial \hat{W}_B}{\partial \varphi}(\varphi_0, a_0, H), \quad (4.20)$$

$$\frac{[\text{sign}(Q)\sqrt{T}]_{UV}^{IR}}{Y_0} = \frac{\partial \hat{W}_B}{\partial a}(\varphi_0, a_0, H), \quad (4.21)$$

From (3.3) and (3.4), the equation of motion for the SM Higgs field on the brane is

$$(X_H(\varphi_0, a_0) + 2S_H(\varphi_0, a_0)|H|^2) H = 0, \quad (4.22)$$

where we also used (4.17). This leads to two solutions H_{\min} for the Higgs field:

$$|H_{\min}|^2 = \begin{cases} 0 & , \\ -\frac{X_H}{2S_H} & \text{for } X_H < 0, \end{cases} \quad (4.23)$$

where we assume positivity of S_H . The physical Higgs mass squared m_H^2 in the two cases is given by

$$m_H^2 = \begin{cases} M_p X_H, & \text{for } X_H \geq 0, \\ -2M_p X_H, & \text{for } X_H < 0, \end{cases} \quad (4.24)$$

from (3.3), where we have also used $T_H = M_p^{-1}$.

When we choose $|H|^2 = |H_{\min}|^2$, the three conditions (4.19), (4.20) and (4.21) can be written as

$$[W]_{UV}^{IR} = \hat{W}_B^{eff}(\varphi_0, a_0) \quad (4.25)$$

$$[S]_{UV}^{IR} = \frac{\partial \hat{W}_B^{eff}}{\partial \varphi}(\varphi_0, a_0), \quad (4.26)$$

$$\frac{[\text{sign}(Q)\sqrt{T}]_{UV}^{IR}}{Y_0} = \frac{\partial \hat{W}_B^{eff}}{\partial a}(\varphi_0, a_0), \quad (4.27)$$

with

$$\hat{W}_B^{eff}(\varphi_0, a_0) \equiv \hat{W}_B(\varphi_0, a_0, H_{\min}) \quad (4.28)$$

To summarize, the full system of bulk and brane field equations boils down to the bulk equations, (2.27, 2.28, 2.29, 2.30) and the three matching conditions (4.25, 4.26, 4.27). Once we impose the IR regularity conditions, the matching conditions (4.5, 4.25, 4.26, 4.27) fix the subleading (vev) boundary conditions on the UV side.

In the following, we explore to what extent the relations between the various integration constants and the bulk solutions are affected by the presence of the brane. For one, as both the integration constants Q_{UV} and q_{UV} are properties of the solution on the UV side alone, the relation between them is unaffected by the brane and hence still given by (2.52), which we reproduce here:

$$Q_{UV} = \text{sign}(Q_{UV}) \frac{\sqrt{q_{UV}}}{\ell} \left(\ell |\varphi_-|^{\frac{1}{\Delta_-}} \right)^4. \quad (4.29)$$

On the other hand in (2.49) the integration constant a_\star was defined in terms of an integral over the whole bulk solution from IR to UV. This expression will be modified in the presence of the brane due to the condition (4.27), to become:

$$\begin{aligned}
a_\star &= -Q_{UV} \int_{u_{UV}}^{u_0} \frac{du}{Y e^{4A}} - Q_{IR} \int_{u_0}^{u_{IR}} \frac{du}{Y e^{4A}} \\
&= - \left(\text{sign}(Q_{UV}) \int_{\varphi(u_{UV})}^{\varphi_0} + \text{sign}(Q_{IR}) \int_{\varphi_0}^{\varphi(u_{IR})} \right) \frac{\sqrt{T}}{YS} d\varphi \\
&= -Q_{IR} \int_{u_{UV}}^{u_{IR}} \frac{du}{Y e^{4A}} + \frac{\partial \hat{W}_B^B}{\partial a} Y_0 e^{4A_0} \int_{u_{UV}}^{u_0} \frac{du}{Y e^{4A}}. \tag{4.30}
\end{aligned}$$

In the last line, the first term is unchanged compared to the case without the brane. The second term appears because of the junction condition (4.27). To arrive at the above we used equation (4.27), (2.9) and (2.30) to write:

$$\frac{\text{sign}(Q_{IR})\sqrt{T_{IR}} - \text{sign}(Q_{UV})\sqrt{T_{UV}}}{Y_0} = \frac{Q_{IR} - Q_{UV}}{Y_0 e^{4A_0}} = \frac{\partial \hat{W}_B^{eff}}{\partial a}(\varphi_0, a_0). \tag{4.31}$$

As we will see, the full system (2.27, 2.28, 2.29, 2.30, 4.25, 4.26, 4.27) permits solutions for generic choices of brane potentials, up to mild assumptions stated below. The solutions can be obtained analytically in the case of small axion backreaction (section 5), otherwise we resort to numerical methods (section 6).

In addition, we require

$$\begin{aligned}
W_{UV}(\varphi_0) &= W_{IR}(\varphi_0) - \hat{W}_B^{eff}(\varphi_0, a_0) > 0, \\
S_{UV}(\varphi_0) &= S_{IR}(\varphi_0) - \frac{\partial \hat{W}_B^{eff}(\varphi_0, a_0)}{\partial \varphi_0} > 0, \tag{4.32}
\end{aligned}$$

which can be regarded as a set of mild constraints on the bulk potentials. The first condition comes from the requirement that the scale factor A asymptotes to $+\infty$ when approaching the UV boundary for $u \rightarrow u_{UV}$. The second condition comes from the requirement that the φ asymptotes to $\varphi_{UV} = 0$ for $u \rightarrow u_{UV}$. These conditions also apply in the case of absence of a running bulk axion, see [7].

Using the equations of the full system, we can calculate the renormalized on-shell action $S_{\text{on-shell}}^{\text{ren}}$, free energy F and the topological susceptibility χ . Here we collect the results, which are given by:

$$S_{\text{on-shell}}^{\text{ren}} = M_p^3 V_4 \ell^3 |\varphi_-|^{\frac{4}{\Delta_-}} (C_{UV}(q_{UV}) - C_{UV,ct}), \tag{4.33}$$

$$F(\varphi_-, \theta_{UV}) = -\text{Min}_{k \in \mathbb{Z}} S_{\text{on-shell}}^{\text{ren}} \tag{4.34}$$

$$\chi = -\text{Min}_k |\varphi_-|^{\frac{4}{\Delta_-}} \frac{(M_p \ell)^3}{N_c^2} \frac{\partial^2 C_{UV}(a_{\star,k})}{\partial a_{\star,k}^2} \Big|_{a_{\star,k} = \frac{\theta_{UV} + 2\pi k}{N_c}} \tag{4.35}$$

with V_4 is the 4-dimensional space-time volume, $C_{UV,ct}$ the free parameter corresponding to the choice of the renormalization scheme, and $C_{UV}(q_{UV})$ the integration constant setting the vev of the operator dual to φ , which depends on q_{UV} (or a_*) in virtue of the IR regularity condition (2.48). The integer k labels the various oblique holographic vacua of the gauge theory. We have introduced a minimization over k to take into account the many-to-one relation between a_* and θ_{UV} (2.46). The details of the computation are given in Appendix A.

5. Solutions in the small axion backreaction approximation

In this section we study solutions of the brane-bulk system analytically by assuming the axion backreaction to the whole system is small. Concretely, we consider a small perturbation around the trivial axion solution $a_* = q_{UV} = Q_{UV} = Q_{IR} = 0$, which will also be referred to as the ‘probe limit’.

We shall calculate the leading corrections in q_{UV} to various quantities. First, we clarify the relation among the various axion-related integration constants q_{UV} , Q_{UV} and Q_{IR} . Recall the relation between Q_{UV} and q_{UV}

$$\ell Q_{UV} = \text{sign}(Q_{UV}) \left(\ell |\varphi_-|^{\frac{1}{\Delta_-}} \right)^4 \sqrt{q_{UV}} \quad (5.1)$$

from (4.29). Note that, for a given q_{UV} one has the freedom to choose $\text{sign}(Q_{UV})$. Then, in the probe limit one can show that Q_{IR} and q_{UV} are related as (see Appendix B for details)

$$\begin{aligned} \ell Q_{IR} &= \frac{\text{sign}(Q_{UV}) \left(\ell |\varphi_-|^{\frac{1}{\Delta_-}} \right)^4}{1 + Y_0 e^{4A_0} \frac{\partial^2 \hat{W}_B^{eff}}{\partial a^2} \int_{u_0}^{u_{IR}} \frac{du}{Y e^{4A}}} \sqrt{q_{UV}} + \mathcal{O}(q_{UV}) \\ &= \frac{\ell Q_{UV}}{1 + Y_0 e^{4A_0} \frac{\partial^2 \hat{W}_B^{eff}}{\partial a^2} \int_{u_0}^{u_{IR}} \frac{du}{Y e^{4A}}} + \mathcal{O}(q_{UV}), \end{aligned} \quad (5.2)$$

where the argument of $\frac{\partial^2}{\partial a^2} \hat{W}_B^{eff}$ is suppressed for simplicity. From (5.2), we observe that the sign of Q_{IR} is same as that of Q_{UV} as long as $\frac{\partial^2}{\partial a^2} \hat{W}_B^{eff} \geq 0$.

Expanding in powers of q_{UV} , the expansion coefficients are defined as follows:

$$W = W^{(q0)} + q_{UV} W^{(q1)} + \mathcal{O}(q_{UV}^2), \quad (5.3)$$

$$S = S^{(q0)} + q_{UV} S^{(q1)} + \mathcal{O}(q_{UV}^2), \quad (5.4)$$

$$T = q_{UV} T^{(q1)} + \mathcal{O}(q_{UV}^2). \quad (5.5)$$

$$\varphi_0 = \varphi_0^{(q0)} + q_{UV} \varphi_0^{(q1)} + \mathcal{O}(q_{UV}^2), \quad (5.6)$$

$$C_{UV} = C_{UV}^{(q0)} + q_{UV} C_{UV}^{(q1)} + \mathcal{O}(q_{UV}^2). \quad (5.7)$$

The leading axion backreaction effects (the quantities with the superscript $(q1)$) can be expressed in terms of the unperturbed quantities (with the superscript $(q0)$). The calculation is straightforward, but lengthy. Therefore, the computation is relegated to Appendix B, and here we focus on the result and its consequences for the sign of the Higgs mass parameter X_H . The readers can find the expressions for $W^{(q1)}$, $S^{(q1)}$, $T^{(q1)}$, $\varphi_0^{(q1)}$ and $C_{UV}^{(q1)}$ in (B.6), (B.7), (B.8), (B.29) and (B.27), respectively.¹⁸

Using the above coefficients of the small- q_{UV} -expansion, the axion field values at the brane position a_0 and axion source a_\star can be expressed as

$$a_0 = -\sqrt{q_{UV}} \operatorname{sign}(Q_{IR}) \int_{\varphi_0^{(q0)}}^{\varphi_{IR}} \frac{\sqrt{T^{(q1)}}}{S^{(q0)} Y} d\varphi + \mathcal{O}(q_{UV}) \equiv g_0 \sqrt{q_{UV}} + \mathcal{O}(q_{UV}), \quad (5.8)$$

$$\begin{aligned} a_\star &= \left(-\operatorname{sign}(Q_{UV}) \int_{\varphi(u_{UV})}^{\varphi_0^{(q0)}} d\varphi \frac{\sqrt{T^{(q1)}}}{S^{(q0)} Y} - \operatorname{sign}(Q_{IR}) \int_{\varphi_0^{(q0)}}^{\infty} d\varphi \frac{\sqrt{T^{(q1)}}}{S^{(q0)} Y} \right) \sqrt{q_{UV}} + \mathcal{O}(q_{UV}) \\ &\equiv g_\star \sqrt{q_{UV}} + \mathcal{O}(q_{UV}). \end{aligned} \quad (5.9)$$

The q_{UV} -expansion of the Higgs mass parameter X_H reads

$$\begin{aligned} X_H &= X_H|_{a=0} + \left(\frac{\partial^2 X}{\partial a^2} g_0^2 + \frac{\partial X_H}{\partial \varphi} \varphi_0^{(q1)} \right) q_{UV} + \mathcal{O}(q_{UV}^2) \\ &= X_H|_{a=0} + \left(\frac{\partial^2 X_H}{\partial a^2} \frac{g_0^2}{g_\star^2} + \frac{\partial X_H}{\partial \varphi} \frac{\varphi_0^{(q1)}}{g_\star^2} \right) \left(\frac{\theta_{UV} + 2\pi k}{N_c} \right)^2 + \mathcal{O} \left(\left(\frac{\theta_{UV} + 2\pi k}{N_c} \right)^4 \right), \end{aligned} \quad (5.10)$$

where we used (2.46) (with c , defined in (2.46) to be equal to 1)¹⁹ and (5.9). In the second line, we assumed CP invariance, i.e.

$$\frac{\partial X}{\partial a}(\varphi_0^{(q0)}, 0) = 0. \quad (5.11)$$

Also, functions on the right hand side of (5.10) are evaluated at $\varphi_0 = \varphi_0^{(q0)}$, $a_0 = 0$.

As one can observe from (5.10), the different solution labelled by $k = 0, 1, \dots, n$ differ in the value of the Higgs mass. From (2.46) we obtain the number of distinct solutions n as

$$n = \left\lfloor \frac{N_c a_\star^{\max}}{2\pi} - \theta_{UV} \right\rfloor + 1, \quad (5.12)$$

where we take $c = 1$ and $\lfloor z \rfloor$ is the maximum integer smaller than or equal to the real number z . Here, a_\star^{\max} is the maximum value of the axion source observed in

¹⁸Apart from the probe limit discussed here, there are other configurations of the brane-bulk system that are amenable to an analytical study. For example, this is the case when the brane is located in the asymptotically UV or IR region of the bulk and the corresponding analysis is recorded in Appendix C.

¹⁹If c is not 1, then a_\star^{\max} should be replaced by a_\star^{\max}/c

[24] (see also section 6). For large N_c , n is a large number, which compares well to a similar number emerging from the chiral Lagrangian, see section 5 of [27]. This multitude of saddle points opens up the following phenomenologically interesting situation. Suppose that we find the branch $k = k_1$ which realizes $X_H|_{k=k_1} \approx 0$ in the region where the small axion backreaction is valid, i.e. $(\theta_{UV} + 2\pi k_1)/N_c \ll 1$. If this is the case, around this saddle point, we can find many other branches realizing $X_H < 0$ with Higgs mass which is smaller than any other scales characterizing the brane-bulk system. The existence of a saddle point with a small Higgs vev therefore arises as a consequence of the multiplicity (and density) of axionic saddle points, similar to the case of the ‘relaxion’ proposal for solving the EW hierarchy problem [28].

In this section, we argued that a small electroweak scale can be realized assuming that the small axion backreaction approximation is applicable. In the next section, we will go beyond the probe limit, and solve the full system numerically. We shall show that solutions with a small Higgs vev persist beyond the probe limit.

6. General numerical solutions

In this section, we explore numerical solutions of the brane-bulk system. Throughout this section, we work with the following choice for the bulk functions V and Y :

$$V = -\frac{1}{\ell^2} \left[12 + \left(\frac{(4 - \Delta_-)\Delta_-}{2} - b^2 V_\infty \right) \varphi^2 + 4V_\infty \sinh^2 \left(\frac{b\varphi}{2} \right) \right], \quad Y = Y_\infty e^{\gamma\varphi}. \quad (6.1)$$

The bulk potential V has an AdS maximum at the origin $\varphi = 0$, and does not have any other extrema. Therefore, the solution in the bulk extends reaches the boundary of field space, $\varphi \rightarrow \pm\infty$. For definiteness, we consider solutions in which $\varphi > 0$.

For large dilaton values the potential asymptotes to

$$V \xrightarrow{\varphi \rightarrow +\infty} -\frac{1}{\ell^2} V_\infty e^{b\varphi} + \mathcal{O}(\varphi^2). \quad (6.2)$$

This choice of bulk functions is the same as in our previous work [24] where axionic RG flow solutions without a brane were studied, and is motivated from top-down string-generated supergravity examples.

In the following, in all numerical examples the parameters in (6.1) are chosen as

$$\Delta_- = 1.2, \quad b = 1.3, \quad \gamma = 1.5, \quad V_\infty = 1, \quad Y_\infty = 1. \quad (6.3)$$

Without loss of generality we also set

$$\ell = 1. \quad (6.4)$$

The set of parameter values is consistent with the bound on γ in (2.44) and the Gubser bound on b in (2.43). The condition (2.44) reads

$$\gamma \geq \frac{8 - 3b^2}{3b} = \frac{293}{390} \simeq 0.75, \quad (6.5)$$

while the Gubser bound (2.43) is given by

$$b \leq \sqrt{\frac{8}{3}} = 2\sqrt{2/3} \simeq 1.63. \quad (6.6)$$

These are satisfied by the choice (6.3).

To set up the numerical study, we also need to specify the brane potentials W_B , X_H and S_H .²⁰ In the following, we shall consider four different choices for the brane potentials, which will be discussed in sections 6.1, 6.2, 6.3 and 6.4. Note that, from (3.3), the mass dimensions of W_B , X_H and S_H are 1, 2 and 3, respectively.

To solve numerically, we impose boundary conditions on the IR end of the flow and then evolve the solutions towards the UV. As the IR is only reached for $\varphi \rightarrow \infty$, in practice boundary conditions are implemented at a finite, but sufficiently large value of φ , where the bulk potential is well-approximated by the leading exponential in (6.2). The appropriate boundary conditions for W_{IR} , S_{IR} and T_{IR} are then given by (2.38), (2.39), (2.40).

Then, we evolve the expressions for W_{IR} , S_{IR} and T_{IR} from the IR towards the UV until we encounter the locus $\varphi = \varphi_0$ where the brane is located. This can be found using only the IR solutions W_{IR} , S_{IR} and T_{IR} as well as the brane potentials and the value of φ for which the following condition is satisfied:

$$\begin{aligned} & \frac{1}{3} \left(W_{IR} - \hat{W}_B^{eff} \right)^2 - \frac{1}{2} \left(S_{IR} - \frac{\partial \hat{W}_B^{eff}}{\partial \varphi} \right)^2 - \\ & - \frac{1}{2Y} \left(\text{sign}(Q_{IR}) \sqrt{T_{IR}} - Y \frac{\partial \hat{W}_B^{eff}}{\partial a} \right)^2 + V \Big|_{\varphi=\varphi_0} = 0, \end{aligned} \quad (6.7)$$

This is just the equation of motion (2.29) for the scalar functions on the UV side, where we substituted for W_{UV} , S_{UV} , T_{UV} using the matching conditions (4.25), (4.26), (4.27). Since the scalar functions W_{IR} , S_{IR} , T_{IR} also satisfy the equation of motion (2.29), the condition (6.7) can be rewritten as

$$-\frac{2}{3} \left(W_{IR} \hat{W}_B^{eff} - \frac{1}{2} \left(\hat{W}_B^{eff} \right)^2 \right) + \left(S_{IR} \frac{\partial \hat{W}_B^{eff}}{\partial \varphi} - \frac{1}{2} \left(\frac{\partial \hat{W}_B^{eff}}{\partial \varphi} \right)^2 \right) + \quad (6.8)$$

²⁰Recall that we are considering a flat brane and hence $R_B = 0$. As a result, the terms multiplying the brane potentials U_B and U_H in (3.2), (3.3) are absent and we can refrain from specifying U_B and U_H .

$$+ \left(\text{sign}(Q_{IR}) \frac{\sqrt{T_{IR}}}{Y} \frac{\partial \hat{W}_B^{eff}}{\partial a} - \frac{Y}{2} \left(\frac{\partial \hat{W}_B^{eff}}{\partial a} \right)^2 \right) \Big|_{\varphi=\varphi_0} = 0.$$

This equation has generically multiple solutions corresponding to multiple possible positions for the brane.

For a given solution, we then calculate the Higgs mass numerically. One priority of this analysis will be to determine whether solutions with a low Higgs mass arise in the fully backreacted setup considered here. The analysis will be performed for the following four choices of brane potentials:

- The brane potentials only depend on the bulk scalar φ , but not on the axion a (Section 6.1). The explicit form of the brane potentials is given in (6.9).
- The Higgs mass function X_H depends linearly on the axion a , while the other brane functions do not depend on a . This is motivated by the original relaxation scenario [28], and by the stringy constructions of (rel)axion monodromy which exhibit an axion-Higgs coupling [52] (Section 6.2). The explicit form of the brane potentials is given in (6.15).
- The brane cosmological constant W_B depends on $\cos(a)$, which is motivated by the standard instanton-generated potential in the dilute gas approximation (Section 6.3). The other brane functions do not depend on a . The explicit form of the brane potentials is given in (6.18).
- The Higgs mass function depends linearly on a , and the brane cosmological constant depends on $\cos(a)$ (Section 6.4). The Higgs self coupling S_H does not depend on a . This is a combination of the ansätze in 6.2 and 6.3. The explicit form of the brane potentials is given in (6.21).

6.1 Brane potential choice 1: No explicit axion dependence

Here we consider the following choice for the brane functions in (3.1):

$$W_B = \frac{\Lambda^4}{M_p^3} \left[-1 - \frac{\varphi}{s} + \left(\frac{\varphi}{s} \right)^2 \right] , \quad (6.9)$$

$$X_H = \frac{\Lambda^2}{M_p} \left[1 + \frac{\varphi}{s_X} - \left(\frac{\varphi}{s_X} \right)^2 \right] , \quad S_H = M_p \left[1 + \left(\frac{\varphi}{s_H} \right)^2 \right] ,$$

where M_p is the bulk Planck mass and s, s_X and s_H are dimensionless constants. We also introduced the parameter Λ which has the interpretation of UV cutoff for the brane theory. Note that (6.9) implies that \hat{W}_B^{eff} is proportional to Λ^4/M_p^3 , as one can observe from (4.15), (4.23) and (4.28). Therefore, it will be convenient to define the quantity

$$\tilde{\Lambda}^4 \equiv \Lambda^4/M_p^3, \quad (6.10)$$

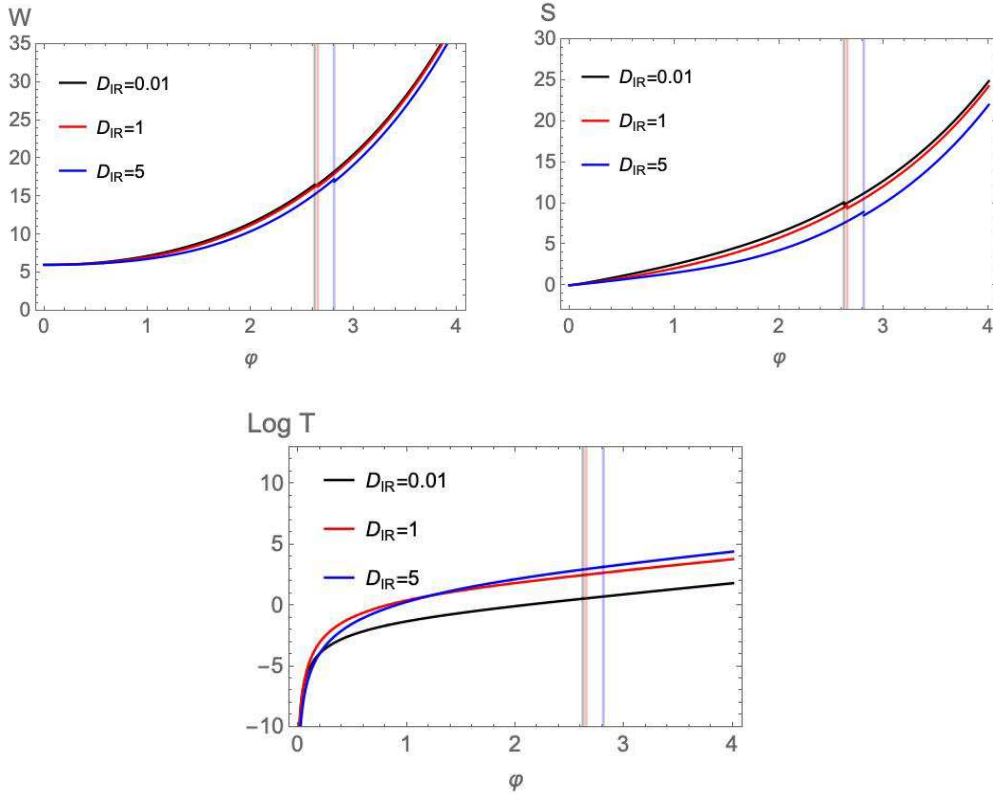


Figure 1: Plots of W , S , T vs. φ for a model with bulk functions (6.1), brane functions (6.9), model parameters (6.3) with (6.11), and $D_{IR} = 0.01, 1, 5$. The vertical line represents the brane position, which is determined by solving (6.12) and (4.32). **Top row, left:** Plot of $W(\varphi)$. **Top row, right:** Plot of $S(\varphi)$. **Bottom row:** Plot of $\log T(\varphi)$.

where $\tilde{\Lambda}$ can be considered as a dimensionless quantity since we set $\ell = 1$. Besides the choice of parameters given in (6.3), here we also set

$$s_X = \frac{2}{3}, \quad s_H = 1, \quad (6.11)$$

and vary s and $\tilde{\Lambda}$.

Here the brane functions do not depend explicitly on a and the junction condition (6.8) reduces to

$$-\frac{2}{3} \left(W_{IR} \hat{W}_B^{eff} - \frac{1}{2} \left(\hat{W}_B^{eff} \right)^2 \right) + \left(S_{IR} \frac{\partial \hat{W}_B^{eff}}{\partial \varphi} - \frac{1}{2} \left(\frac{\partial \hat{W}_B^{eff}}{\partial \varphi} \right)^2 \right) \Bigg|_{\varphi=\varphi_0} = 0. \quad (6.12)$$

In figure 1 we plot solutions for W , S , and T for the parameter choices (5.12), (6.11), $s = 1$, $\tilde{\Lambda} = 1$.²¹ The three solutions plotted correspond to the three choices

²¹ $\tilde{\Lambda} = 1$ corresponds to a brane cutoff scale Λ that is much smaller than the bulk Planck scale.

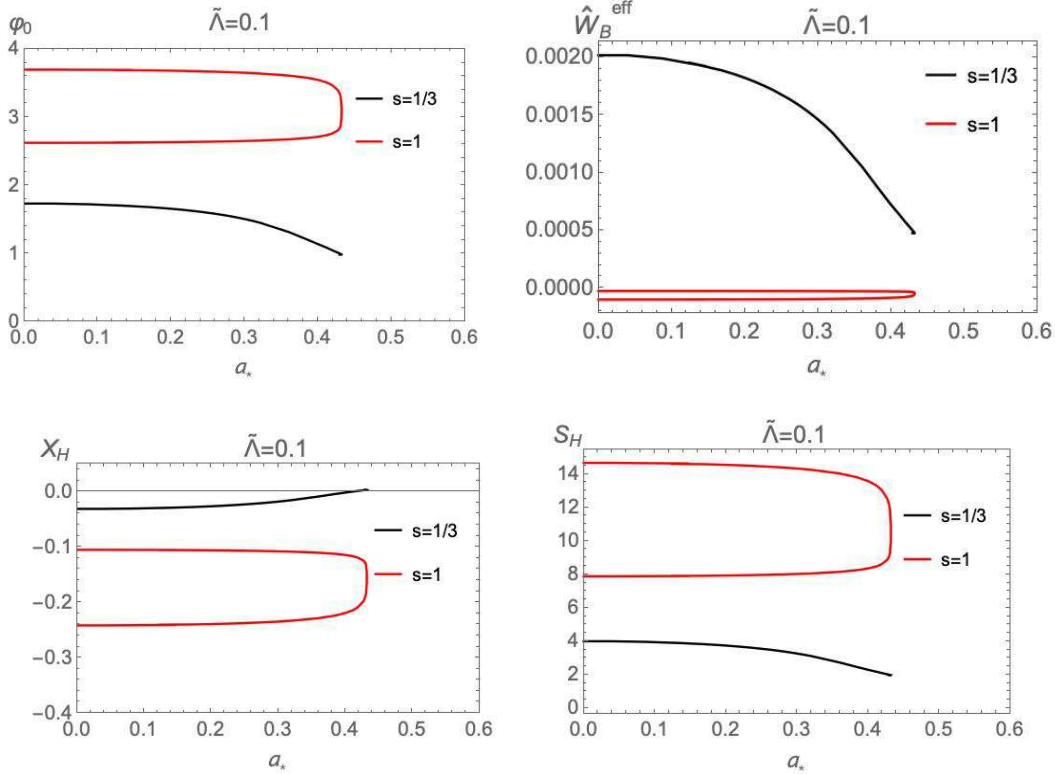


Figure 2: Plots of φ_0 , \hat{W}_B^{eff} , X_H and S_H vs. a_* for a model with bulk functions (6.1) and brane functions (6.9). The bulk parameters are (6.3), and the brane parameters are (6.11), $\tilde{\Lambda} = 0.1$, and $s = 1/3, 1$. **Top row, left:** Plot of φ_0 . **Top row, right:** Plot of $\hat{W}_B^{eff}(\varphi_0, a_0)$. **Bottom row, left:** Plot of $X_H(\varphi_0, a_0)$. **Bottom row, right:** Plot of $S_H(\varphi_0, a_0)$.

$D_{IR} = 0.01, 1$ and 5 for the axion-related integration constant D_{IR} . The vertical lines indicate the brane position φ_0 for the three different choices of D_{IR} . There are two solutions to (6.12) satisfying (4.32). To be specific, in figure 1 we only display the solution with the smaller value of φ_0 . Note that the functions W and S are discontinuous at φ_0 because of the junction conditions (4.25) and (4.26). The function T is continuous, consistent with (4.27), as here the brane functions are independent of a , (6.9). However, T is not smooth. The first derivative of T is not continuous at φ_0 , which follows from (2.28) and the discontinuity of W and S . We also checked that the numerical result is consistent with the UV and IR asymptotic expansions (2.34, 2.35, 2.36, 2.38, 2.39, 2.40).

The main observation is that even though the brane functions in (6.9) do not depend explicitly on the axion a , the equilibrium brane position φ_0 is affected by axion backreaction. Here, we controlled the strength of axion backreaction by adjusting the integration constant D_{IR} at the IR end of the flow. A shift in D_{IR} resulted in a (small but nevertheless non-vanishing) shift in φ_0 .

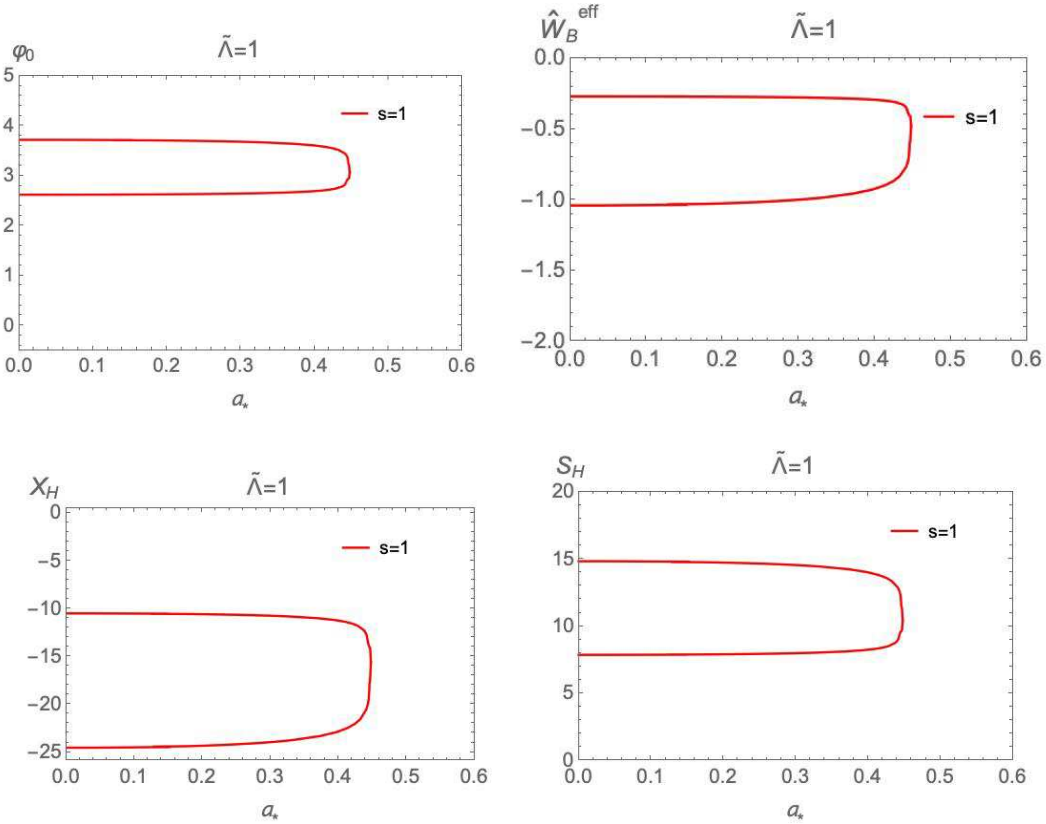


Figure 3: Plots of φ_0 , \hat{W}_B^{eff} , X_H and S_H vs. a_* for a model with bulk functions (6.1) and brane functions (6.9). The bulk parameters are (6.3), and the brane parameters are (6.11), $\tilde{\Lambda} = 1$, and $s = 1$. **Top row, left:** Plot of φ_0 . **Top row, right:** Plot of $\hat{W}_B^{eff}(\varphi_0, a_0)$. **Bottom row, left:** Plot of $X_H(\varphi_0, a_0)$. **Bottom row, right:** Plot of $S_H(\varphi_0, a_0)$.

In the following, we shall also examine in more detail how the brane equilibrium position φ_0 and the brane functions \hat{W}_B^{eff} , X_H and S_H evaluated at φ_0 are affected by axion backreaction. However, rather than controlling D_{IR} , the axion integration constant in the IR, it will be more convenient to dial the value of a_* , the axion integration constant in the UV, as this has a physical interpretation as the axion source in the dual field theory.²²

As examples of the types of solutions, we show the results one obtains for a few representative (but in no way special) values of the remaining unfixed parameters,

²²In practice, when solving numerically, we implement boundary conditions in the IR and hence we need to specify D_{IR} . Then, for a given solution, we read off the corresponding values of a_* and φ_0 . Scanning over all values of D_{IR} we can then determine a_* , φ_0 as functions of D_{IR} , i.e. $a_*(D_{IR})$, $\varphi_0(D_{IR})$. Inverting $a_*(D_{IR})$ then allows us to obtain $\varphi_0(a_*)$ from $\varphi_0(D_{IR})$. In this way we can also determine $\hat{W}_B^{eff}(\varphi_0)$, $X_H(\varphi_0)$ and $S_H(\varphi_0)$ as functions of a_* .

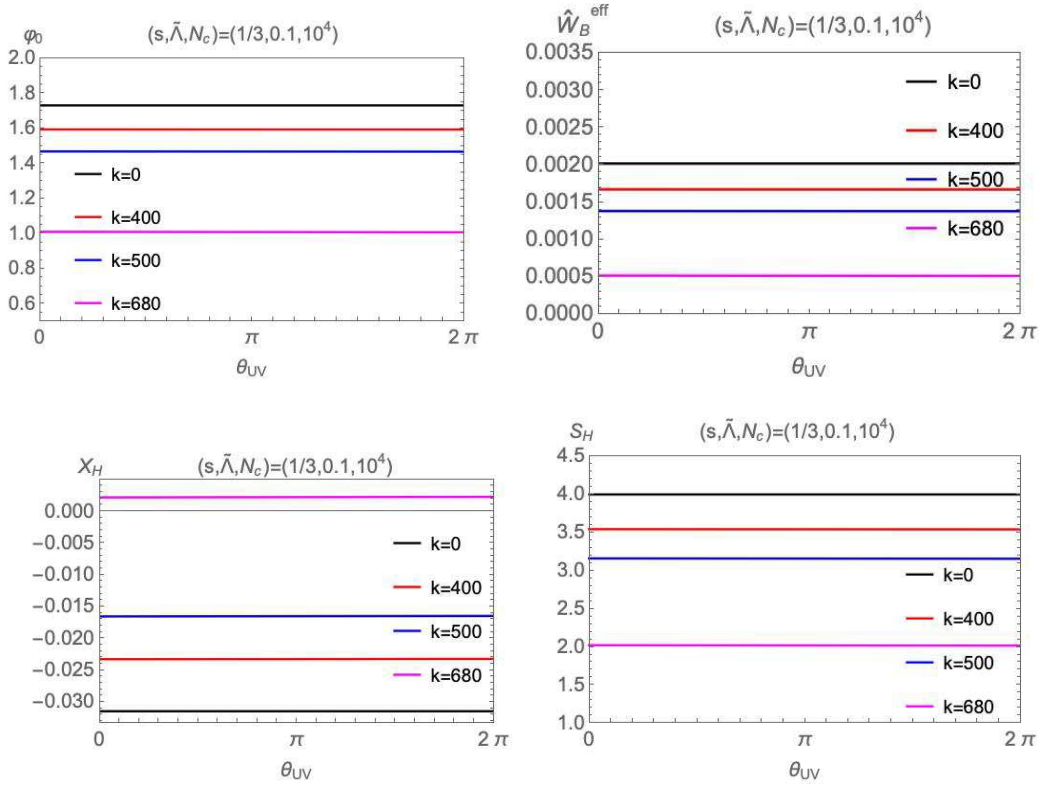


Figure 4: Plots of φ_0 , \hat{W}_B^{eff} , X_H and S_H vs. θ_{UV} for a model with bulk functions (6.1) and brane functions (6.9). We take $s = 1/3$, $\tilde{\Lambda} = 0.1$ and $N_c = 10^4$. Other parameters are (6.3) and (6.11). Only the $k = 0, 400, 500, 680$ branches are shown for the illustration. **Top row, left:** Plot of φ_0 . **Top row, right:** Plot of $\hat{W}_B^{eff}(\varphi_0, a_0)$. **Bottom row, left:** Plot of $X_H(\varphi_0, a_0)$. **Bottom row, right:** Plot of $S_H(\varphi_0, a_0)$.

namely we take

$$s = \frac{1}{3}, \quad 1 \quad \tilde{\Lambda} = 0.1, \quad 1 \quad (6.13)$$

Notice that choosing $\tilde{\Lambda}$ (defined in equation (6.10)) of order one or smaller in AdS units means that we are restricting the UV cut-off Λ to be much smaller than the Planck scale. Indeed, reinstating the AdS length in equation (6.10), we find that

$$\frac{\Lambda^4 \ell}{M_p^3} \sim O(1) \quad \Rightarrow \quad \Lambda^4 \sim \frac{M_p^3}{\ell} \ll M_p^4, \quad (6.14)$$

where the last inequality comes from the requirement that the bulk geometry is classical, $\ell \gg M_p^{-1}$.

In figures 2 and 3, we plot the values of φ_0 , \hat{W}_B^{eff} , X_H and S_H as functions of a_* for the bulk parameters (5.12), brane parameters (6.11) and the combination of parameters chosen in (6.13). We make the following observations.

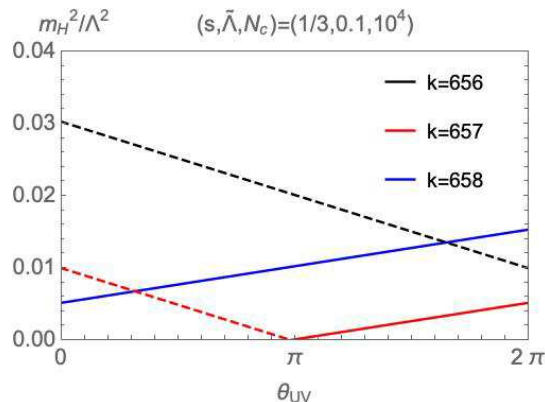


Figure 5: Plot of the Higgs mass squared m_H^2 (4.24) in units of Λ^2 vs. θ_{UV} for a model with bulk functions (6.1) and brane functions (6.9). The model parameters are (6.3), (6.11), $s = 1/3$, $\tilde{\Lambda} = 0.1$, $N_c = 10^4$. We plot the lines with $k = 656, 657, 658$, corresponding to the branches realizing the small Higgs mass. Note that, for $0 \leq \theta_{UV} \lesssim \pi$, the symmetric ($X_H > 0$) and broken ($X_H < 0$) phase correspond to $k \geq 658$ and $k \leq 657$, respectively. For $\pi \lesssim \theta_{UV} < 2\pi$, the symmetric and broken phases correspond to $k \geq 657$ and $k \leq 656$. In the figure, the symmetric and broken phases are represented by the solid and dashed lines, respectively.

- The range of a_\star is typically bounded with an upper limit a_\star^{\max} whose precise value depends on the model parameters. This property of axionic RG flows was already observed in absence of the brane in [24], but it also persists when a brane is included. In figures 2, 3 and all following plots of functions of a_\star , we display the functions over their complete domain of support $0 < a_\star < a_\star^{\max}$.
- For the parameter choice $s = 1/3$, $\tilde{\Lambda} = 1$ there exist solutions to the junction condition (6.12), however, these do not satisfy the overshooting constraint (D.10) in Appendix D (i.e. the solutions miss the fixed point in the UV). Thus, as stated there, we should discard these solutions and this is why we refrain from plotting the corresponding numerical results in figure 3.
- The brane cosmological constant \hat{W}_B^{eff} is generically of the same magnitude as $\tilde{\Lambda}^4$, as can be seen in the top right panels of figures 2 and 3. Nevertheless, the brane worldvolume is flat by construction, i.e. the solutions exhibit self-tuning of the cosmological constant as advertised.
- In addition to realising this self-tuning mechanism for the cosmological constant, the second objective of this work is to seek for solutions with low Higgs mass (and vev). As follows from the discussion in sec. 4, a small Higgs mass can be attained if X_H is small. This is the case in the vicinity of $X_H \approx 0$ and thus we are particularly interested in solutions where X_H as a function of a_\star

changes sign. For the parameter choices considered here, a sign change in X_H exists, but only on the branch of solutions with $s = 1/3$, $\tilde{\Lambda} = 0.1$, see fig. 2. We shall study the solutions on this branch in more detail next.

So far we were considering φ_0 , \hat{W}_B^{eff} , X_H and S_H as a function of the UV parameter a_\star in figures 2 and 3. A related UV parameter is θ_{UV} , the theta angle of the dual field theory supported on the UV boundary. Note that the identification between a_\star and θ_{UV} , recorded in (2.46), is many-to-one, i.e. one fixed value of θ_{UV} corresponds to many different discrete values of a_\star . Following the notation in (2.46) we can label the various vacua associated with a single value for θ_{UV} by the integer k . As all these different vacua for a given θ_{UV} have different values of a_\star , all these different vacua will generically possess different values for φ_0 , \hat{W}_B^{eff} , X_H and S_H . For large values of N_c the various vacua for fixed θ_{UV} are ‘dense’ in a_\star -space, as follows straightforwardly from (2.46). To illustrate this we consider the branch of solutions with $s = 1/3$, $\tilde{\Lambda} = 0.1$ in fig. 2, but using (2.46) we plot the brane functions φ_0 , \hat{W}_B^{eff} , X_H and S_H as functions of θ_{UV} . This is shown in fig. 4 where for better visibility, we only plot results for $k = 0, 400, 500, 680$.²³

Then, as long as X_H as a function of a_\star changes sign, there will typically exist a finite (but possibly large) number of fixed- θ_{UV} vacua with $X_H \approx 0$ and hence a small Higgs mass. Here we find that this is the case for the branches of solutions with k in the vicinity of $k \sim 657$. In figure 5, we plot of ratio of Higgs mass m_H^2 defined in (4.24) and the scale Λ appearing in (6.9) for the branches with $k = 656, 657, 658$.²⁴ Notice that the ratio m_H^2/Λ^2 is independent of Λ and M_p , and we do not need to specify the values of these parameters. The scale Λ sets both size of the cosmological constant and the naive Higgs mass parameter X_H on the brane and can be understood as the UV cutoff scale of the brane theory. We hence refer to the Higgs mass as small if

$$m_H^2 \ll \Lambda^2 .$$

In figure 5 we observe that $m_H^2/\Lambda^2 \sim \mathcal{O}(10^{-2})$ for a generic value of θ_{UV} on these branches, but the precise value is also a consequence of our choice $N_c = 10^4$. Branches with smaller values can be obtained if N_c is chosen larger.

To summarise, the example considered here is a brane-world model that realizes self-tuning of the cosmological constant, but also possesses a (potentially) large number of saddle points, some with a small Higgs mass. Therefore it can be seen as

²³As the overall range of a_\star is bounded, there is a finite number of saddle points associated with a fixed value of θ_{UV} . Here, with the choice $c = 1$, $N_c = 10^4$ and the observed value $a_\star^{\max} \sim 0.4$ we find that the total number of fixed- θ_{UV} saddle points is ~ 680 , see e.g. eq. (5.12).

²⁴Note that, for $0 \leq \theta_{UV} \lesssim \pi$, the symmetric and broken phases for the Higgs correspond to $k \geq 658$ and $k \leq 657$, respectively. For $\pi \lesssim \theta_{UV} < 2\pi$, the symmetric and broken phases correspond to $k \geq 657$ and $k \leq 656$. In figure 5, the symmetric and broken phases are represented by the solid and dashed lines, respectively.

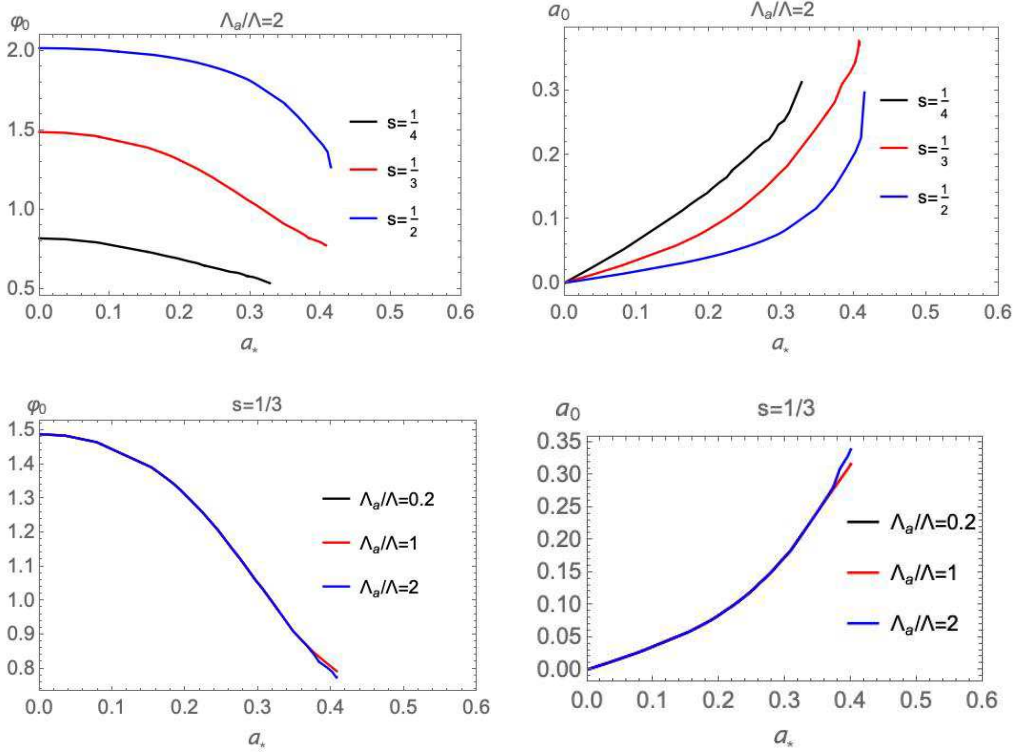


Figure 6: Plots of φ_0 and a_0 vs. a_* for a model with bulk functions (6.1) and brane functions (6.15). The bulk parameters are (6.3), and the brane parameters are (6.16), $\text{sign}(Q_{IR}) = -1$, $s = 1/4, 1/3, 1/2$ and $\Lambda_a/\Lambda = 0.2, 1, 2$. **Top row, left:** Plot of φ_0 for $s = 1/4, 1/3, 1/2$ and $\Lambda_a/\Lambda = 2$. **Top row, right:** Plot of a_0 for $s = 1/4, 1/3, 1/2$ and $\Lambda_a/\Lambda = 2$. **Bottom row, left:** Plot of φ_0 for $s = 1/3$ and $\Lambda_a/\Lambda = 0.2, 1, 2$. The various plots are near-indistinguishable. **Bottom row, right:** Plot of a_0 for $s = 1/3$ and $\Lambda_a/\Lambda = 0.2, 1, 2$. The various plots are near-indistinguishable.

a proof of principle that a simultaneous self-tuning of the cosmological constant and the EW breaking scale is possible. The crucial condition for achieving this is that X_H as a function of a_* changes sign for some value of a_* . However, for the choice of brane functions considered here, i.e. (6.9), a sign change in $X_H(a_*)$ does not occur for generic choice of the model parameters $s, \tilde{\Lambda}$. In the following section we shall hence consider a different choice of brane functions to see whether this short-coming of the example considered here can be overcome.

6.2 Brane potential choice 2: linear axion dependence of Higgs mass parameter

Here we make the following choice for the brane potentials in (3.3):

$$W_B = \frac{\Lambda^4}{M_p^3} \left[-1 - \frac{\varphi}{s} + \left(\frac{\varphi}{s} \right)^2 \right] = \tilde{\Lambda}^4 \left[-1 - \frac{\varphi}{s} + \left(\frac{\varphi}{s} \right)^2 \right] , \quad (6.15)$$

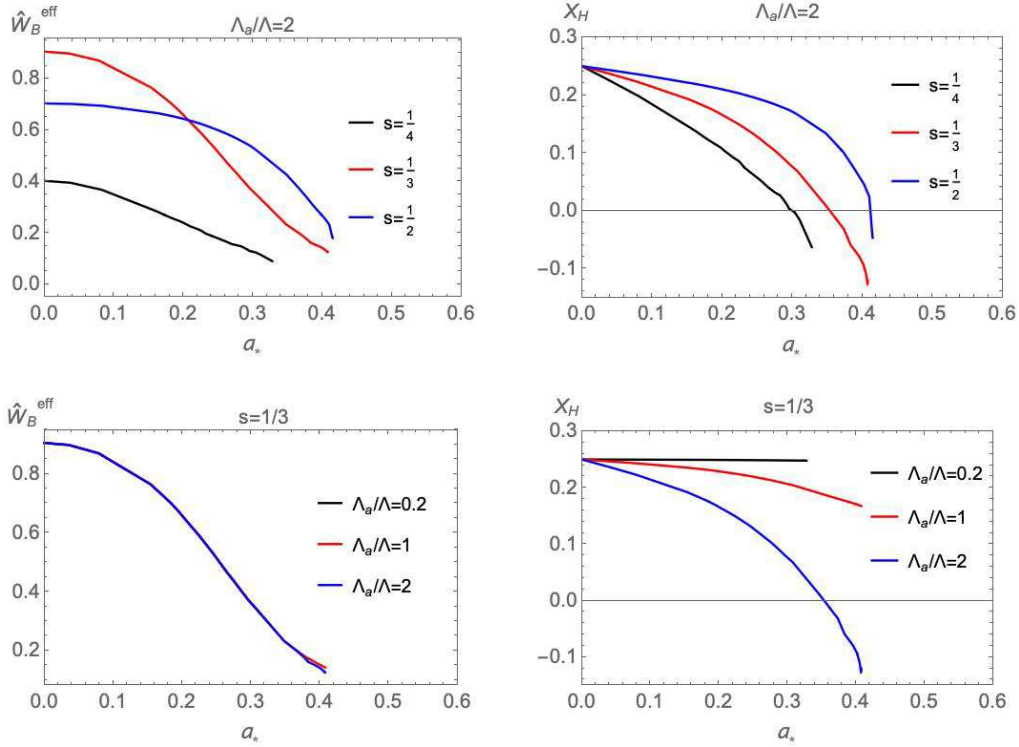


Figure 7: Plots of \hat{W}_B^{eff} (**left**) and X_H (**right**) at the brane position vs. a_* for a model with bulk functions (6.1) and brane functions (6.15). The bulk parameters are (6.3), and the brane parameters are (6.16), $\text{sign}(Q_{IR}) = -1$, $s = 1/4, 1/3, 1/2$ and $\Lambda_a/\Lambda = 0.2, 1, 2$. For top row panels, the brane position equation (6.8) with (4.32) have at most one solution for each s . For $s = 1/2$, the solution exists only for $D_{IR} \lesssim 1.5$. **Top row, left:** Plot of \hat{W}_B^{eff} for $s = 1/4, 1/3, 1/2$ and $\Lambda_a/\Lambda = 2$. **Top row, right:** Plot of X_H for $s = 1/4, 1/3, 1/2$ and $\Lambda_a/\Lambda = 2$. **Bottom row, left:** Plot of \hat{W}_B^{eff} for $s = 1/3$ and $\Lambda_a/\Lambda = 0.2, 1, 2$. The various plots are near-indistinguishable. **Bottom row, right:** Plot of X_H for $s = 1/3$ and $\Lambda_a/\Lambda = 0.2, 1, 2$.

$$X_H = \frac{\Lambda^2}{M_p} \left(1 - \frac{\Lambda_a^2}{\Lambda^2} a \right) = M_p^{1/2} \tilde{\Lambda}^2 \left(1 - \frac{\Lambda_a^2}{\Lambda^2} a \right) \quad , \quad S_H = M_p,$$

where Λ_a is a constant. The bulk potential and axion kinetic function are still given by (6.1) with parameters (6.3). The main difference with respect to the scenario examined in section 6.1 is the explicit axion dependence of the Higgs mass function X_H . Here we consider a linear dependence on the axion as in the original relaxion scenario [28] or as realised in the string-inspired setting of [52].

We further choose

$$\tilde{\Lambda} = 0.5, \tag{6.16}$$

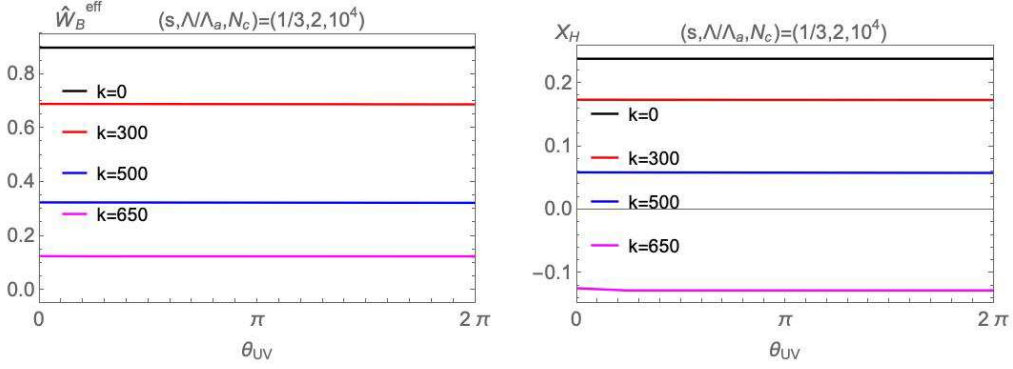


Figure 8: Plots of \hat{W}_B^{eff} (**left**) and X_H (**right**) at the brane position vs. θ_{UV} for a model with bulk functions (6.1) and brane functions (6.15). The model parameters are (6.3), (6.16), $s = 1/3$, $\Lambda_a/\Lambda = 2$, $N_c = 10^4$. Here the branches for $k = 0, 300, 500, 650$ are shown.

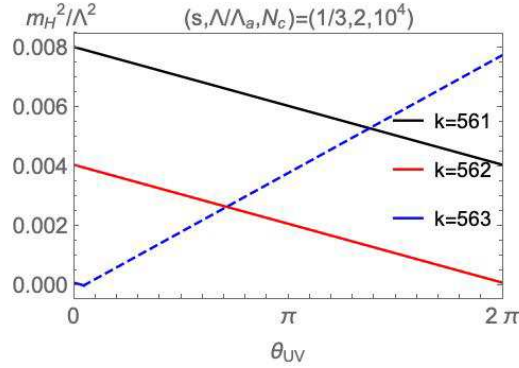


Figure 9: Plot of the Higgs mass squared m_H^2 (4.24) in units of Λ^2 vs. θ_{UV} for a model with bulk functions (6.1) and brane functions (6.15). The model parameters are (6.3), (6.16), $s = 1/3$, $\Lambda_a/\Lambda = 2$, $N_c = 10^4$. We plot the lines with $k = 561, 562, 563$, corresponding to the branches realizing the small Higgs mass. Note that, for $0 \leq \theta_{UV} \lesssim 0.05\pi$, the symmetric and broken phase correspond to $k \leq 563$ and $k \geq 564$, respectively. For $0.05\pi \lesssim \theta_{UV} < 2\pi$, the symmetric and broken phases correspond to $k \leq 562$ and $k \geq 563$. In the figure, the symmetric and broken phases are represented by the solid and dashed lines, respectively.

and vary s and Λ_a/Λ . We take the following as representative values:

$$s = \frac{1}{4}, \frac{1}{3}, \frac{1}{2}, \quad \frac{\Lambda_a}{\Lambda} = 0.2, 1, 2. \quad (6.17)$$

We again derive the brane position by solving (6.8) and (4.32). As in section 6.1 we can plot the various brane quantities as functions of a_* . In fig. 6 we hence display φ_0, a_0 vs. a_* , while in fig. 7 we show the brane cosmological constant \hat{W}_B^{eff}

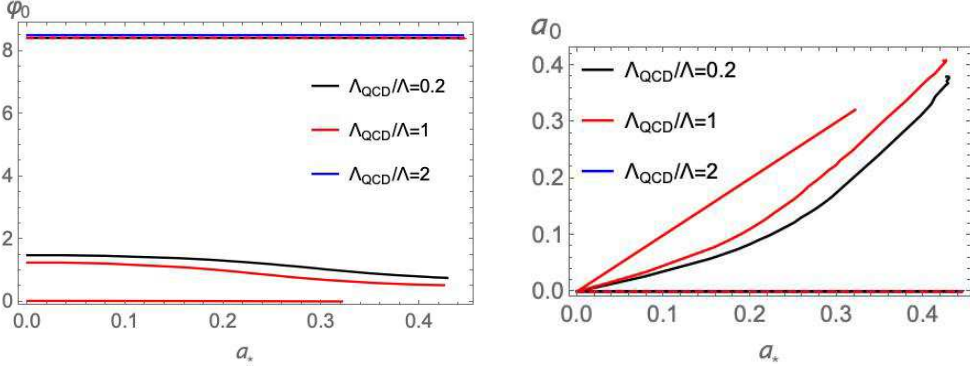


Figure 10: Plots of φ_0 (**left**) and a_0 (**right**), i.e. the values of φ and a at the brane position, vs. a_* for a model with bulk functions (6.1) and brane functions (6.18). The bulk parameters are (6.3), and the brane parameters are (6.19), and $\Lambda_{QCD}/\Lambda = 0.2, 1, 2$. There are two, three and one solutions of the brane position equation (6.8) with (4.32) for $\Lambda_{QCD}/\Lambda = 0.2, 1, 2$, respectively. In the left (right) panel, the three lines for $\varphi_0 \sim 8.5$ ($a_0 \sim 0$) almost overlap one another.

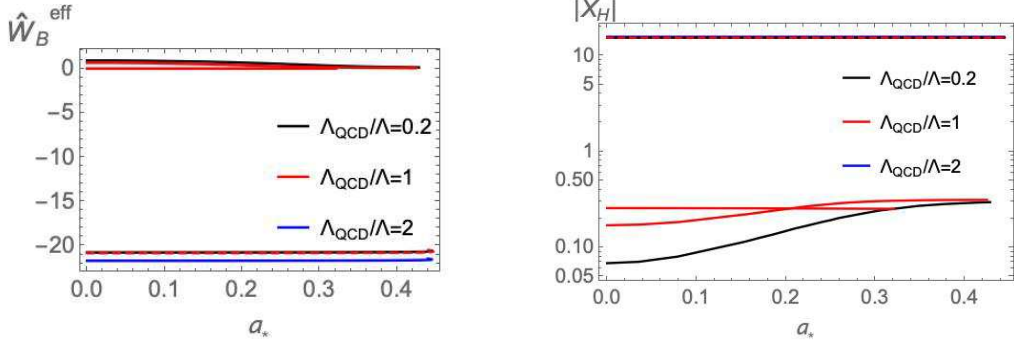


Figure 11: Plots of \hat{W}_B^{eff} (**left**) and $|X_H|$ (**right**) at the brane position vs. a_* for a model with bulk functions (6.1) and brane functions (6.18). The bulk parameters are (6.3), and the brane parameters are (6.19), and $\Lambda_{QCD}/\Lambda = 0.2, 1, 2$. There are two, three and one solutions of the brane position equation (6.8) with (4.32) for $\Lambda_{QCD}/\Lambda = 0.2, 1, 2$, respectively. In the left panel, three lines $\hat{W}_B^{eff} \sim 0$ almost overlap one another while two lines $\hat{W}_B^{eff} \sim -21$ also overlap one another. In the right panel, three lines at $|X_H| \sim 15$ almost overlap one another.

and the Higgs mass parameter X_H as functions of a_* . The top row panels in figures 6, 7 correspond to $\Lambda_a/\Lambda = 2$ with $s = 1/4, 1/3, 1/2$. There is only one branch of solutions to the junction conditions for every parameter choice here. The bottom row panels in figures 6, 7 correspond to $\Lambda_a/\Lambda = 0.2, 1, 2$ with $s = 1/3$.

We are mainly interested in the possibility of solutions with a small Higgs mass. Recall that such solutions generically exist if X_H as a function of a_* exhibits a sign

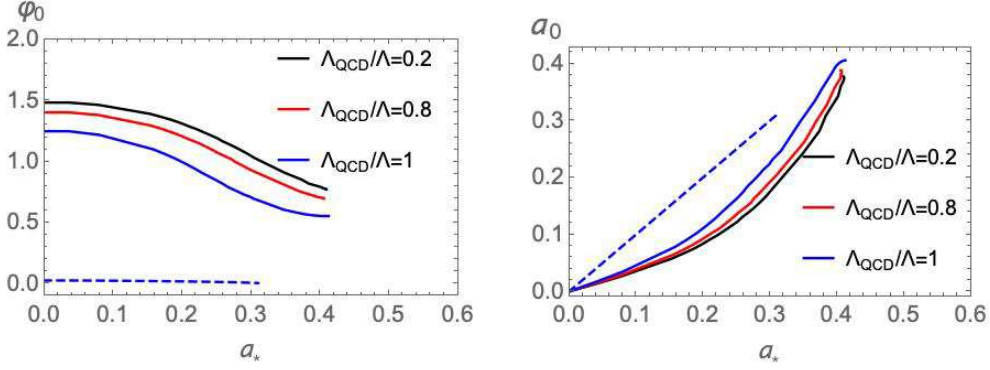


Figure 12: Plots of φ_0 (**left**) and a_0 (**right**), i.e. the values of φ and a at the brane position, vs. a_* for a model with bulk functions (6.1) and brane functions (6.21). The bulk parameters are (6.3), and the brane parameters are (6.22) and $\Lambda_{QCD}/\Lambda = 0.2, 0.8, 1$. For $\Lambda_{QCD}/\Lambda = 0.2$, there are two solutions of (6.8) with (4.32), which we denote by the solid and dashed lines.

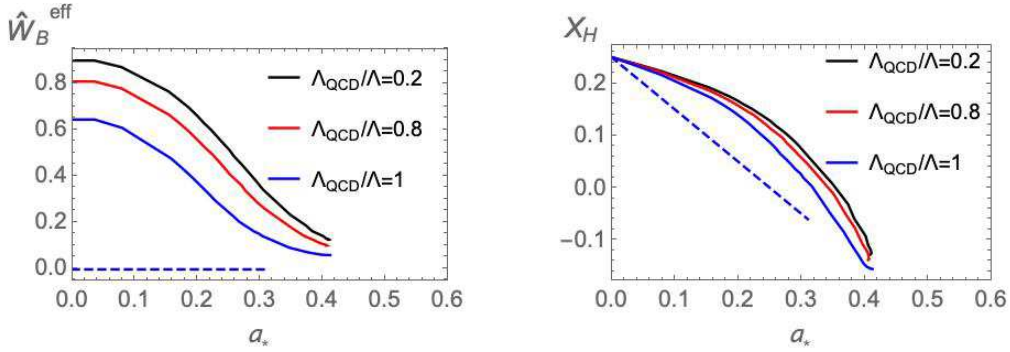


Figure 13: Plots of \hat{W}_B^{eff} (**left**) and X_H (**right**) at the brane position vs. a_* for a model with bulk functions (6.1) and brane functions (6.21). The bulk parameters are (6.3), and the brane parameters are (6.22) and parameters. For $\Lambda_{QCD}/\Lambda = 0.2$, there are two solutions of (6.8) with (4.32), which we denote by the solid and dashed lines.

change (see the discussion in section 6.1). Here we find that this is the case for all solutions we considered with $\Lambda_a/\Lambda = 2$. Overall, we observe that for the brane functions considered here it is much easier to find solutions where $X_H(a_*)$ changes sign compared to the choice for the brane functions in sec. 6.1. That is, an explicit axion-dependence in X_H as in (6.15) is advantageous for finding solutions with a small Higgs mass.

Using (2.46) we can again write a function of a_* as a multi-branched function of θ_{UV} as we have done in sec. 6.1. To be specific, we pick the example with model parameters $s = 1/3$, $\Lambda_a/\Lambda = 2$ which exhibits a sign change in $X_H(a_*)$. In figure 8 we

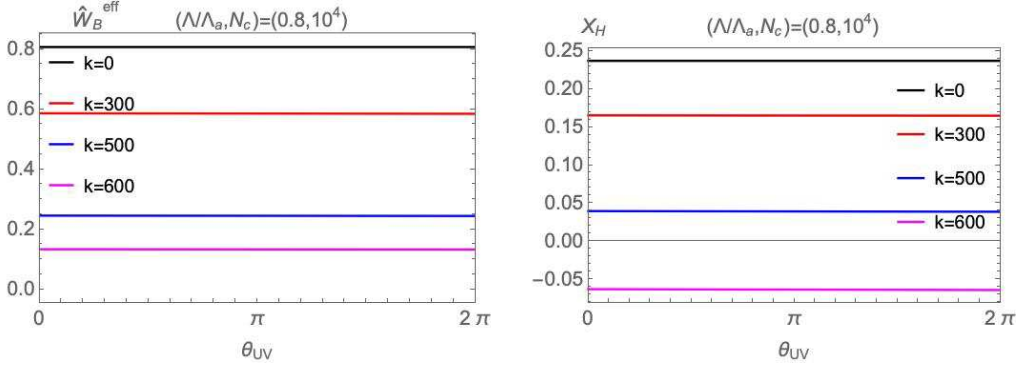


Figure 14: Plots of \hat{W}_B^{eff} and X_H at the brane position vs. θ_{UV} for a model with bulk functions (6.1) and brane functions (6.21). The bulk parameters are (6.3), and the brane parameters are (6.22), $\Lambda_{QCD}/\Lambda = 0.8$, and $N_c = 10^4$.

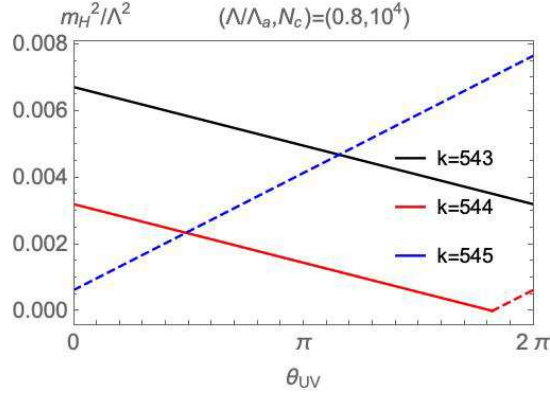


Figure 15: Plot of the Higgs mass squared m_H^2 (4.24) at the brane position vs. θ_{UV} for a model with bulk functions (6.1) and brane functions (6.21). The model parameters are (6.3), (6.22), $\Lambda_{QCD}/\Lambda = 0.8$, and $N_c = 10^4$. We plot the lines with $k = 543, 544, 545$, corresponding to the branches realizing the small Higgs mass. In the figure, the symmetric and broken phases are represented by the solid and dashed lines, respectively.

then plot \hat{W}_B^{eff} and X_H as functions of θ_{UV} for this model, further choosing $c = 1$ and $N_c = 10^4$. For better visibility we only show the branches with $k = 0, 300, 500, 650$. Then, for this example, we can find that the branches with the lowest value of the Higgs mass can be found for $k \sim 562$. In figure 9 we plot of ratio of Higgs mass squared m_H^2 defined in (4.24) and the scale Λ for the branches with $k = 561, 562, 563$. In the figure, solid and dashed lines correspond to solutions with intact and broken EW symmetry, respectively. For the branches displayed one finds $m_H^2/\Lambda^2 = \mathcal{O}(10^{-3})$, i.e. the solutions exhibit a hierarchy between $|m_H|$ and the UV cutoff scale on the brane Λ . The numerical separation between $|m_H|$ and Λ can be further increased by

choosing a larger value for N_c .

6.3 Brane potential choice 3: axion cosine potential

Once more, the bulk potential and axion kinetic function are given by (6.1) with parameter choice (6.3). For the brane potentials (3.3) we now take

$$\begin{aligned} W_B &= \frac{1}{M_p^3} \left\{ \Lambda^4 \left[-1 - \frac{\varphi}{s} + \left(\frac{\varphi}{s} \right)^2 \right] + \Lambda_{QCD}^4 \cos(a) \right\} \\ &= \tilde{\Lambda}^4 \left[-1 - \frac{\varphi}{s} + \left(\frac{\varphi}{s} \right)^2 + \frac{\Lambda_{QCD}^4}{\Lambda^4} \cos(a) \right], \end{aligned} \quad (6.18)$$

$$X_H = \frac{\Lambda^2}{M_p} \left[1 + \frac{\varphi}{s_X} - \left(\frac{\varphi}{s_X} \right)^2 \right] = M_p^{1/2} \tilde{\Lambda}^2 \left[1 + \frac{\varphi}{s_X} - \left(\frac{\varphi}{s_X} \right)^2 \right], \quad S_H = M_p,$$

where Λ_{QCD} is a dimension one parameter. That is, here we revert to an axion-independent Higgs mass parameter X_H as in section 6.1, but now the brane potential W_B is given a periodic dependence on a as observed in the instanton-generated potential axion potential in QCD. We take

$$s = 1/3, \quad s_X = 1, \quad \tilde{\Lambda} = 0.5, \quad (6.19)$$

and vary Λ_{QCD}/Λ . As representative values, we take

$$\frac{\Lambda_{QCD}}{\Lambda} = 0.2, 1, 2. \quad (6.20)$$

The dilaton and axion field value at the brane position as functions of a_* are plotted in figure 10 with the parameters (6.3), (6.19), and $\Lambda_{QCD}/\Lambda = 0.2, 1, 2$. For the same parameter set, the brane cosmological constant \hat{W}_B^{eff} and the absolute value of Higgs mass parameter $|X_H|$ are shown in figure 11 as functions of a_* . There are two, three and one solutions of the brane position equation (6.8) with (4.32) for $\Lambda_{QCD}/\Lambda = 0.2, 1, 2$, respectively. The brane cosmological constant \hat{W}_B^{eff} is generically of the order $\sim \tilde{\Lambda}^4$. For the parameter values chosen here X_H does not change sign as a function of a_* , nor does it closely approach zero anywhere. For the (generic) parameter choices considered here, we are not able to find solutions with a small Higgs mass. Therefore, we conclude that the sinusoidal axion dependence of the brane potential W_B is generically not helpful for the existence of saddle points with a small Higgs mass.

6.4 Brane potential choice 4: $\Lambda_{QCD} + \Lambda_a$

In the final numerical example we include both a periodic axion dependence in W_B as in section 6.3 while at the same time allowing for a linear dependence of X_H on a

as in section 6.2. Hence here the brane potentials are given by

$$\begin{aligned}
W_B &= \frac{1}{M_p^3} \left\{ \Lambda^4 \left[-1 - \frac{\varphi}{s} + \left(\frac{\varphi}{s} \right)^2 \right] + \Lambda_{QCD}^4 \cos(a) \right\} \\
&= \tilde{\Lambda}^4 \left\{ \left[-1 - \frac{\varphi}{s} + \left(\frac{\varphi}{s} \right)^2 \right] + \frac{\Lambda_{QCD}^4}{\Lambda^4} \cos(a) \right\}, \tag{6.21}
\end{aligned}$$

$$X_H = \frac{\Lambda^2}{M_p} \left(1 - \frac{\Lambda_a^2}{\Lambda^2} a \right), \quad S_H = M_p.$$

with

$$s = 1/3, \quad \tilde{\Lambda} = 0.5, \quad \Lambda_a/\Lambda = 2. \tag{6.22}$$

As in the previous subsection, we vary Λ_{QCD}/Λ and we show results for the representative values:

$$\frac{\Lambda_{QCD}}{\Lambda} = 0.2, 0.8, 1. \tag{6.23}$$

In figure 12 we plot the dilaton and axion at the brane locus, φ_0 , a_0 , as functions of a_* for $\Lambda_{QCD}/\Lambda = 0.2, 0.8, 1$. In figure 13 we plot the corresponding values for \hat{W}_B^{eff} and X_H at the brane locus as functions of a_* . Note that modifying Λ_{QCD}/Λ does not affect the solutions much, as φ_0, a_0 in fig. 13 or \hat{W}_B^{eff}, X_H in fig. 14 do not differ significantly for different values of Λ_{QCD}/Λ . Hence the effect of the $\cos(a)$ -term in W_B on the overall solution is fairly mild. However, from fig. 13 we observe that for all parameter choices considered the Higgs mass parameter as a function of a_* exhibit a sign change. This can be traced back to the linear axion-dependence of X_H as in section 6.2, which facilitates the appearance of a sign change in $X_H(a_*)$. As observed previously, this sign change will guarantee the existence of saddle points with a small Higgs mass, which therefore arise generically in the model considered here.

Focussing on the solution with $\Lambda_{QCD}/\Lambda = 0.8$ we once more rewrite \hat{W}_B^{eff} and X_H as multi-branched functions of θ_{UV} with the help of (2.46). Here we choose $c = 1$ and $N_c = 10^4$. The corresponding plots can be seen in fig. 14 where for visibility we only display the branches for $k = 0, 300, 500, 600$. For this solution the minimal value for the Higgs mass squared is observed on the branches with $k \sim 544$. In fig. 15 we plot of ratio of Higgs mass squared m_H^2 defined in (4.24) and the scale Λ defined in (6.22) for the branches with $k = 543, 544, 545$. In the figure, solid and dashed lines correspond to solutions with intact and broken EW symmetry, respectively. For the branches displayed one finds $m_H^2/\Lambda^2 = \mathcal{O}(10^{-3})$ for generic θ_{UV} , i.e. the solutions exhibit a hierarchy between $|m_H|$ and the UV cutoff scale on the brane Λ . The numerical separation between $|m_H|$ and Λ can be further increased by choosing a larger value for N_c .

6.5 Summary of the section

Our goal in this section has been to numerically check the existence of vacua which realize the self-tuning of the cosmological constant as well as a large electroweak hierarchy. A small Higgs mass is obtained if the Higgs mass parameter X_H as a function of a_* exhibits at least one zero. If this happens, we expect that, around this value, we will have electroweak symmetry breaking with a small Higgs mass. Then, for any value of θ_{UV} , as long as there exist branches that satisfy

$$c \frac{\theta_{UV} + 2\pi k}{N_c} \approx a_{*,0} \quad (6.24)$$

these correspond to vacua with a small Higgs mass. We performed a numerical analysis for static solutions of our brane-bulk system for four types of the brane potentials (6.9, 6.15, 6.18, 6.21). Here we summarize the main observations from this section.

- In section 6.1, we used brane potentials (6.9) which only depend on the bulk scalar φ , but not the axion a . In this case the effect of axion backreaction on brane quantities only enters via a shift in the value of the brane position φ_0 . We observed that φ_0 typically exhibits $\mathcal{O}(1)$ shifts when we take into account the axion backreaction (Top row, left panel in figure 2). Correspondingly, the effective Higgs potential on the brane changes. In particular, we find that (for certain choices of model parameters) there exist solutions where the Higgs mass parameter X_H crosses zero as a function of the axion source. In this case, we find that there exist saddle points which allow for a small Higgs mass (figure 5).
- In section 6.2, we used a brane potential (6.15), where the Higgs mass function X_H depends linearly on the axion a . If this linear coupling is large enough, by increasing the value of the axion source, the Higgs mass parameter X_H generically changes sign as a function of the axion source (figure 7). The model is reminiscent of the relaxion scenario whose mechanism will be compared to our setup in section 7.
- In section 6.3, we used brane potentials where the brane cosmological constant depends on the axion as $\sim \cos(a)$, with a coefficient of the order of SM scales, see (6.18). This is the standard QCD-instanton-generated potential. The effect of $\cos(a)$ on the dynamics is mild. It only slightly changes the brane position φ_0 . For the parameter choices given in section 6.3, we do not obtain a sign change of X_H . All branches parameterized by k have the same sign for X_H .
- In section 6.4, we used the brane potentials (6.21). Here the Higgs mass function depends linearly on the axion a , and the brane cosmological constant is

proportional to $\cos(a)$. This is a combination of the ansätze in 6.2 and 6.3. As in section 6.2, we can easily obtain solutions with a “small” Higgs mass (figure 15). The effect of $\cos(a)$ on the brane cosmological constant and Higgs mass is not large even if we take Λ_{QCD} to be of the order of the cutoff Λ (figure 13).

7. The gauge hierarchy problem and outlook

A formulation of solutions in brane-world models in terms of holographic RG flows has been shown to be advantageous for realizing self-tuning of the cosmological constant [7]. Here we observe that generalizing to axionic RG flow solutions leads to further promising applications in brane-world phenomenology. As discussed in section 6, thanks to the relation (2.46), adding a non-trivial axion provides an avenue for obtaining a large number of inequivalent vacua (parametrized by a different periodicity branch of the θ -angle and therefore a different parameter a_\star) over which to scan,²⁵ with possibly different physical properties such as the Higgs mass and vev. This may help finding a stabilized vacuum with a naturally small value of the Higgs mass, as in the relaxion scenario [28].

Indeed, in figures 4, 8, and 14, we found that different values of the Higgs mass are realized in different axionic saddle points labelled by k . Especially, when the Higgs mass squared parameter X_H crosses zero as a function of the axion source a_\star , the Higgs expectation value is much smaller than the cutoff scale of the brane physics Λ . This can be obtained in one of the axionic vacua parametrized by k , for sufficiently large N_c , as we observed in figures 5, 9, and 15.

A first question is whether the setup can accommodate a large hierarchy of scales, like many orders of magnitude as the naive version of the cosmological constant problem suggests.²⁶ This has two sub-questions, the first addressing the cosmological constant self-tuning mechanism and the second the existence of small Higgs mass vacua. These two questions are currently under study.

If the answer to the previous two questions is in the affirmative, the next question to ask is how the vacuum realizing the light Higgs mass is selected in our world. If the vacuum with a small Higgs mass minimizes the free energy (4.34), then the system evolves to this state after a sufficiently long time.

On the other hand, if the vacuum with a small Higgs mass does not minimize the free energy (4.34), this state could be realized as a metastable vacuum. In the absence of the brane, it is well known that the minimum free energy occurs for minimal values of $k = 0, 1$. However, the brane contributes importantly to the free energy and the minimization problem becomes complex, especially as it is affected by the scalar-dependent functions on the brane.

²⁵Different mechanisms to scan the Higgs mass are proposed in [53, 54, 55, 56].

²⁶The actual hierarchy scale may be smaller as running bulk fields may also contribute to this.

As was done already for the self-tuning setup, the relevant dynamics is the bulk motion of the brane that will generate the associated cosmology. This was studied in the absence of the axion in [38, 28, 19] in the probe approximation, which is solvable. What was found is that the setup corresponds to a brane moving in a radial bulk potential whose minimum (or minima) are at the positions which correspond to a stabilised flat brane, where the vacuum energy is cosmologically invisible. Once the brane starts in a different bulk position it will move generating a non-trivial brane cosmology. This motion is affected, beyond the initial velocity and potential, by the presence of matter densities on the brane and brane-bulk energy exchange, [39, 40].

In our case, we have two effects which can happen in tandem, and which can change the position of the brane: the first is a semiclassical tunneling that interpolates between different k -bulk solutions; the second is classical brane motion in a single bulk solution which will also be affected by the axion.

For the second effect, we expect a similar behavior to the one mentioned above, but now the brane motions will also be affected by the axion. The solutions we found for different values of the integer k (the oblique vacua of the dual QFT) will correspond to the minima of the effective potential felt by the brane. It is important to find how the system may evolve to the metastable vacuum by studying the associated cosmology. At the same time, the lifetime of this vacuum should be long enough. An alternative possibility is to rely on anthropic arguments for the Higgs mass [41, 42, 43, 44, 45].

We finally compare our scenario to the standard relaxion scenario [28]. The scalar potential of the relaxion model is given by

$$V = (\Lambda^4 - \Lambda^2 g \tilde{a} + \dots) + (\Lambda^2 - g \tilde{a} + \dots) |H|^2 + \Lambda_{QCD}^4 \cos\left(\frac{\tilde{a}}{f_a}\right), \quad (7.1)$$

where Λ is the cutoff scale, \tilde{a} is the relaxion, f_a is the relaxion decay constant, and g is the shift-symmetry-breaking small parameter which has mass dimension one. In order to obtain the vacua, a certain balance between the ga term and $\cos(a)$ needs to be imposed,

$$\Lambda^2 g \sim \frac{\Lambda_{QCD}^4}{f_a}, \quad (7.2)$$

which indicates that the parameter g needs to be hierarchically small.

On the other hand, in our brane potential (6.15), such an extreme fine-tuning of couplings is not required, because the existence of the multiple axionic vacua emerges naturally from holography (2.46). From the 4d dual field theory viewpoint, the brane scalar potential can be written as

$$V = (\Lambda^2 - \Lambda_a^2 a) \frac{|\tilde{H}|^2}{T_H} + \dots \sim \left(\Lambda^2 - \frac{\Lambda_a^2}{N_c} (\theta_{UV} + 2\pi k) \right) \frac{|\tilde{H}|^2}{T_H} + \dots, \quad (7.3)$$

where the canonical Higgs field is

$$\tilde{H} \equiv \frac{M_P}{\sqrt{T_H(\varphi_0, a_0)}} H. \quad (7.4)$$

and ... in eq. (7.3) stands for terms in the scalar potential other than the Higgs mass term. In the second expression for V in eq. (7.3), we used $a \sim (\theta_{UV} + 2\pi k)/N_c$ assuming that $a \sim a_*$ and $c = 1$ in (2.46).²⁷ From (7.3) and for large N_c , the coupling between the θ_{UV} and \tilde{H} is suppressed. In this sense, in our scenario, the breaking of the shift symmetry of θ_{UV} is small, as in the relaxion model.

Acknowledgements

We would like to thank Pascal Anastasopoulos, Mina Arvanitaki, Panos Betzios, Savas Dimopoulos, Matti Järvinen and Olga Papadoulaki for discussions.

This work was supported in part by the European Union via the Advanced ERC grant SM-GRAV, No 669288. LW also acknowledges support from the European Research Council under the European Union's Horizon 2020 research and innovation programme (grant agreement No 758792, project GEODESI).

²⁷This assumes that the equilibrium position of the brane is near the IR end point where the value of a becomes very small.

APPENDIX

A. Calculation of on-shell action, free energy and topological susceptibility

In this Appendix, we present the calculation of the on-shell action and free energy. The bulk and brane actions are given in (2.1, 3.2, 3.3). The relevant calculation of the Einstein-dilaton-axion theory without the brane was performed in [24].

First, we calculate the on-shell bulk action. From the metric ansatz (2.4), we obtain

$$R = -8\ddot{A} - 20\dot{A}^2 = \frac{1}{2}\dot{\varphi}^2 + \frac{1}{2}Y\dot{a}^2 + \frac{5}{3}V. \quad (\text{A.1})$$

In the second equality, (2.5) and (2.6) are used. Substituting (A.1) into (2.1), the bulk on-shell action is

$$\begin{aligned} S_{\text{bulk, on-shell}} &= M_p^3 \int d^4x \left(\int_{u_0}^{u_{IR}} du + \int_{u_{UV}}^{u_0} du \right) e^{4A} \left[R - \frac{1}{2}\dot{\varphi}^2 - \frac{1}{2}Y\dot{a}^2 - V \right] + S_{GHY} \\ &= \frac{2}{3}M_p^3 V_4 \left(\int_{u_0}^{u_{IR}} du + \int_{u_{UV}}^{u_0} du \right) e^{4A} V + S_{GHY} \\ &= -2M_p^3 V_4 \left\{ \left(\left[e^{4A} \dot{A} \right]_{u_{IR}} - \left[e^{4A} \dot{A} \right]_{u_0+\epsilon} \right) + \left(\left[e^{4A} \dot{A} \right]_{u_0-\epsilon} - \left[e^{4A} \dot{A} \right]_{u_{UV}} \right) \right\} + S_{GHY} \end{aligned} \quad (\text{A.2})$$

where V_4 is the 4-dimensional space-time volume, (A.1) has been used in the second line, and in the third line, we used

$$V = -3\ddot{A} - 12\dot{A}^2. \quad (\text{A.3})$$

For the Gibbons-Hawking-York term, we obtain

$$S_{GHY} = -8M_p^3 V_4 \left\{ \left(\left[e^{4A} \dot{A} \right]_{u_{UV}} - \left[e^{4A} \dot{A} \right]_{u_0-\epsilon} \right) + \left(\left[e^{4A} \dot{A} \right]_{u_0+\epsilon} - \left[e^{4A} \dot{A} \right]_{u_{IR}} \right) \right\}. \quad (\text{A.4})$$

Here we are exclusively interested in solutions which have a behavior in the IR (i.e. for $\varphi \rightarrow +\infty$) as described in section 2.2. The corresponding expression for W and A as functions of φ can be read from the equations (2.26, 2.38, 2.40). Using these expressions and (2.24), the IR contribution to the on-shell action can be shown to give

$$\left[e^{4A} \dot{A} \right]_{\text{IR}} \sim \left[e^{4A} W \right]_{\varphi \rightarrow +\infty} \sim e^{-\frac{8-3b^2}{6b}\varphi}. \quad (\text{A.5})$$

Note that if the parameter b satisfies the Gubser bound (2.43) the exponent in the above is negative and the IR contribution vanishes.

Combining (2.24), (A.2) and (A.4) we arrive at

$$\begin{aligned}
S_{\text{bulk, on-shell}} &= -6M_p^3 V_4 \left\{ \left[e^{4A} \dot{A} \right]_{uUV} - \left[\frac{1}{6} e^{4A_0} W \right]_{UV}^{IR} \right\} \\
&= -6M_p^3 V_4 \left[e^{4A} \dot{A} \right]_{uUV} + M_p^3 V_4 e^{4A_0} W_B^{eff}(\varphi_0, a_0),
\end{aligned} \tag{A.6}$$

Next, we calculate the on-shell brane action starting from (3.1, 3.2, 3.3). As for S_g , the only nonzero term is the brane cosmological constant term W_B by using (2.4). Similarly, we can observe that the first and last terms in (3.3) vanish on-shell. Therefore, we obtain

$$\begin{aligned}
S_{\text{brane, on-shell}} &= M_p^3 V_4 e^{4A_0} \left[-W_B(\varphi_0, a_0) - X(\varphi_0) |H|^2 - S_H(\varphi_0) |H|^4 \right] \\
&= -M_p^3 V_4 e^{4A_0} W_B^{eff}(\varphi_0, a_0),
\end{aligned} \tag{A.7}$$

where W_B^{eff} is defined in (4.28).

In total, the on-shell action is

$$S_{\text{on-shell}} = S_{\text{bulk, on-shell}} + S_{\text{brane, on-shell}} = -6M_p^3 V_4 \left[e^{4A} \dot{A} \right]_{uUV} = M_p^3 V_4 \left[e^{4A} W \right]_{UV}, \tag{A.8}$$

where (2.24) is used in the last equality. This is the same form as the case without the brane [24]. As we can observe from (2.26, 2.34, 2.36), the on-shell action as written in (A.8) is divergent and requires renormalization. The procedure of renormalization is same as for the case without the brane. The divergences can be removed by adding a counterterm S_{ct} to the on-shell action (see e.g. [58]), with S_{ct} given by

$$S_{ct} = -M_p^3 \left[\int d^4 x \sqrt{|\gamma|} W_{ct}(\varphi) \right]_{\substack{u=\ell \log \epsilon \\ \varphi=\varphi(\ell \log \epsilon)}} = -(M_p \ell)^3 V_4 |\varphi_-|^{\frac{4}{\Delta_-}} \left[\Lambda^4 \ell W_{ct}(\varphi_\epsilon) \right], \tag{A.9}$$

where

$$\Lambda \equiv \frac{e^{A(u)}}{\ell |\varphi_-|^{1/\Delta_-}} \Big|_{u=\ell \log \epsilon}. \tag{A.10}$$

The function W_{ct} is defined as the solution of equation (2.29) with $T = 0$, i.e.

$$\frac{1}{3} W_{ct}^2 - \frac{1}{2} (W'_{ct})^2 + V = 0. \tag{A.11}$$

One can show that the renormalized on-shell action can be written as

$$S_{\text{on-shell}}^{\text{ren}} = M_p^3 V_4 \ell^3 |\varphi_-|^{\frac{4}{\Delta_-}} (C_{UV}(q_{UV}) - C_{UV,ct}). \tag{A.12}$$

As in the case without the brane, $C_{UV,ct}$ is a free parameter corresponding to the choice of the renormalization scheme, and $C_{UV}(q_{UV})$ depends on q_{UV} (or a_*) through

the IR regularity condition. The relation between q_{UV} and a_* is given through (4.30) and (B.14). The free energy is given by $-S_{\text{on-shell}}^{\text{ren}}$:

$$\begin{aligned} F_k &\equiv -S_{\text{on-shell}}^{\text{ren}} = - (M_p \ell)^3 V_4 |\varphi_-|^{\frac{4}{\Delta_-}} (C_{UV}(q_{UV,k}) - C_{UV,ct}), \\ &= - (M_p \ell)^3 V_4 |\varphi_-|^{\frac{4}{\Delta_-}} \left[C_{UV} \left(\frac{\theta_{UV} + 2\pi k}{N_c} \right) - C_{UV,ct} \right]. \end{aligned} \quad (\text{A.13})$$

where we have written the k -dependence of q_{UV} explicitly for clarity. Note that this exhibits several features familiar from QCD. The parameter φ_- corresponds to the mass scale of the theory and is the analogue of Λ_{QCD} .²⁸ Further, like in QCD, there is another dimensionless coupling which here is given by θ_{UV} . As C_{UV} is a dimensionless parameter, it only depends on the dimensionless coupling θ_{UV} (through q_{UV}). Then, we can recognize in (A.13) the structure of the free energy familiar from large N_c QCD [25, 59, 26], i.e.

$$F_k \sim \Lambda_{\text{QCD}}^4 V \left(\frac{\theta_{UV} + 2\pi k}{N_c} \right). \quad (\text{A.14})$$

This is a general feature of holographic QCD-like theories [60].

The physical free energy is the minimization over k of the free energies F_k for fixed θ_{UV} .

$$F(\varphi_-, \theta_{UV}) = \text{Min}_{k \in \mathbb{Z}} F_k(\varphi_-, \theta_{UV}). \quad (\text{A.15})$$

The topological susceptibility becomes

$$\chi \equiv \frac{1}{V_4} \frac{\partial^2 F}{\partial \theta_{UV}^2} = - \text{Min}_k |\varphi_-|^{\frac{4}{\Delta_-}} \frac{(M_p \ell)^3}{N_c^2} \frac{\partial^2 C_{UV}(a_{*,k})}{\partial a_{*,k}^2} \Big|_{a_{*,k} = \frac{\theta_{UV} + 2\pi k}{N_c}} \quad (\text{A.16})$$

A.1 Small axion backreaction approximation

At small q_{UV} , the free energy can be written as

$$\begin{aligned} F_k &= F^{(q0)} + q_{UV,k} F^{(q1)} + \mathcal{O}(q_{UV,k}^2) \\ &= - (M_p \ell)^3 V_4 |\varphi_-|^{\frac{4}{\Delta_-}} \left[(C_{UV}^{(q0)} - C_{UV,ct}) + C_{UV}^{(q1)} q_{UV,k} + \mathcal{O}(q_{UV,k}^2) \right], \end{aligned} \quad (\text{A.17})$$

where the expression of $C_{UV}^{(q1)}$ can be found in (B.27).

Next, from (B.28), we observe that

$$q_{UV,k} = \frac{1}{f^2} a_{*,k}^2 \quad (\text{A.18})$$

²⁸In the case at hand φ_- is a dimensionful coupling, but one can also modify the setup so that the operator deforming the UV theory is marginally relevant like the QCD coupling. This can be achieved by setting the mass term to zero the UV expansion of the potential, in which case the running is driven by the cubic or higher terms [46]. Alternatively one can realize the UV as a runaway AdS solution, as in the Improved Holographic QCD models [49]. In either case, the scale Λ_{QCD} is dynamically generated.

at leading order for small axion backreaction. Note that $q_{UV,k}$ is positive due to equations (2.26) and (2.36), and the constant f is defined by the last line of (B.28). Then, the free energy becomes

$$F_k = F^{(q_0)} - V_4 |\varphi_-|^{\frac{4}{\Delta_-}} (M_p \ell)^3 \frac{C_{UV}^{(q_1)}}{f^2} a_{*,k}^2 + \mathcal{O}((a_{*,k})^4). \quad (\text{A.19})$$

Note that the subsubleading term is $\mathcal{O}(a_{*,k}^4)$ because we assume CP invariance.

Finally, using the relation (2.46) between a_* and the theta-parameter θ_{UV} one obtains

$$F_k = F^{(q_0)} - V_4 |\varphi_-|^{\frac{4}{\Delta_-}} \frac{(M_p \ell)^3 C_{UV}^{(q_1)}}{N_c^2 f^2} (\theta_{UV} + 2\pi k)^2 + \mathcal{O}(N_c^{-2}). \quad (\text{A.20})$$

From the definition (A.16) of the topological susceptibility, we obtain

$$\chi = -2 |\varphi_-|^{\frac{4}{\Delta_-}} \frac{(M_p \ell)^3 C_{UV}^{(q_1)}}{N_c^2 f^2} + \mathcal{O}(N_c^{-2}), \quad (\text{A.21})$$

at leading order for small axion backreaction. The leading order of χ is $\mathcal{O}(N_c^0)$ because we identify $(M_p \ell)^3 \sim N_c^2$ in holography.

B. Small axion backreaction approximation

First, we derive the relation between Q_{IR} and q_{UV} . From (4.29) and (4.31), Q_{IR} is

$$\begin{aligned} Q_{IR} &= \text{sign}(Q_{UV}) \frac{\sqrt{q_{UV}}}{\ell} \left(\ell |\varphi_-|^{\frac{1}{\Delta_-}} \right)^4 + Y_0 e^{4A_0} \frac{\partial \hat{W}_B^{eff}}{\partial a}(\varphi_0, a_0) \quad (\text{B.1}) \\ &= \text{sign}(Q_{UV}) \frac{\sqrt{q_{UV}}}{\ell} \left(\ell |\varphi_-|^{\frac{1}{\Delta_-}} \right)^4 - Y_0 e^{4A_0} \frac{\partial^2 \hat{W}_B^{eff}}{\partial a^2}(\varphi_0, 0) Q_{IR} \int_{u_0}^{u_{IR}} \frac{du}{Y e^{4A}} + \mathcal{O}(q_{UV}), \end{aligned}$$

from which we obtain

$$\ell Q_{IR} = \frac{\text{sign}(Q_{UV}) \left(\ell |\varphi_-|^{\frac{1}{\Delta_-}} \right)^4}{1 + Y_0 e^{4A_0} \frac{\partial^2 \hat{W}_B^{eff}}{\partial a^2} \int_{u_0}^{u_{IR}} \frac{du}{Y e^{4A}}} \sqrt{q_{UV}} + \mathcal{O}(q_{UV}) = \frac{\ell Q_{UV}}{1 + Y_0 e^{4A_0} \frac{\partial^2 \hat{W}_B^{eff}}{\partial a^2} \int_{u_0}^{u_{IR}} \frac{du}{Y e^{4A}}} + \mathcal{O}(q_{UV}), \quad (\text{B.2})$$

where the argument of $\frac{\partial^2 \hat{W}_B^{eff}}{\partial a^2}$ is suppressed. In the following, we do not write the argument of the functions to avoid clutter. All the functions are evaluated at the brane position in the trivial axion solution.

Next, we shall calculate the perturbation of the bulk equations of motion (2.27), (2.28) and (2.29) to derive the corrections to W , S and T . At the linear order in q_{UV} , the bulk equations are

$$S^{(q_1)} = W^{(q_1)} - \frac{T^{(q_1)}}{Y S^{(q_0)}}, \quad (\text{B.3})$$

$$\frac{T'(q_1)}{T(q_1)} = \frac{4}{3} \frac{W'(q_0)}{S(q_0)}, \quad (\text{B.4})$$

$$S^{(q_0)} W'(q_1) = \frac{T'(q_1)}{2Y} + \frac{2}{3} W^{(q_0)} W'(q_1). \quad (\text{B.5})$$

The general solution of (B.3), (B.4), (B.5) is

$$\ell W^{(q_1)} = \lim_{\varphi(u_{UV}) \rightarrow 0} \left[e^{\frac{2}{3} \int_{\varphi(u_{UV})}^{\varphi} d\varphi' \frac{W^{(q_0)}}{S^{(q_0)}}} \left(F_1 + \frac{F_2}{2} \int_{\varphi(u_{UV})}^{\varphi} d\varphi' \frac{e^{\frac{2}{3} \int_{\varphi(u_{UV})}^{\varphi'} d\varphi'' \frac{W^{(q_0)}}{S^{(q_0)}}}}{Y \ell S^{(q_0)}} \right) \right], \quad (\text{B.6})$$

$$\ell S^{(q_1)} = \lim_{\varphi(u_{UV}) \rightarrow 0} \left[\frac{2}{3} \frac{W^{(q_0)}}{S^{(q_0)}} e^{\frac{2}{3} \int_{\varphi(u_{UV})}^{\varphi} d\varphi' \frac{W^{(q_0)}}{S^{(q_0)}}} \left(F_1 + \frac{F_2}{2} \int_{\varphi(u_{UV})}^{\varphi} d\varphi' \frac{e^{\frac{2}{3} \int_{\varphi(u_{UV})}^{\varphi'} d\varphi'' \frac{W^{(q_0)}}{S^{(q_0)}}}}{Y \ell S^{(q_0)}} \right) \right. \quad (\text{B.7})$$

$$\left. - \frac{F_2}{2Y \ell S^{(q_0)}} e^{\frac{4}{3} \int_{\varphi(u_{UV})}^{\varphi} d\varphi' \frac{W^{(q_0)}}{S^{(q_0)}}} \right],$$

$$\ell^2 T^{(q_1)} = \lim_{\varphi(u_{UV}) \rightarrow 0} F_2 e^{\frac{4}{3} \int_{\varphi(u_{UV})}^{\varphi} d\varphi' \frac{W^{(q_0)}}{S^{(q_0)}}}, \quad (\text{B.8})$$

where F_1, F_2 are integration constants. There are four integration constants $F_1^{UV}, F_1^{IR}, F_2^{UV}$ and F_2^{IR} corresponding to the UV and IR regions. The IR regularity condition (Gubser's bound) imposes

$$F_1^{IR} + \frac{F_2^{IR}}{2} \int_{\varphi(u_{UV})}^{\infty} d\varphi' \frac{e^{\frac{2}{3} \int_{\varphi(u_{UV})}^{\varphi'} d\varphi'' \frac{W^{(q_0)}}{S^{(q_0)}}}}{Y \ell S^{(q_0)}} = 0. \quad (\text{B.9})$$

From the UV limit of (B.6) and (B.8), we obtain

$$F_1^{UV} = C_{UV}^{(q_1)} |\varphi(u_{UV})|^{\frac{4}{\Delta_-}}, \quad (\text{B.10})$$

$$F_2^{UV} = |\varphi(u_{UV})|^{\frac{8}{\Delta_-}}, \quad (\text{B.11})$$

where (2.34) are used.

In order to deduce the value of the integration constants, we need to use the junction conditions. For $q_{UV} = 0$, the junction conditions (4.25) and (4.26) become

$$[W^{(q_0)}]_{UV}^{IR} = \hat{W}_B^{eff}, \quad (\text{B.12})$$

$$[S^{(q_0)}]_{UV}^{IR} = [W'^{(q_0)}]_{UV}^{IR} = \frac{\partial \hat{W}_B^{eff}}{\partial \varphi}. \quad (\text{B.13})$$

We notice that, to have a consistent solution without axion, we must have

$$\frac{\partial \hat{W}_B^{eff}}{\partial a} = 0, \quad (\text{B.14})$$

from (4.27). Moreover, we assume CP invariance:

$$\frac{\partial^2 \hat{W}_B^{eff}}{\partial a \partial \varphi} = 0, \quad (\text{B.15})$$

which shall be used in (B.17).

At linear order in q_{UV} , by using (B.15) and (B.13), (4.25) and (4.26) become

$$[W^{(q1)}]_{UV}^{IR} + \frac{\partial \hat{W}_B^{eff}}{\partial \varphi} \varphi_0^{(q1)} = \frac{\partial^2 \hat{W}_B^{eff}}{\partial a^2} g^2 + \frac{\partial \hat{W}_B^{eff}}{\partial \varphi} \varphi_0^{(q1)}, \quad (\text{B.16})$$

$$[S^{(q1)}]_{UV}^{IR} + \left[\frac{\partial^2 W^{(q0)}}{\partial \varphi^2} \right]_{UV}^{IR} \varphi_0^{(q1)} = \frac{\partial^3 \hat{W}_B^{eff}}{\partial \varphi \partial a^2} g^2 + \frac{\partial^2 \hat{W}_B^{eff}}{\partial \varphi^2} \varphi_0^{(q1)}, \quad (\text{B.17})$$

where g is defined in (5.8), while the last junction condition (4.27) is

$$\left[\text{sign}(Q) \sqrt{T^{(q1)}} \right]_{UV}^{IR} = \frac{\partial \hat{W}_B^{eff}}{\partial a^2} Y_0 g. \quad (\text{B.18})$$

The first condition (B.16) fixes $W^{UV(q1)}(\varphi_0)$ in terms of $W^{IR(q1)}(\varphi_0)$:

$$W_{UV}^{(q1)}(\varphi_0) = W_{IR}^{(q1)}(\varphi_0) - \frac{\partial^2 \hat{W}_B^{eff}}{\partial a^2} g^2. \quad (\text{B.19})$$

The second junction condition determines the perturbation of the brane position $\varphi_0^{(q1)}$,

$$\varphi_0^{(q1)} = \frac{[S^{(q1)}]_{UV}^{IR} - \frac{\partial^3 \hat{W}_B^{eff}}{\partial \varphi \partial a^2} g^2}{\frac{\partial^2 \hat{W}_B^{eff}}{\partial \varphi^2} - \left[\frac{\partial^2 W^{(q0)}}{\partial \varphi^2} \right]_{UV}^{IR}}. \quad (\text{B.20})$$

Now we can calculate the integration constants, $(F_1^{UV}, F_1^{IR}, F_2^{UV}, F_2^{IR})$, using the junction conditions. By using (5.8) and (B.8), the condition (B.18) leads to

$$\begin{aligned} \lim_{\varphi(u_{UV}) \rightarrow 0} F_2^{IR} \left(1 + \frac{\partial \hat{W}_B^{eff}}{\partial a^2} Y_0 \int_{\varphi_0^{(q0)}}^{\infty} \frac{e^{\frac{2}{3} \int_{\varphi(u_{UV})}^{\varphi} d\varphi' \frac{W^{(q0)}}{S^{(q0)}}}}{Y \ell S^{(q0)}} d\varphi \right)^2 &= \lim_{\varphi(u_{UV}) \rightarrow 0} F_2^{UV} e^{\frac{4}{3} \int_{\varphi(u_{UV})}^{\varphi_0^{(q0)}} d\varphi' \frac{W^{(q0)}}{S^{(q0)}}} \\ &= \lim_{\varphi(u_{UV}) \rightarrow 0} |\varphi(u_{UV})|^{\frac{8}{\Delta-}} e^{\frac{4}{3} \int_{\varphi(u_{UV})}^{\varphi_0^{(q0)}} d\varphi' \frac{W^{(q0)}}{S^{(q0)}}}, \end{aligned} \quad (\text{B.21})$$

where (B.11) is used in the last equality.

From (B.19), we obtain

$$\lim_{\varphi(u_{UV}) \rightarrow 0} e^{\frac{2}{3} \int_{\varphi(u_{UV})}^{\varphi_0^{(q0)}} d\varphi' \frac{W^{(q0)}}{S^{(q0)}}} \left([F_1]_{UV}^{IR} + \frac{[F_2]_{UV}^{IR}}{2} \int_{\varphi(u_{UV})}^{\varphi_0^{(q0)}} d\varphi' \frac{e^{\frac{2}{3} \int_{\varphi(u_{UV})}^{\varphi'} d\varphi'' \frac{W^{(q0)}}{S^{(q0)}}}}{Y \ell S^{(q0)}} \right) \quad (\text{B.22})$$

$$= \lim_{\varphi(u_{UV}) \rightarrow 0} \frac{\partial^2 \hat{W}_B^{eff}}{\partial a^2} F_2^{IR} \left(\int_{\varphi_0^{(q_0)}^{\varphi_{IR}}} e^{\frac{2}{3} \int_{\varphi(u_{UV})}^{\varphi} d\varphi' \frac{W(q_0)}{S(q_0)}} d\varphi \right)^2.$$

By combining (B.22) with (B.9), (B.11), (B.21), The integration constants are given by

$$\frac{F_1^{UV}}{|\varphi(u_{UV})|^{\frac{8}{\Delta_-}}} = -\frac{1}{2} \int_{\varphi(u_{UV})}^{\varphi_0^{(q_0)}} d\varphi' \frac{e^{\frac{2}{3} \int_{\varphi(u_{UV})}^{\varphi'} d\varphi'' \frac{W(q_0)}{S(q_0)}}}{Y \ell S(q_0)}, \quad (\text{B.23})$$

$$\frac{\left(\int_{\varphi_0^{(q_0)}}^{\infty} \frac{e^{\frac{2}{3} \int_{\varphi(u_{UV})}^{\varphi} d\varphi' \frac{W(q_0)}{S(q_0)}}}{Y \ell S(q_0)} d\varphi \right) \left(\frac{1}{2} e^{\frac{4}{3} \int_{\varphi(u_{UV})}^{\varphi_0^{(q_0)}} d\varphi' \frac{W(q_0)}{S(q_0)}} + \frac{\partial^2 \hat{W}_B^{eff}}{\partial a^2} \int_{\varphi_0^{(q_0)}}^{\infty} \frac{e^{\frac{2}{3} \int_{\varphi(u_{UV})}^{\varphi} d\varphi' \frac{W(q_0)}{S(q_0)}}}{Y \ell S(q_0)} d\varphi \right)}{\left(1 + \frac{\partial \hat{W}_B^{eff}}{\partial a^2} Y_0 \int_{\varphi_0^{(q_0)}}^{\infty} \frac{e^{\frac{2}{3} \int_{\varphi(u_{UV})}^{\varphi} d\varphi' \frac{W(q_0)}{S(q_0)}}}{Y \ell S(q_0)} d\varphi \right)^2},$$

$$\frac{F_1^{IR}}{|\varphi(u_{UV})|^{\frac{8}{\Delta_-}}} = -\frac{1}{2} \frac{e^{\frac{4}{3} \int_{\varphi(u_{UV})}^{\varphi_0^{(q_0)}} d\varphi' \frac{W(q_0)}{S(q_0)}} \int_{\varphi(u_{UV})}^{\infty} d\varphi' \frac{e^{\frac{2}{3} \int_{\varphi(u_{UV})}^{\varphi'} d\varphi'' \frac{W(q_0)}{S(q_0)}}}{Y \ell S(q_0)}}{\left(1 + \frac{\partial \hat{W}_B^{eff}}{\partial a^2} Y_0 \int_{\varphi_0^{(q_0)}}^{\infty} \frac{e^{\frac{2}{3} \int_{\varphi(u_{UV})}^{\varphi} d\varphi' \frac{W(q_0)}{S(q_0)}}}{Y \ell S(q_0)} d\varphi \right)^2}, \quad (\text{B.24})$$

$$\frac{F_2^{UV}}{|\varphi(u_{UV})|^{\frac{8}{\Delta_-}}} = 1, \quad (\text{B.25})$$

$$\frac{F_2^{IR}}{|\varphi(u_{UV})|^{\frac{8}{\Delta_-}}} = \frac{e^{\frac{4}{3} \int_{\varphi(u_{UV})}^{\varphi_0^{(q_0)}} d\varphi' \frac{W(q_0)}{S(q_0)}}}{\left(1 + \frac{\partial \hat{W}_B^{eff}}{\partial a^2} Y_0 \int_{\varphi_0^{(q_0)}}^{\infty} \frac{e^{\frac{2}{3} \int_{\varphi(u_{UV})}^{\varphi} d\varphi' \frac{W(q_0)}{S(q_0)}}}{Y \ell S(q_0)} d\varphi \right)^2}. \quad (\text{B.26})$$

From (B.10) and (B.23), we obtain

$$C_{UV}^{(q_1)} = -\frac{1}{2} \int_{\varphi(u_{UV})}^{\varphi_0^{(q_0)}} d\varphi' \frac{e^{\frac{2}{3} \int_{\varphi(u_{UV})}^{\varphi'} d\varphi'' \frac{W(q_0)}{S(q_0)}}}{Y \ell S(q_0)} - \quad (\text{B.27})$$

$$\frac{\left(\int_{\varphi_0^{(q_0)}}^{\infty} \frac{e^{\frac{2}{3} \int_{\varphi(u_{UV})}^{\varphi} d\varphi' \frac{W(q_0)}{S(q_0)}}}{Y \ell S(q_0)} d\varphi \right) \left(\frac{1}{2} e^{\frac{4}{3} \int_{\varphi(u_{UV})}^{\varphi_0^{(q_0)}} d\varphi' \frac{W(q_0)}{S(q_0)}} + \frac{\partial^2 \hat{W}_B^{eff}}{\partial a^2} \int_{\varphi_0^{(q_0)}}^{\infty} \frac{e^{\frac{2}{3} \int_{\varphi(u_{UV})}^{\varphi} d\varphi' \frac{W(q_0)}{S(q_0)}}}{Y \ell S(q_0)} d\varphi \right)}{\left(1 + \frac{\partial \hat{W}_B^{eff}}{\partial a^2} Y_0 \int_{\varphi_0^{(q_0)}}^{\infty} \frac{e^{\frac{2}{3} \int_{\varphi(u_{UV})}^{\varphi} d\varphi' \frac{W(q_0)}{S(q_0)}}}{Y \ell S(q_0)} d\varphi \right)^2}.$$

By using (4.30), (B.8), (B.25), (B.26), the axion source is, to leading order,

$$\frac{a_*}{\sqrt{q_{UV}}} = -\text{sign}(Q_{UV}) \int_{\varphi(u_{UV})}^{\varphi_0^{(q_0)}} d\varphi \frac{\sqrt{T(q_1)}}{S(q_0) Y} - \text{sign}(Q_{IR}) \int_{\varphi_0^{(q_0)}}^{\infty} d\varphi \frac{\sqrt{T(q_1)}}{S(q_0) Y} \quad (\text{B.28})$$

$$= -\text{sign}(Q_{UV}) \sqrt{F_2^{UV}} \int_{\varphi(u_{UV})}^{\varphi_0^{(q_0)}} d\varphi \frac{e^{\frac{2}{3} \int_{\varphi(u_{UV})}^{\varphi} d\varphi' \frac{W(q_0)}{S(q_0)}}}{Y \ell S(q_0)} - \text{sign}(Q_{IR}) \sqrt{F_2^{IR}} \int_{\varphi_0^{(q_0)}}^{\infty} d\varphi \frac{e^{\frac{2}{3} \int_{\varphi(u_{UV})}^{\varphi} d\varphi' \frac{W(q_0)}{S(q_0)}}}{Y \ell S(q_0)}$$

$$\begin{aligned}
&= - \lim_{\varphi(u_{UV}) \rightarrow 0} |\varphi(u_{UV})|^{\frac{4}{\Delta_-}} \left[\text{sign}(Q_{UV}) \int_{\varphi(u_{UV})}^{\varphi_0^{(q_0)}} d\varphi \frac{e^{\frac{2}{3} \int_{\varphi(u_{UV})}^{\varphi} d\varphi' \frac{W(q_0)}{S(q_0)}}}{Y \ell S(q_0)} \right. \\
&+ \text{sign}(Q_{IR}) \left. \frac{e^{\frac{2}{3} \int_{\varphi(u_{UV})}^{\varphi_0^{(q_0)}} d\varphi' \frac{W(q_0)}{S(q_0)}}}{\left| 1 + \frac{\partial \hat{W}_B^{eff}}{\partial a^2} Y_0 \int_{\varphi_0^{(q_0)}}^{\infty} \frac{e^{\frac{2}{3} \int_{\varphi(u_{UV})}^{\varphi} d\varphi' \frac{W(q_0)}{S(q_0)}}}{Y \ell S(q_0)} d\varphi \right|} \int_{\varphi_0^{(q_0)}}^{\infty} d\varphi \frac{e^{\frac{2}{3} \int_{\varphi(u_{UV})}^{\varphi} d\varphi' \frac{W(q_0)}{S(q_0)}}}{Y \ell S(q_0)} \right]
\end{aligned}$$

Here $\text{sign}(Q_{UV})$ is a free parameter, and $\text{sign}(Q_{IR})$ is determined by (5.2).

Finally, we provide the dilaton and axion at the brane position ((B.20) and (5.8)) in terms of the unperturbed quantities:

$$\begin{aligned}
\varphi_0^{(q_1)} &= \frac{1}{\frac{\partial^2 \hat{W}_B^{eff}}{\partial \varphi^2} - \left[\frac{\partial^2 W(q_0)}{\partial \varphi^2} \right]_{UV}^{IR}} \left\{ \frac{2}{3} e^{\frac{2}{3} \int_{\varphi(u_{UV})}^{\varphi_0^{(q_0)}} d\varphi' \frac{W(q_0)}{S(q_0)}} \left(\left[\frac{W(q_0) F_1}{S(q_0)} \right]_{UV}^{IR} + \right. \right. & (B.29) \\
&+ \left. \left[\frac{W(q_0) F_2}{2S(q_0)} \right]_{UV}^{IR} \int_{\varphi(u_{UV})}^{\varphi_0^{(q_0)}} d\varphi' \frac{e^{\frac{2}{3} \int_{\varphi(u_{UV})}^{\varphi'} d\varphi'' \frac{W(q_0)}{S(q_0)}}}{Y \ell S(q_0)} \right) - \frac{1}{2Y_0} \left[\frac{F_2}{\ell S(q_0)} \right]_{UV}^{IR} e^{\frac{4}{3} \int_{\varphi(u_{UV})}^{\varphi_0^{(q_0)}} d\varphi' \frac{W(q_0)}{S(q_0)}} - \\
&\left. - \frac{\partial^3 \hat{W}_B^{eff}}{\partial \varphi \partial a^2} F_2^{IR} \left(\int_{\varphi_0^{(q_0)}}^{\varphi_{IR}} \frac{e^{\frac{2}{3} \int_{\varphi(u_{UV})}^{\varphi} d\varphi' \frac{W(q_0)}{S(q_0)}}}{Y \ell S(q_0)} d\varphi \right)^2 \right\},
\end{aligned}$$

$$a_0 = -\text{sign}(Q_{IR}) \sqrt{F_2^{IR}} \int_{\varphi_0^{(q_0)}}^{\infty} d\varphi \frac{e^{\frac{2}{3} \int_{\varphi(u_{UV})}^{\varphi} d\varphi' \frac{W(q_0)}{S(q_0)}}}{Y \ell S(q_0)} + \mathcal{O}(q_{UV}), \quad (B.30)$$

where $(F_1^{UV}, F_1^{IR}, F_2^{UV}, F_2^{IR})$ are given in (B.23), (B.24), (B.25), (B.26) in terms of the unperturbed quantities, and (5.8) and (B.7) are used in (B.29), while (B.8) is used in (B.30).

The calculations of the on-shell axion, free energy and topological susceptibility in the small axion backreaction are given in Appendix A.1, where the known large- N_c result [25, 59, 26] is reproduced.

C. Brane equilibrium position in the near-UV or near-IR regions: analytic results

C.1 Brane equilibrium position in the near-UV region

Suppose that φ_0 is close to the $\varphi(u_{UV}) = 0$, and we can use the UV asymptotic expressions at the locus of the brane position. By using the junction conditions (4.25), (4.26), (4.27) and the UV asymptotic expressions for the scalar functions (2.34), (2.35), (2.36), we obtain

$$\frac{1}{\ell} (C_{IR} - C_{UV}) |\varphi_0|^{\frac{4}{\Delta_-}} = \hat{W}_B^{eff}(\varphi_0, a_0), \quad (C.1)$$

$$\frac{1}{\ell} \frac{4}{\Delta_-} (C_{IR} - C_{UV}) |\varphi_0|^{\frac{4}{\Delta_-} - 1} = \frac{\partial \hat{W}_B^{eff}}{\partial \varphi}(\varphi_0, a_0), \quad (\text{C.2})$$

$$\frac{1}{\ell} \left(\text{sign}(Q_{IR}) \sqrt{q_{IR}} - \text{sign}(Q_{UV}) \sqrt{q_{UV}} \right) |\varphi_0|^{\frac{4}{\Delta_-}} = Y_0 \frac{\partial \hat{W}_B^{eff}}{\partial a}(\varphi_0, a_0), \quad (\text{C.3})$$

at leading order in φ_0 . Here C_{IR} and q_{IR} are the integration constant appearing in the UV expansions of the scalar functions (W_{IR}, S_{IR}, T_{IR}).

By solving (C.1), (C.2) and (C.3), one can express the IR integration constants C_{IR} and q_{IR} and the brane position φ_0 in terms of the UV integration constants. If $\hat{W}_B^{eff}(\varphi_0, a_0) \neq 0$, from the first two equations (C.1) and (C.2), one can see that φ_0 is determined by solving

$$\varphi_0 \frac{\partial \log \hat{W}_B^{eff}}{\partial \varphi}(\varphi_0, a_0) = \frac{4}{\Delta_-}, \quad (\text{C.4})$$

where a_0 is related to the function of φ_0 through

$$a_0 = -\text{sign}(Q_{IR}) \int_{\varphi_0}^{\varphi(u_{IR})} \frac{\sqrt{T}}{YS}. \quad (\text{C.5})$$

By using the solution for φ_0 we can determine C_{IR} and q_{IR} as

$$C_{IR} = C_{UV} + |\varphi_0|^{-\frac{4}{\Delta_-}} \ell \hat{W}_B^{eff}(\varphi_0, a_0), \quad (\text{C.6})$$

$$\text{sign}(Q_{IR}) \sqrt{q_{IR}} = \text{sign}(Q_{UV}) \sqrt{q_{UV}} + |\varphi_0|^{-\frac{4}{\Delta_-}} \ell Y_0 \frac{\partial \hat{W}_B^{eff}}{\partial a}(\varphi_0, a_0). \quad (\text{C.7})$$

On the other hand, if $\hat{W}_B^{eff}(\varphi_0, a_0) = 0$, then $C_{IR} = C_{UV}$ but (C.7) is still valid. The brane position is determined by the condition $\frac{\partial \hat{W}_B^{eff}}{\partial a}(\varphi_0, a_0) = 0$.

C.2 Brane equilibrium position in the near-IR region

Suppose that the brane is in the region where the IR asymptotic expansions (2.38), (2.39), (2.40) can be used. Again we can obtain relations among the various integration constants analytically in this case. The junction conditions (4.25), (4.26), (4.27) lead to

$$-\frac{1}{2} \frac{D_{IR} - D_{UV}}{\frac{b}{2} + \gamma - \frac{4}{3b}} e^{(\frac{8}{3b} - \frac{b}{2} - \gamma)\varphi_0} - E_{UV} e^{\frac{4}{3b}\varphi_0} = \ell \hat{W}_B^{eff}(\varphi_0, a_0), \quad (\text{C.8})$$

$$-\frac{D_{IR} - D_{UV}}{2} \frac{\frac{b}{2} + \gamma}{\frac{b}{2} + \gamma - \frac{4}{3b}} e^{(\frac{8}{3b} - \frac{b}{2} - \gamma)\varphi_0} - \frac{4E_{UV}}{3b} e^{\frac{4}{3b}\varphi_0} = \ell \frac{\partial \hat{W}_B^{eff}}{\partial \varphi}(\varphi_0, a_0), \quad (\text{C.9})$$

$$\sqrt{\frac{bW_\infty}{2Y_\infty}} \left(\text{sign}(Q_{IR}) \sqrt{D_{IR}} - \text{sign}(Q_{UV}) \sqrt{D_{UV}} \right) e^{(\frac{4}{3b} - \gamma)\varphi_0} = \ell \frac{\partial \hat{W}_B^{eff}}{\partial a}(\varphi_0, a_0), \quad (\text{C.10})$$

where D_{UV} and E_{UV} are the integration constant appearing in the IR expansion of the scalar functions (W_{UV}, S_{UV}, T_{UV}) on the UV side of the brane:

$$\ell W_{UV} = W_\infty e^{\frac{b}{2}\varphi} - \frac{D_{UV}}{2} \frac{1}{\frac{b}{2} + \gamma - \frac{4}{3b}} e^{(\frac{8}{3b} - \frac{b}{2} - \gamma)\varphi} + E_{UV} e^{\frac{4}{3b}\varphi} + \dots, \quad (\text{C.11})$$

$$\ell S_{UV} = \frac{b}{2} W_\infty e^{\frac{b}{2}\varphi} - \frac{D_{UV}}{2} \frac{\frac{b}{2} + \gamma}{\frac{b}{2} + \gamma - \frac{4}{3b}} e^{(\frac{8}{3b} - \frac{b}{2} - \gamma)\varphi} + \frac{4E_{UV}}{3b} e^{\frac{4}{3b}\varphi} + \dots, \quad (\text{C.12})$$

$$\ell^2 T_{UV} = \frac{b}{2} D_{UV} W_\infty Y_\infty e^{\frac{8}{3b}\varphi} + \dots. \quad (\text{C.13})$$

Note that the integration constant E has to be set to zero in (W_{IR}, S_{IR}, T_{IR}) due to Gubser's bound.

From (2.44) we observe

$$\frac{8}{3b} - \frac{b}{2} - \gamma \leq \frac{4}{3b}. \quad (\text{C.14})$$

Therefore, the left hand side of (C.8) and (C.9) is generally dominated by the E_{UV} term, and we neglect $D_{IR} - D_{UV}$ term in the following. Combining (C.8) with (C.9), we obtain

$$\frac{\partial \log \hat{W}_B^{eff}}{\partial \varphi}(\varphi_0, a_0) = \frac{4}{3b}, \quad (\text{C.15})$$

for $\hat{W}_B^{eff}(\varphi_0, a_0) \neq 0$. The position φ_0 can be deduced from this equation. The integration constants are determined by

$$E_{UV} = -\ell \frac{\partial \hat{W}_B^{eff}}{\partial \varphi}(\varphi_0, a_0) e^{-\frac{4}{3b}\varphi_0}, \quad (\text{C.16})$$

$$\text{sign}(Q_{IR}) \sqrt{D_{IR}} = \text{sign}(Q_{UV}) \sqrt{D_{UV}} + \sqrt{\frac{2Y_\infty}{bW_\infty Y_\infty}} \ell \frac{\partial \hat{W}_B^{eff}}{\partial a}(\varphi_0, a_0) e^{-(\frac{4}{3b} - \gamma)\varphi_0}. \quad (\text{C.17})$$

In the case of $\hat{W}_B^{eff}(\varphi_0, a_0) = 0$, we get $E_{UV} = 0$, and φ_0 is determined by solving $\frac{\partial \hat{W}_B^{eff}}{\partial \varphi}(\varphi_0, a_0) = 0$. Then, D_{UV} is fixed by (C.17).

D. Overshooting constraint

One can show that there exists an additional constraint on the brane potential W_B , if the solution for W on the UV side of the brane is to exhibit the expected UV asymptotics recorded in (2.34). For simplicity, we construct the argument in the case without a bulk axion and generalise to case with bulk axion later. In the absence of a bulk axion the equation of motion for W_{UV} can be written as

$$W'_{UV} = \sqrt{\frac{2}{3} W_{UV}^2 + 2V}. \quad (\text{D.1})$$

which is (2.29) with $S_{UV} = W'_{UV}$ as follows from (2.27) in absence of the axion. The function W_{UV} is then given by the solution to (D.1) subject to the boundary condition

$$\lim_{\epsilon \rightarrow 0} W_{UV}(\varphi_0 - \epsilon) \equiv W_0, \quad (\text{D.2})$$

where we assume $W_0 > 6$. To construct the argument, it will be useful to introduce an auxiliary function \tilde{W} , which is defined as the solution to

$$\tilde{W}' = \sqrt{\frac{2}{3}\tilde{W}^2 - 24} \quad , \quad \tilde{W}(\varphi_0) = W_0. \quad (\text{D.3})$$

By definition, the function \tilde{W} is monotonic in φ . Equation (D.3) can be solved analytically to find

$$\frac{\tilde{W}(\varphi)}{3} = \tilde{C}e^{\sqrt{\frac{2}{3}}(\varphi-\varphi_0)} + \tilde{C}^{-1}e^{-\sqrt{\frac{2}{3}}(\varphi-\varphi_0)}, \quad (\text{D.4})$$

with

$$\tilde{C} = \frac{W_0}{6} + \sqrt{\left(\frac{W_0}{6}\right)^2 - 1}. \quad (\text{D.5})$$

The solution (D.4) is valid only for

$$\varphi \geq \varphi_{\min}, \quad \text{with} \quad \varphi_{\min} = \varphi_0 - \sqrt{\frac{3}{2}} \log \tilde{C}, \quad (\text{D.6})$$

as for $\varphi = \varphi_{\min}$ one finds

$$\tilde{W}(\varphi_{\min}) = 6, \quad (\text{D.7})$$

and the square root in (D.3) vanishes.

From (6.1), we have that $V > -12$. Then, as a consequence of the definition of \tilde{W} in (D.3) it follows that

$$\tilde{W}(\varphi) < W_{UV}(\varphi) \quad \text{for} \quad \varphi < \varphi_0. \quad (\text{D.8})$$

For W_{UV} to exhibit the desired UV behaviour of a RG flow solution, we require $W_{UV}(0) = 6$. Then, consistency of the condition $W_{UV}(0) = 6$ with the property (D.8) and the monotonicity of \tilde{W} require

$$\varphi_{\min} > 0, \quad \Rightarrow \quad e^{\sqrt{\frac{4}{3}}\varphi_0} > \tilde{C}. \quad (\text{D.9})$$

This provides a non-trivial constraint on the brane potential through the dependence of \tilde{C} on W_0 .

We numerically check this constraint in fig. 16. The condition (D.9) can be interpreted as a lower bound on φ_0 . In the top row panel we plot this bound on φ_0 as a function of W_0 . In the bottom row panels, we numerically solve (D.1) and (D.3) for W_{UV} and \tilde{W} , respectively. The left panel corresponds to a parameter choice which does not satisfy (D.9). We observe that $W_{UV}(0) = 6$ is not realized in this case. On the other hand, the parameter choice in the right panel satisfies (D.9), and $W_{UV}(0) = 6$ can be attained.

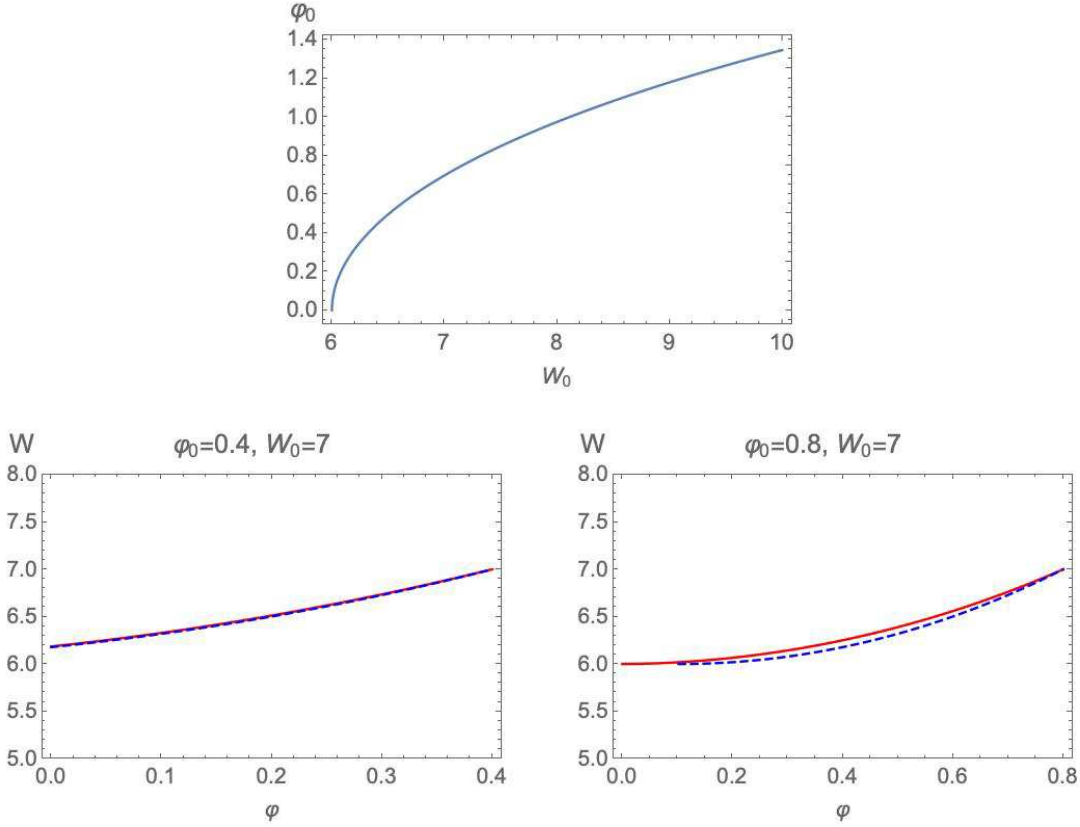


Figure 16: **Top row:** Lower bound on φ_0 as a function of W_0 as arising from the constraint (D.9). **Bottom row, left:** Plot of W_{UV} and \tilde{W} vs. φ by solving (D.1) and (D.3) for the parameter choice $\varphi_0 = 0.4$ and $W_0 = 7$. The solid and dashed lines correspond to W_{UV} and \tilde{W} , respectively. For this parameter choice $W_{UV}(0) = 6$ is not realized. **Bottom row, right:** Plot of W_{UV} and \tilde{W} vs. φ by solving (D.1) and (D.3) for the parameter choice $\varphi_0 = 0.8$ and $W_0 = 7$. The solid and dashed lines correspond to W_{UV} and \tilde{W} , respectively. For this parameter we find $W_{UV}(0) = 6$.

Inserting for \tilde{C} with (D.5) and substituting for $W_0 = W_{UV}(\varphi_0)$ using the junction condition (4.25), the condition (D.9) can be written as

$$e^{\sqrt{\frac{2}{3}}\varphi} \left(\frac{W_{IR} - \hat{W}_B^{eff}}{6} + \sqrt{\left(\frac{W_{IR} - \hat{W}_B^{eff}}{6} \right)^2 - 1} \right)^{-1} \Big|_{\varphi=\varphi_0} > 1 \quad (\text{D.10})$$

where φ_0 is determined by (6.8). We expect a similar condition to also exist in the presence of nontrivial axion backreaction, but an analytical statement along the lines of the argument above is more difficult in this case and is left for future work. Instead, in the numerical examples including axion backreaction considered here, we check explicitly whether the condition $\lim_{\varphi \rightarrow 0} W_{UV} = 6$ is satisfied, at least within

our numerical precision. If a solution does not satisfy this condition it is discarded. Hence, all numerical examples shown in sec. 6 exhibit $\lim_{\varphi \rightarrow 0} W_{UV} = 6$ as expected for a RG flow solution.

E. Positivity constraints

In this appendix we give a preliminary assessment of the question: can the mixing of the Higgs with the bulk modes lead to the emergence of ghost-like or tachyonic instabilities? As we shall see, the detailed answer will depend on the specific features of the model. Nevertheless, some general conclusions can be drawn which show that, broadly speaking, this is not an issue that would make the theory inconsistent.

In what follows we analyze this question at the level of linear perturbations around a self-tuning vacuum. The answer about stability is read off from the action at the quadratic level in the fluctuations: the absence of ghosts requires positivity of kinetic terms, whereas the absence of tachyons implies constraints on the mass matrix.

The model contains tensor modes (which come from the traceless and transverse part of the bulk graviton) and scalar modes. The latter are a mixture of the trace part of the metric fluctuations, of the bulk dilaton and axion fluctuations, of the brane-localized Higgs, plus the fluctuations in the brane position around equilibrium. Tensor modes are healthy (i.e. non-ghost like and with a positive definite mass) if both the brane and bulk Einstein-Hilbert term have the correct sign, which we assume to be always true in the models under considerations. In the absence of brane-localized fields, the conditions for stability of the Einstein-dilaton theory were analyzed in [7], and the addition of the axion does not change the pictures qualitatively (as long as its bulk and brane kinetic terms are healthy). However, new and qualitatively different constraints may arise from the mixing of the brane-localized Higgs with the bulk KK modes, which is a new feature in this model with respect to [7].

Since the Higgs on the brane does not affect tensor fluctuations at linear order, we restrict the analysis to scalar perturbations. The bulk perturbations are also unaffected by the Higgs. However the matching conditions are modified.

To simplify the discussion, we make one more simplification: we neglect the bulk axion and we consider a model of Einstein-dilaton 5d gravity (with generic bulk and brane-induced terms up to two derivatives) coupled to the brane-Higgs field. In other words, we set $a = 0$ everywhere in the action (2.1), (3.2) and (3.3). This does not change the picture qualitatively. In the presence of a (backreacting) axion, one would first need to diagonalize the bulk fluctuations before performing the analysis, and add another set of KK modes for the corresponding new bulk field. However, as long as the axion has healthy brane and bulk kinetic terms, this will not change the qualitative picture.

This appendix extends to the present model the techniques described in detail in Section 5 of [7], and we refer the reader to that work for more details.

E.1 Linear Perturbations

The relevant bulk perturbations in the scalar sector (with a convenient gauge fixing, see [7] for details) are:

$$ds^2 = a(r)^2 \{ (1 + 2\phi)dr^2 + [(1 + 2\psi)\eta_{\mu\nu} + 2\partial_\mu\partial_\nu E]dx^\mu dx^\nu \}, \quad \varphi = \bar{\varphi}(r), \quad (\text{E.1})$$

where ϕ, E, ψ are small perturbations which depend on (r, x^μ) . We use a gauge where the dilaton is unperturbed in the bulk.

On the brane, we have two more perturbations: the fluctuation in the brane position,

$$r_{brane}(x_\mu) = r_0 + \rho(x_\mu), \quad (\text{E.2})$$

and the perturbation in the Higgs field, which we parametrize as²⁹

$$H = (v_0 + h(x))e^{i\theta(x)}, \quad (\text{E.3})$$

where $v_0 \geq 0$ and $h(x)$ is a real scalar.

We follow closely the discussion in [7], section 3 and 5, and appendix D. This leads to a quadratic action for the perturbation, which is a modified version of equation (5.9) of [7]. We define the doublet:

$$\Psi = \begin{pmatrix} \psi_{UV} \\ \psi_{IR} \end{pmatrix}, \quad (\text{E.4})$$

where $\psi_{UV}(r)$ is in principle defined for $r > r_0$ and $\psi_{IR}(r)$ for $r < r_0$, but we can extend them over the whole range of r with no consequence.

The bulk+brane action at quadratic order reads,

$$\begin{aligned} S_5 = & -\frac{M_p^3}{2} \int d^4x \left[\int dr [\partial_r \Psi^\dagger \mathcal{B}(r) \partial_r \Psi + \partial_\mu \Psi^\dagger \mathcal{B}(r) \partial^\mu \Psi] \right. \\ & + \Psi^\dagger(r_0) \Sigma \hat{\Gamma}_1 \Psi(r_0) - \partial_\mu \Psi^\dagger(r_0) \Sigma \hat{\Gamma}_2 \partial^\mu \Psi(r_0) \\ & + T_H a_0^2 [\partial_\mu h \partial^\mu h + a_0^2 m_H^2 h^2 + v_0^2 \partial_\mu \theta \partial^\mu \theta] \\ & \left. + a_0^4 \frac{\partial^2 \hat{W}_B}{\partial \varphi \partial H} \Big|_{\varphi_0, H_0} \hat{\chi}(r_0) h + 6a_0^2 U_H(\varphi_0) v_0 \partial^\mu \hat{\psi}(r_0) \partial_\mu h \right]. \quad (\text{E.5}) \end{aligned}$$

²⁹For simplicity we take a $U(1)$ Higgs. For the SM Higgs we have 3 goldstones instead of one

The factors of $a_0 \equiv a(r_0)$ come from the induced metric on the brane, $\gamma_{\mu\nu} = a_0^2 \eta_{\mu\nu}$. The first two lines in equation (E.5) have the same form as equation (5.9) in [7]. The 2×2 matrices $\mathcal{B}(r)$ and Σ are:

$$\mathcal{B}(r) = \begin{pmatrix} e^{2B_{UV}} \theta(r_0 - r) & 0 \\ 0 & e^{2B_{IR}} \theta(r - r_0) \end{pmatrix}, \quad \Sigma \equiv \begin{pmatrix} -e^{2B_{UV}(r_0)} & 0 \\ 0 & e^{2B_{IR}(r_0)} \end{pmatrix}, \quad (\text{E.6})$$

where on each side $e^{2B} = a^3(r)z^2(r)$ and $z = a\bar{\varphi}'/a'$. The matrices $\hat{\Gamma}_1$ and $\hat{\Gamma}_2$ are given explicitly in (D.79) in [7], where now W_B and U_B have to be replaced everywhere by \hat{W}_B and \hat{U}_B from equations (4.15-4.16).

The last line in the quadratic action (E.5) contains the mixing between the Higgs fluctuation and the bulk fields. Notice that the $U(1)$ Goldstone mode is decoupled from the rest. Notice also that the mixing is very simply written in terms of $\hat{\psi}(r_0)$ and $\hat{\chi}(r_0)$, the gauge-invariant fluctuations which couple to the dilaton charge and trace of the stress-tensor, respectively:

$$\hat{\psi}(r_0) = \psi(r_0) + \frac{a'(r_0)}{a(r_0)}\rho, \quad \hat{\chi}(r_0) = \bar{\varphi}'(r_0)\rho. \quad (\text{E.7})$$

They also correspond to the ‘‘heavy’’ and ‘‘light’’ scalar fluctuations [7]. Interestingly, the first one has only a mass-mixing with h , the second only kinetic mixing. In the gauge we are using, they are given by the following linear combinations of $\psi_{UV}(r)$ and $\psi_{IR}(r)$:

$$\hat{\chi}(r_0) = -\frac{[\psi]}{[1/z]}, \quad \hat{\psi}(r_0) = \frac{[z\psi]}{[z]}, \quad (\text{E.8})$$

where [...] denotes the jump across the brane.

To summarize, when we compare (E.5) with the quadratic action found in [7], the effect of the Higgs field is to change W_B, U_B into \hat{W}_B, \hat{U}_B and to generate the mixing terms in the last line. Notice that the mixing is proportional to the Higgs vev v_0 : this is manifest in the second term on the last line in (E.5), and the first term is explicitly:

$$\frac{\partial^2 \hat{W}_B}{\partial \varphi \partial H} = 2X'_H(\varphi)v_0 + 4S'_H(\varphi)v_0^3. \quad (\text{E.9})$$

Therefore, the mixing vanishes in the trivial Higgs vacuum $v_0 = 0$.

E.2 KK expansion

In order to understand the effect of the mixing, we expand the action on ‘‘Kaluza-Klein’’ modes with eigenvalue m^2 for the radial Hamiltonian. These modes have form:

$$\Psi(r, x^\mu) = \Psi(r)\phi(x), \quad (\text{E.10})$$

where the radial wave-function Ψ satisfies (for $r \neq r_0$):

$$-\mathcal{B}^{-1} \frac{d}{dr} \left(\mathcal{B}(r) \frac{d\Psi(r)}{dr} \right) = m^2 \Psi(r), \quad (\text{E.11})$$

plus the boundary condition:

$$\Psi'(r_0) = \left(\hat{\Gamma}_1 + \hat{\Gamma}_2 m^2 \right) \Psi(r_0). \quad (\text{E.12})$$

This radial problem plus boundary conditions define a self-adjoint radial Hamiltonian with orthogonal eigenstates. If we expand a generic normalizable function $\Psi(r, x^\mu)$ in a complete basis of radial eigenstates, insert in (E.5), and integrate over the bulk, we obtain at quadratic order an effective 4d action which is a sum over decoupled 4d KK modes, except for the last line in (E.5), where each mode separately mixes with the brane Higgs field:

$$S = M_p^3 \sum_n S^{(n)}, \quad (\text{E.13})$$

$$\begin{aligned} S^{(n)} = & -\frac{1}{2} \int d^4x \mathcal{N}_n [\partial^\mu \phi_n \partial_\mu \phi_n + m_n^2 \phi_n^2] + a_0^2 T_H [\partial_\mu h \partial^\mu h + a_0^2 m_H^2 h^2] \\ & + a_0^2 \lambda_n \phi_n h + a_0 q_n \partial^\mu \phi_n \partial_\mu h \end{aligned} \quad (\text{E.14})$$

with

$$\mathcal{N}_n = \int_{r < r_0} dr e^{2B_{UV}} \psi_{UV,n}^2 + \int_{r > r_0} dr e^{2B_{IR}} \psi_{IR,n}^2 - \Psi_n^\dagger(r_0) \Sigma \hat{\Gamma}_2 \Psi_n(r_0), \quad (\text{E.15})$$

and

$$\lambda_n \equiv a_0^2 (2X'_H(\varphi_0) v_0 + 4S'_H(\varphi_0) v_0^3) \hat{\chi}_n(r_0), \quad q_n \equiv 6a_0 U_H(\varphi_0) v_0 \hat{\psi}_n(r_0), \quad (\text{E.16})$$

where $\Psi_n(r)$ are the radial (doublet) eigenfunctions corresponding to the n -th eigenvalue m_n^2 . We see that the mixing terms are proportional to the values of the radial eigenfunctions taken on the brane.

We have written equation (E.13) for the case of a discrete KK spectrum. For a continuous spectrum, the mass m becomes a continuous variable and the sums are replaced by integrals. We continue to write the symbol of “sum” but it is understood that this may represent both cases.

The action (E.13) describes an infinite tower of four-dimensional scalar modes with masses m_n , plus the Higgs field. All of the modes do not mix with each other but only with the Higgs. To check whether there are ghosts and/or tachyons we have to separately analyse the kinetic mixing and then the mass mixing.

E.2.1 Ghosts

To unmix the kinetic terms, it is sufficient to shift each mode by an appropriate multiple of h . Define:

$$\phi_n = \tilde{\phi}_n - \frac{a_0 q_n}{2\mathcal{N}_n} h. \quad (\text{E.17})$$

This redefinition diagonalizes the kinetic action,

$$S_{kin} = -\frac{M_p^3}{2} \left[\sum_n \mathcal{N}_n \int d^4x \left(\partial^\mu \tilde{\phi}_n \partial_\mu \tilde{\phi}_n \right) + a_0^2 \left(T_H - \sum_n \frac{q_n^2}{2\mathcal{N}_n} \right) \int d^4x \partial_\mu h \partial^\mu h \right]. \quad (\text{E.18})$$

From this expression we see that the mixing only affects the kinetic term of the Higgs, and leaves unchanged the KK kinetic terms. Absence of ghosts requires that:

1. All the $\mathcal{N}_n > 0$. If this is the case, none of the KK modes are ghosts. A sufficient condition for this was obtained in [7] (equation (5.19)). Here, it has to be satisfied with the effective superpotentials \hat{W}_B and \hat{U}_B , which contain the Higgs vev v_0 and the new functions X_H and S_H .
2. On top of that, the Higgs must not be a ghost, i.e. we need:

$$T_H > \Delta Q, \quad \Delta Q \equiv \sum_n \frac{q_n^2}{2\mathcal{N}_n}, \quad (\text{E.19})$$

where q_n is defined in (E.16) and \mathcal{N}_n in (E.15). Under the assumption that point 1 holds, i.e. if no KK mode is a ghost, then ΔQ is the sum (or integral) of non-negative terms. In section E.3, we show that the sum is finite and we will evaluate it in simple cases.

E.2.2 Tachyons

Let us assume that there are no ghosts, i.e. all kinetic terms are positive definite. Then, the absence of tachyons is equivalent to the positivity of the mass eigenvalues of the KK system. We can again disentangle the Higgs from the KK modes by redefining:

$$\phi_n = \tilde{\phi}_n - \frac{a_0^2 \lambda_n}{2\mathcal{N}_n m_n^2} h. \quad (\text{E.20})$$

Notice that this new redefinition does not remove the kinetic mixing, but this doesn't matter for the discussion of the sign of the mass eigenvalues, as long as the kinetic matrix is positive definite (i.e. there are no ghosts). If this is the case, we only need to look at the eigenvalues of the mass terms which after the redefinition (E.20) take the form:

$$S_{mass} = -\frac{M_p^3}{2} \int d^4x \left[\sum_n \mathcal{N}_n m_n^2 \tilde{\phi}_n^2 + a_0^4 \left(T_H m_H^2 - \sum_n \frac{\lambda_n^2}{2\mathcal{N}_n m_n^2} \right) h^2 \right]. \quad (\text{E.21})$$

Absence of tachyons requires:

1. All KK masses-squared have to be positive. A sufficient conditions for this to happen was derived in [7] (equation (5.25) there) and the same holds here except that one has to replace W_B with \hat{W}_B .
2. The Higgs must not be a tachyon, i.e.

$$m_H^2 > \Delta M^2, \quad \Delta M^2 \equiv \frac{1}{T_H} \sum_n \frac{\lambda_n^2}{2\mathcal{N}_n m_n^2}, \quad (\text{E.22})$$

where λ_n is defined in (E.16) and \mathcal{N}_n in (E.15). We shall estimate ΔM^2 in the next section.

E.3 Simple models estimates

Having obtained a general expression for the effective Higgs kinetic and mass terms which include the KK contribution, we now proceed to assess the positivity of these terms. We do that in two simple toy-models which roughly mimic the situation of two general classes of theories: those in which the bulk spectrum is discrete, and those in which it is continuous.

E.3.1 Discrete models

These arise if the bulk potential $V(\varphi)$ is such that as $\varphi \rightarrow +\infty$

$$V \sim \exp b\varphi, \quad b > \sqrt{\frac{2}{3}} \quad \text{or} \quad V \sim \varphi^P \exp \sqrt{\frac{2}{3}}\varphi, \quad P > 0. \quad (\text{E.23})$$

In this case, the KK spectrum is gapped and discrete, and the KK masses m_n behave asymptotically as:

$$m_n^2 \simeq \begin{cases} k^2 n^{2P} & b = \sqrt{\frac{2}{3}} \text{ and } 0 < P < 1, \\ k^2 n^2 & b = \sqrt{\frac{2}{3}} \text{ and } P \geq 1 \quad \text{or } b > \sqrt{\frac{2}{3}}, \end{cases} \quad (\text{E.24})$$

where k is the IR scale of the holographic model.

Except for the subclass with $b = \sqrt{2/3}$ and $0 < P < 1$, all other cases above lead to the same KK spectrum asymptotics as a one-dimensional compactification on a circle of radius $R = 1/k$. Therefore, in order to make estimates in these models, we shall use as a proxy the model constituted by a brane localized in a flat 5-dimensional bulk, compactified on a circle of radius R , and with an induced Einstein-Hilbert term on the brane characterized by a crossover scale r_c . This model was discussed in detail in [64]. The crossover scale is given by $r_c = M_4^2/M_p^3$, which in the full holographic model is (roughly) given by $\hat{U}(\varphi_0, H_0)$ [7]. This is parametrically similar to the DGP setup in bulk AdS space, with $R \leftrightarrow \ell$ as analyzed in [17].

Before we continue, we pause to assess whether this simple circle compactification can capture the qualitative features of the full holographic model. The main difference between the full holographic setup and the toy model is the presence, in the latter, of a normalizable zero mode for bulk fields (including the graviton), due to which the model matches GR on very large scales. In the holographic model this mode is not part of the spectrum, since the bulk volume is infinite on the UV side. However this is irrelevant for the effect we are studying, i.e. the mixing of the Higgs field with the entire tower of KK modes. Another difference is the fact that the 5th dimension in the toy model is flat whereas in the holographic model it is warped. However, this does not affect the features of the KK states, except for the fact that in the toy model the IR scale k is simply the inverse radius, as shown in [17].

In [64] analytical expressions were obtained for the masses m_n , wave-function normalizations \mathcal{N}_n , and values of the wave-function at the brane position (which we set at $r = 0$) $\psi_n(0)$ for the tower of KK modes. We use wave-functions which are normalized to unity in the bulk, i.e. such that (in the real model) the first two terms in (E.15) add up to one. Then we have:

$$m_n^2 = \frac{n^2}{R^2}, \quad \mathcal{N}_n = 1 + r_c |\psi_n(0)|^2, \quad \psi_n(0) = \frac{1}{\sqrt{2\pi R}} \frac{1}{\sqrt{1 + \frac{r_c^2 m_n^2}{4}}}. \quad (\text{E.25})$$

With these expressions we can easily estimate the sums in equations (E.19) and (E.22). The result is controlled by the value of the dimensionless quantity r_c/R . Since the fifth dimension is flat, we can choose the constant scale factor to be $a = 1$. Therefore we do not have factors of a_0 around in our equations.

Higgs kinetic term correction. First, notice that the normalization factor \mathcal{N}_n is given explicitly by:

$$\mathcal{N}_n = 1 + \frac{r_c/R}{1 + \frac{r_c^2 n^2}{4R^2}}. \quad (\text{E.26})$$

No matter the value of r_c/R , the above expression is always near unity, therefore we make the approximation:

$$\mathcal{N}_n \approx 1. \quad (\text{E.27})$$

The correction ΔQ to the Higgs kinetic term in (E.19) is then given by:

$$\Delta Q = (6U_H v_0)^2 \frac{1}{2\pi R} \sum_{n=1}^{\infty} \frac{1}{1 + \frac{r_c^2 n^2}{4R^2}}. \quad (\text{E.28})$$

We can distinguish two cases:

1. $r_c/R \gg 1$.

This is the case in which there is no five-dimensional regime for gravitational

propagation [64, 7]. We can drop the “1” in the denominator of (E.28) for any $n > 0$, and we can estimate the sum as

$$\sum_n \frac{1}{1 + \frac{r_c^2 n^2}{4R^2}} \approx \frac{4R^2}{r_c^2} \sum_{n=1}^{\infty} \frac{1}{n^2}. \quad (\text{E.29})$$

The series converges to a finite constant and we arrive at (dropping numerical factors of order one):

$$\Delta Q \sim (U_H v_0)^2 \frac{R}{r_c^2}, \quad \frac{r_c}{R} \gg 1. \quad (\text{E.30})$$

2. $r_c/R \ll 1$.

In this case gravity has an intermediate five-dimensional (DGP-like) regime, over distances $r_c < r < R$. In this regime we introduce the quantity $N = [R/r_c] \gg 1$ (where [...] denotes the integer part) and we can approximate the sum as follows:

$$\sum_n \frac{1}{1 + \frac{r_c^2 n^2}{4R^2}} \approx \sum_{n=1}^N 1 + \frac{4R^2}{r_c^2} \sum_{n=N}^{+\infty} \frac{1}{n^2} \approx \text{const.} \frac{R}{r_c}. \quad (\text{E.31})$$

In the last approximation, we have used the fact that the first term evaluates to $N \approx R/r_c$, and that the sum in the second term is, for $N \gg 1$, the remainder of the sum of inverse squared integers, which behaves as $1/N$ asymptotically. Dropping again factors of order one, we arrive at:

$$\Delta Q \sim (U_H v_0)^2 \frac{1}{r_c}, \quad \frac{r_c}{R} \ll 1. \quad (\text{E.32})$$

We can understand the extra suppression factor R/r_c in case 1 compared to case 2 from the fact that, in the regime $R/r_c \gg 1$ there is a large number of KK modes which contribute and are unsuppressed on the brane: those with masses above the compactification scale $1/R$ but below the cross-over scale $1/r_c$.

Higgs mass term correction. The Higgs has a quadratic non-derivative coupling only to heavy bulk modes. We can incorporate this fact in our toy model by supposing that the bulk field which gives rise to the KK spectrum has a bulk mass M_0 , and the spectrum is then:

$$m_n^2 = M_0^2 + \frac{n^2}{R^2}. \quad (\text{E.33})$$

This does not affect the KK normalization nor the value of the wavefunction on the brane, which are still as in (E.25). The correction ΔM^2 to the Higgs mass is then obtained from equation (E.22):

$$\Delta M^2 \simeq \frac{F_0^2}{T_H} \frac{1}{2\pi R} \sum_{n=1}^{\infty} \frac{1}{\left(1 + \frac{r_c^2 n^2}{4R^2}\right) \left(M_0^2 + \frac{n^2}{R^2}\right)}, \quad (\text{E.34})$$

where we have approximated again $\mathcal{N}_n \simeq 1$ and we have defined:

$$F_0 = (2X'_H(\varphi_0)v_0 + 4S'_H(\varphi_0)v_0^3). \quad (\text{E.35})$$

There are two dimensionless parameters which control the result:

$$\frac{R}{r_c}, \quad RM_0. \quad (\text{E.36})$$

1. $r_c/R \gg 1$ and $M_0 \ll 1/R$.

In this case the sum can be approximated by

$$\frac{R^4}{r_c^2} \sum_{n=1}^{\infty} \frac{1}{n^4} = \text{const.} \frac{R^4}{r_c^2}, \quad (\text{E.37})$$

and we obtain:

$$\Delta M^2 \approx \frac{F_0^2 R^3}{T_H r_c^2}. \quad (\text{E.38})$$

2. $r_c/R \gg 1$ and $M_0 \gg 1/R$.

In this case we can neglect the “1” only in the first factor the denominator of the general term of the sum in (E.34). Therefore:

$$\sum_{n=1}^{\infty} \frac{1}{\left(1 + \frac{r_c^2 n^2}{4R^2}\right) \left(M_0^2 + \frac{n^2}{R^2}\right)} \approx \frac{R^2}{r_c^2} \sum_{n=1}^{\infty} \frac{1}{n^2 \left(M_0^2 + \frac{n^2}{R^2}\right)}. \quad (\text{E.39})$$

Introducing $N = [M_0 R] \gg 1$ we can approximate the last expression as:

$$\frac{R^2}{r_c^2} \left(\frac{1}{M_0^2} \sum_{n=1}^N \frac{1}{n^2} + R^2 \sum_{n=N}^{\infty} \frac{1}{n^4} \right) \approx \text{const.} \frac{R^2}{r_c^2 M_0^2}. \quad (\text{E.40})$$

In the last approximation we have used the fact that the remainder of the series of $1/n^4$ from N scales as N^{-3} so the second term in equation (E.40) gives a contribution $\sim 1/(r_c^2 M_0^4)$, which is negligible with respect to the first term, $R^2/(r_c^2 M_0^2)$. From (E.40) we arrive at:

$$\Delta M^2 \approx \frac{F_0^2 R}{T_H r_c^2 M_0^2}. \quad (\text{E.41})$$

3. $r_c/R \ll 1$ and $M_0 \ll 1/R$.

In this case the roles of the first and second factor in the denominator of the summand in (E.34) are interchanged, and proceeding as in case 3 we obtain:

$$\Delta M^2 \approx \frac{F_0^2}{T_H} R. \quad (\text{E.42})$$

4. $r_c/R \ll 1$ and $M_0 \gg 1/R$.

Define two large integers $N_1 = R/r_c$ and $N_2 = M_0 R$. Proceeding as in the cases above, the dominant part of the series is the sum of the first N_1 or N_2 terms, whichever is smaller. We then find that the sum evaluates to:

$$\sum_{n=1}^{\infty} \frac{1}{\left(1 + \frac{r_c^2 n^2}{4R^2}\right) \left(M_0^2 + \frac{n^2}{R^2}\right)} \approx \begin{cases} \frac{R}{M_0} & M_0 < \frac{1}{r_c}, \\ \frac{R}{M_0^2 r_c} & M_0 > \frac{1}{r_c}, \end{cases} \quad (\text{E.43})$$

which leads to:

$$\Delta M^2 \approx \begin{cases} \frac{F_0^2}{T_H} \frac{1}{M_0} & M_0 < \frac{1}{r_c}, \\ \frac{F_0^2}{T_H} \frac{1}{M_0^2 r_c} & M_0 > \frac{1}{r_c}. \end{cases} \quad (\text{E.44})$$

E.3.2 Continuous models (abridged)

Bulk potentials with a softer behavior at infinity than (E.23) lead to geometries with a continuous KK spectrum. A toy model which mimics this case is the single-brane RS model with induced gravity on the brane, where the bulk is a cut-off AdS_5 space-time. The two relevant parameters now are the bulk curvature scale k , and the crossover scale r_c , still given by M_4^2/M_p^3 . As in the previous subsection, the main difference between the toy model and the complete holographic setup is that the former contains a zero-mode which mediates four-dimensional interactions at large distances, while in the latter this mode is projected out. However, this is not important since we are interested in the effect of the (continuous) tower of massive modes.

This model was analyzed in [17] where one can find analytic expressions (in terms of Bessel functions) for the KK wave-functions evaluated on the brane. We need the large-mass and small-mass asymptotic behavior:

$$\psi_m(r_0) = \begin{cases} \frac{\sqrt{m/k}}{1+kr_c} & m/k \ll 1, \\ \frac{1}{\sqrt{1+r_c^2 m^2/4}} & m/k \gg 1, \end{cases} \quad (\text{E.45})$$

where now m is a continuous mass parameter. The wave-functions are plane-wave normalized in the IR, and we still have $\mathcal{N}_m \simeq 1$. We can set again $a_0 = 1$. With this choice, all mass scales appearing in the equations are to be understood as measured by brane observers.

The sums in the previous section turn into integrals over m . It turns out that, when evaluated, these integrals lead exactly to the same estimates as in the previous subsection, with the substitution $R \rightarrow 1/k$. The reason is that the suppression of the wave function on the brane for large mass in (E.45) is the same as found for the flat

compactification on a circle, equation (E.25). The fact that most of the effect comes from summing over a large number of modes makes the difference between sums and integrals negligible.

E.4 General remarks

Based on the results we have found in this appendix that, whether or not there are instabilities clearly depends on the details of the model parameters and superpotentials. However we can draw a few general conclusions.

- The KK corrections to the Higgs kinetic term and mass are always finite when we sum over the whole KK tower.
- The corrections are proportional to the Higgs vev and the various “superpotential” coupling the Higgs to the dilaton and the curvature.
- Depending on the model features, the effects scale with different combinations of R and r_c (kinetic term), or R, r_c and M_0 (mass term). To have definite results, one has to look at a concrete model. However, notice that in the regime which is likely the most pheno-friendly ($r_c \gg R$ or $r_c \gg 1/k$) the corrections are always suppressed by powers of the of small numbers R/r_c or $1/kr_c$. In this regime, we can obtain more insight by rephrasing the estimates (E.30) and (E.38-E.41) in terms of the four-dimensional Planck scale M_4 , using the relation:

$$M_4^2 = M_p^3 r_c. \quad (\text{E.46})$$

Recall also that the Higgs and its vev v_0 we are using are in units of M_p (the bulk Planck scale), and that $T_H = M_p^{-1}$. Using these relations, we can rewrite (E.30) as

$$\frac{\Delta Q}{T_H} \approx U_H^2 v_{phys}^2 \frac{R}{r_c} \left(\frac{1}{r_c M_4} \right)^{2/3}, \quad (\text{E.47})$$

where $v_{phys} \equiv v_0 M_p$ is the physical Higgs vev with dimension of energy. The quantity (E.47) must be smaller than unity if we want the Higgs boson not to turn into a ghost. This can be easily achieved naturally for reasonable values of U_H , due to the suppression factor R/r_c and especially to the huge suppression by $r_c M_4$, which is roughly the ratio between the 4d Planck scale and a macroscopic (astrophysical or cosmological) scale.

Similarly, we can write the ratio between the Higgs mass and the mass correction in equations (E.38) and (E.41) (limiting ourselves to the case $R \ll r_c$) as:

$$\frac{\Delta M^2}{m_H^2} \approx (X'_0)^2 R^2 \frac{v_{phys}^2}{m_H^2} \frac{R}{r_c} \left(\frac{1}{r_c M_4} \right)^{2/3}, \quad M_0 \ll 1/R, \quad (\text{E.48})$$

or

$$\frac{\Delta M^2}{m_H^2} \approx \frac{(X'_0)^2 v_{phys}^2 R}{M_0^2 m_H^2 r_c} \left(\frac{1}{r_c M_4} \right)^{2/3}, \quad M_0 \gg 1/R. \quad (\text{E.49})$$

In both cases the large suppression factors R/r_c and especially $(r_c M_4)^{2/3}$ make it very plausible that one does not need any fine tuning to make $\Delta M^2/m_H^2$ small, thereby preventing the Higgs from turning tachyonic. In writing equations (E.48-E.49) we have neglected the term proportional to S'_0 in F_0 (see equation) because it is suppressed by even more powers of the four-dimensional Planck scale.

- Given that the results are the same for the softest of non-confining potential (i.e. a cosmological constant) as for “steep” confining potentials, it is reasonable to assume that the same results will hold in the intermediate classes of general non-confining potentials (i.e. $0 < b < \sqrt{2/3}$) as well as “soft” confining potentials (i.e. $b = \sqrt{2/3}$, $0 < P < 1$).

References

- [1] A. Arvanitaki, S. Dimopoulos, V. Gorbenko, J. Huang and K. Van Tilburg, “A small weak scale from a small cosmological constant,” JHEP **1705** (2017) 071; [ArXiv:1609.06320][hep-ph].
- [2] G. Dvali and A. Vilenkin, “Cosmic attractors and gauge hierarchy,” Phys. Rev. D **70** (2004) 063501; [ArXiv:hep-th/0304043].
- [3] G. Dvali, “Large hierarchies from attractor vacua,” Phys. Rev. D **74** (2006) 025018; [ArXiv:hep-th/0410286].
- [4] G. Dvali, “Cosmological Relaxation of Higgs Mass Before and After LHC and Naturalness,” [ArXiv:1908.05984][hep-ph].
- [5] M. Shaposhnikov and D. Zenhausern, “Quantum scale invariance, cosmological constant and hierarchy problem,” Phys. Lett. B **671** (2009) 162; [ArXiv:0809.3406][hep-th].
- [6] S. J. Huber and Q. Shafi, “Cosmological constant, gauge hierarchy and warped geometry,” Phys. Rev. D **68** (2003) 023503; [ArXiv:hep-ph/0207232].
- [7] C. Charmousis, E. Kiritsis and F. Nitti, “Holographic self-tuning of the cosmological constant,” JHEP **1709** (2017) 031; [ArXiv:1704.05075][hep-th].
- [8] L. Randall and R. Sundrum, “An Alternative to compactification,” Phys. Rev. Lett. **83**, 4690 (1999); [ArXiv:hep-th/9906064];
L. Randall and R. Sundrum, “A Large mass hierarchy from a small extra dimension,” Phys. Rev. Lett. **83**, 3370 (1999); [ArXiv:hep-ph/9905221].

- [9] S. Fichtel, “*Braneworld Effective Field Theories–Holography, Consistency and Conformal Effects*,” JHEP **2004** (2020) 016; [ArXiv:1912.12316][hep-th].
- [10] E. Kiritsis, “*Gravity and axions from a random UV QFT*,” EPJ Web Conf. **71** (2014) 00068; [ArXiv:1408.3541][hep-ph].
- [11] S. L. Dubovsky and M. V. Libanov, “*On brane induced gravity in warped backgrounds*,” JHEP **0311** (2003) 038; [ArXiv:hep-th/0309131].
- [12] G. R. Dvali, G. Gabadadze and M. Porrati, “*4-D gravity on a brane in 5-D Minkowski space*,” Phys. Lett. B **485** (2000) 208; [ArXiv:hep-th/0005016].
- [13] D. Z. Freedman, S. S. Gubser, K. Pilch and N. P. Warner, “*Renormalization group flows from holography supersymmetry and a c theorem*,” Adv. Theor. Math. Phys. **3** (1999), 363-417; [ArXiv:hep-th/9904017];
D. Z. Freedman, S. S. Gubser, K. Pilch and N. P. Warner, “*Continuous distributions of D3-branes and gauged supergravity*,” JHEP **07** (2000), 038 [ArXiv:hep-th/9906194];
K. Pilch and N. P. Warner, “*N=2 supersymmetric RG flows and the IIB dilaton*,” Nucl. Phys. B **594** (2001), 209-228; [ArXiv:hep-th/0004063].
- [14] O. DeWolfe, D. Z. Freedman, S. S. Gubser and A. Karch, “*Modeling the fifth-dimension with scalars and gravity*,” Phys. Rev. D **62**, 046008 (2000); [ArXiv:hep-th/9909134].
- [15] N. Arkani-Hamed, S. Dimopoulos, N. Kaloper and R. Sundrum, “*A Small cosmological constant from a large extra dimension*,” Phys. Lett. B **480**, 193 (2000); [ArXiv:hep-th/0001197]. S. Kachru, M. B. Schulz and E. Silverstein, “*Selftuning flat domain walls in 5-D gravity and string theory*,” Phys. Rev. D **62**, 045021 (2000); [ArXiv:hep-th/0001206].
- [16] C. Csaki, J. Erlich, C. Grojean and T. J. Hollowood, “*General properties of the selftuning domain wall approach to the cosmological constant problem*,” Nucl. Phys. B **584**, 359 (2000); [hep-th/0004133].
- [17] E. Kiritsis, N. Tetradis and T. N. Tomaras, “*Induced gravity on RS branes*,” JHEP **0203** (2002) 019; [ArXiv:hep-th/0202037].
- [18] J. K. Ghosh, E. Kiritsis, F. Nitti and L. T. Witkowski, “*De Sitter and Anti-de Sitter branes in self-tuning models*,” JHEP **1811**, 128 (2018); [ArXiv:1807.09794][hep-th].
- [19] A. Amariti, C. Charmousis, D. Forcella, E. Kiritsis and F. Nitti, “*Brane cosmology and the self-tuning of the cosmological constant*,” JCAP **1910** (2019) no.10, 007; [ArXiv:1904.02727][hep-th].
- [20] I. Antoniadis, E. Kiritsis and T. N. Tomaras, “*A D-brane alternative to unification*,” Phys. Lett. B **486** (2000) 186; [ArXiv:hep-ph/0004214];
“*D-brane standard model*,” Fortsch. Phys. **49** (2001) 573; [ArXiv:hep-th/0111269];

- I. Antoniadis, E. Kiritsis, J. Rizos and T. N. Tomaras, “*D-branes and the standard model*,” Nucl. Phys. B **660** (2003) 81; [ArXiv:hep-th/0210263].
- [21] P. Anastasopoulos and E. Kiritsis, “*The Anomalous magnetic moment of the muon in the D-brane realization of the standard model*,” JHEP **0205** (2002) 054; [ArXiv:hep-ph/0201295].
- [22] P. Anastasopoulos, T. P. T. Dijkstra, E. Kiritsis and A. N. Schellekens, “*Orientifolds, hypercharge embeddings and the Standard Model*,” Nucl. Phys. B **759** (2006) 83; [ArXiv:hep-th/0605226].
- [23] C. Coriano, N. Irges and E. Kiritsis, “*On the effective theory of low-scale orientifold string vacua*,” Nucl. Phys. B **746** (2006) 77 [ArXiv:hep-ph/0510332].
- [24] Y. Hamada, E. Kiritsis, F. Nitti and L. T. Witkowski, “*Axion RG flows and the holographic dynamics of instanton densities*,” J. Phys. A **52** (2019) no.45, 454003; [ArXiv:1905.03663][hep-th].
- [25] E. Witten, “*Large N Chiral Dynamics*,” Annals Phys. **128** (1980) 363.
- [26] E. Witten, “ *θ dependence in the large N limit of four-dimensional gauge theories*,” Phys. Rev. Lett. **81** (1998) 2862; [ArXiv:hep-th/9807109].
- [27] D. Arean, I. Iatrakis, M. Jarvinen and E. Kiritsis, “*CP-odd sector and θ dynamics in holographic QCD*,” Phys. Rev. D **96** (2017) no.2, 026001; [ArXiv:1609.08922][hep-ph].
- [28] P. W. Graham, D. E. Kaplan and S. Rajendran, “*Cosmological Relaxation of the Electroweak Scale*,” Phys. Rev. Lett. **115** (2015) no.22, 221801; [ArXiv:1504.07551][hep-ph].
- [29] N. Arkani-Hamed, L. Motl, A. Nicolis and C. Vafa, “*The String landscape, black holes and gravity as the weakest force*,” JHEP **0706** (2007) 060; [ArXiv:hep-th/0601001].
- [30] P. Svrcek and E. Witten, “*Axions In String Theory*,” JHEP **0606** (2006) 051; [ArXiv:hep-th/0605206].
- [31] T. Rudelius, “*Constraints on Axion Inflation from the Weak Gravity Conjecture*,” JCAP **1509** (2015) 020; [ArXiv:1503.00795][hep-th].
- [32] M. Montero, A. M. Uranga and I. Valenzuela, “*Transplanckian axions!?*,” JHEP **1508** (2015) 032; [ArXiv:1503.03886][hep-th].
- [33] F. Baume and E. Palti, “*Backreacted Axion Field Ranges in String Theory*,” JHEP **1608** (2016) 043; [ArXiv:1602.06517]hep-th].
- [34] A. Hebecker, P. Henkenjohann and L. T. Witkowski, “*Flat Monodromies and a Moduli Space Size Conjecture*,” JHEP **1712** (2017) 033; [ArXiv:1708.06761]hep-th].

- [35] C. Kounnas, F. Zwirner and I. Pavel, “Towards a dynamical determination of parameters in the minimal supersymmetric standard model,” Phys. Lett. B **335** (1994) 403; [ArXiv:hep-ph/9406256].
- [36] S. Dimopoulos, G. F. Giudice and N. Tetradis, “Disoriented and plastic soft terms: A Dynamical solution to the problem of supersymmetric flavor violations,” Nucl. Phys. B **454** (1995) 59; [ArXiv:hep-ph/9504296].
- [37] S. Dubovsky, A. Lawrence and M. M. Roberts, “Axion monodromy in a model of holographic gluodynamics,” JHEP **1202** (2012) 053; [ArXiv:1105.3740][hep-th].
- [38] A. Kehagias and E. Kiritsis, “Mirage cosmology,” JHEP **9911** (1999) 022; [ArXiv:hep-th/9910174].
- [39] E. Kiritsis, G. Kofinas, N. Tetradis, T. N. Tomaras and V. Zarikas, “Cosmological evolution with brane bulk energy exchange,” JHEP **0302** (2003) 035; [ArXiv:hep-th/0207060].
- [40] E. Kiritsis, “Holography and brane-bulk energy exchange,” JCAP **0510** (2005) 014; [ArXiv:hep-th/0504219].
- [41] V. Agrawal, S. M. Barr, J. F. Donoghue and D. Seckel, “Viable range of the mass scale of the standard model,” Phys. Rev. D **57** (1998) 5480; [ArXiv:hep-ph/9707380].
- [42] T. Damour and J. F. Donoghue, “Constraints on the variability of quark masses from nuclear binding,” Phys. Rev. D **78** (2008) 014014; [ArXiv:0712.2968][hep-ph].
- [43] J. F. Donoghue, K. Dutta, A. Ross and M. Tegmark, “Likely values of the Higgs vev,” Phys. Rev. D **81** (2010) 073003; [ArXiv:0903.1024][hep-ph].
- [44] L. J. Hall, D. Pinner and J. T. Ruderman, “The Weak Scale from BBN,” JHEP **1412** (2014) 134; [ArXiv:1409.0551][hep-ph].
- [45] U. G. Meissner, “Anthropic considerations in nuclear physics,” Sci. Bull. **60** (2015) no.1, 43; [ArXiv:1409.2959][hep-th].
- [46] E. Kiritsis, F. Nitti and L. S. Pimenta, “Exotic RG Flows from Holography,” Fortsch. Phys. **65** (2017) no.2, 1600120; [ArXiv:1611.05493][hep-th].
- [47] J. K. Ghosh, E. Kiritsis, F. Nitti and L. T. Witkowski, “Holographic RG flows on curved manifolds and quantum phase transitions,” JHEP **1805** (2018) 034; [ArXiv:1711.08462][hep-th].
- [48] E. Witten, “Anti-de Sitter space, thermal phase transition, and confinement in gauge theories,” Adv. Theor. Math. Phys. **2** (1998) 505 [ArXiv:hep-th/9803131].
- [49] U. Gursoy and E. Kiritsis, “Exploring improved holographic theories for QCD: Part I,” JHEP **0802** (2008) 032; [ArXiv:0707.1324][hep-th];

- U. Gursoy, E. Kiritsis and F. Nitti, “*Exploring improved holographic theories for QCD: Part II*,” JHEP **0802** (2008) 019; [ArXiv:0707.1349][hep-th];
- U. Gursoy, E. Kiritsis, L. Mazzanti, G. Michalogiorgakis and F. Nitti, “*Improved Holographic QCD*,” Lect. Notes Phys. **828** (2011) 79; [ArXiv:1006.5461][hep-th].
- [50] S. S. Gubser, “*Curvature singularities: The Good, the bad, and the naked*,” Adv. Theor. Math. Phys. **4** (2000) 679; [ArXiv:hep-th/0002160].
- [51] U. Gursoy, E. Kiritsis, L. Mazzanti and F. Nitti, “*Holography and Thermodynamics of 5D Dilaton-gravity*,” JHEP **0905**, 033 (2009); [ArXiv:0812.0792][hep-th].
- [52] L. E. Ibanez, M. Montero, A. Uranga and I. Valenzuela, “*Relaxion Monodromy and the Weak Gravity Conjecture*,” JHEP **1604** (2016) 020; [ArXiv:1512.00025][hep-th].
- [53] A. Herraez and L. E. Ibanez, “*An Axion-induced SM/MSSM Higgs Landscape and the Weak Gravity Conjecture*,” JHEP **1702** (2017) 109; [ArXiv:1610.08836][hep-th].
- [54] G. F. Giudice, A. Kehagias and A. Riotto, “*The Selfish Higgs*,” JHEP **1910** (2019) 199; [ArXiv:1907.05370][hep-ph].
- [55] N. Kaloper and A. Westphal, “*A Goldilocks Higgs*,” Phys. Lett. B **808** (2020), 135616; [ArXiv:1907.05837][hep-th].
- [56] H. M. Lee, “*Relaxation of Higgs mass and cosmological constant with four-form fluxes and reheating*,” JHEP **2001** (2020) 045; [ArXiv:1908.04252][hep-ph].
- [57] K. Skenderis and M. Taylor, “*Kaluza-Klein holography*,” JHEP **05** (2006), 057; [ArXiv:hep-th/0603016].
- [58] I. Papadimitriou, “*Holographic Renormalization of general dilaton-axion gravity*,” JHEP **1108** (2011) 119; [ArXiv:1106.4826][hep-th].
- [59] C. Vafa and E. Witten, “*Parity Conservation in QCD*,” Phys. Rev. Lett. **53** (1984) 535.
- [60] E. Kiritsis, W. Li and F. Nitti, “*On the gluonic operator effective potential in holographic Yang-Mills theory*,” JHEP **1504**, 125 (2015); [ArXiv:1410.1091][hep-th].
- [61] C. Charmousis, B. Gouteraux, B. S. Kim, E. Kiritsis and R. Meyer, “*Effective Holographic Theories for low-temperature condensed matter systems*,” JHEP **11** (2010), 151; [ArXiv:1005.4690][hep-th].
- [62] B. Gouteraux and E. Kiritsis, “*Generalized Holographic Quantum Criticality at Finite Density*,” JHEP **12** (2011), 036; [ArXiv:1107.2116][hep-th].
- [63] E. Kiritsis, “*Dissecting the string theory dual of QCD*,” Fortsch. Phys. **57** (2009), 396-417; [ArXiv:0901.1772][hep-th].
- [64] G. R. Dvali, G. Gabadadze, M. Kolanovic and F. Nitti, “*The Power of brane induced gravity*,” Phys. Rev. D **64** (2001) 084004; [ArXiv:hep-ph/0102216].